GENERAL ELECTRIC REVIEW

A MONTHLY MAGAZINE FOR ENGINEERS

Manager, M. P. RICE   Editor, JOHN R. HEWETT   Associate Editor, E. C. SANDERS

Subscription Rates: United States and Mexico, $3.00 per year; Canada, $3.25 per year; Foreign, $3.50 per year; payable in advance. *Library and Student Rates:* United States and Mexico, $2.00 per year; Canada, $2.25 per year; Foreign, $2.50 per year; payable in advance.

Remit by post-office or express money order, bank check, or draft, made payable to the *General Electric Review*, Schenectady, N. Y.

Advertising forms close on the first day of the month preceding date of issue.

Entered as second-class matter, March 26, 1912, at the post-office at Schenectady, N. Y., under the Act of March, 1879.

Vol. XXVII, No. 12

Copyright 1924
by General Electric Company

DECEMBER, 1924

CONTENTS

PAGE

Frontispiece: George E. Emmons, Retiring Vice President in Charge of Manufacturing, General Electric Company 776

Editorial: George E. Emmons: A Sketch of His Career and Character 777

The Turbine Designer's Wind Tunnel 780
By LORING WIRT

Electric Trucks for Store Door Delivery of Freight 793
By R. MACRAE

Study of Crystal Structure and Its Applications: Part II 795
By W. P. DAVEY

Relighting Atlantic City's Boardwalk 803
By T. P. BROWN

Studies of Electric Discharges in Gases at Low Pressures: Part V 810
By IRVING LANGMUIR and HAROLD MOTT-SMITH, JR.

The Steinmetz Memorial Scholarships 820
By C. M. RIPLEY

Oil Circuit Breaker Investigations to Determine Interrupting Capacities 822
By J. D. HILLIARD

Studies in the Projection of Light: Part XV 830
By FRANK BENFORD

Library Section 839

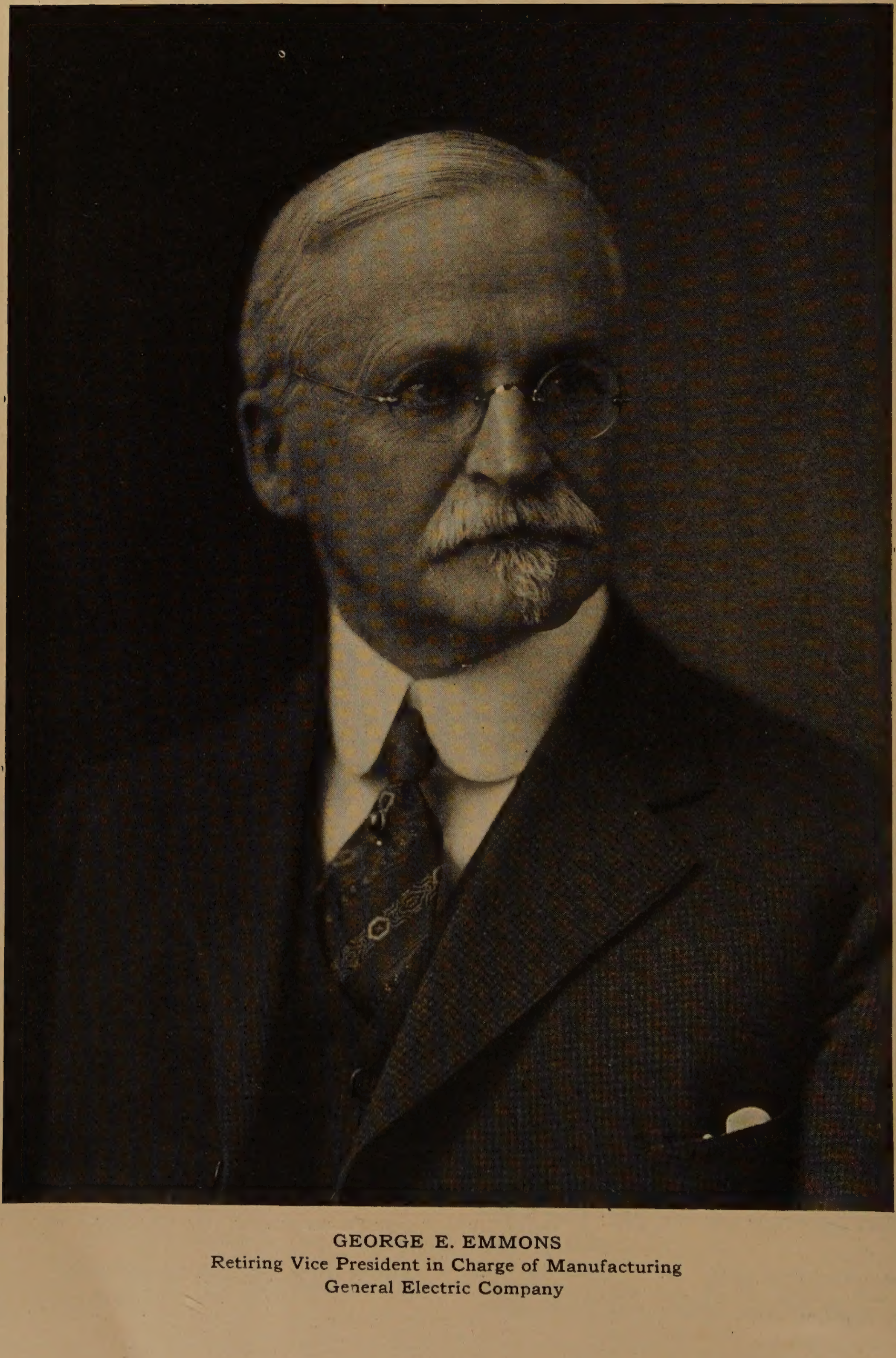

GEORGE E. EMMONS
Retiring Vice President in Charge of Manufacturing
General Electric Company

GENERAL ELECTRIC REVIEW

GEORGE E. EMMONS: A SKETCH OF HIS CAREER AND CHARACTER

To give a most deserved and special recognition to Mr. George E. Emmons on the occasion of his retirement as Vice President in Charge of Manufacturing of the General Electric Company, we are this month publishing a recent portrait of him as the frontispiece and are devoting the editorial page to a sketch of him prepared for this purpose by Mr. John T. Broderick who, through years of intimate association with Mr. Emmons, is ably fitted to perform this official act of friendship.—EDITOR.

Abraham Lincoln said the Almighty must be partial to common people because He made so many of them. So far as normal contacts and spontaneous sympathies go, our retiring chief belongs to that favored class—the common people. No one has ever heard him boast of any blue blood, though it is equally certain that no one has ever seen in him the slightest trace of a yellow taint. His, palpably, is that red blood that flows in the veins of so many of the men who have made our country what it is—the world's industrial center. To be sure, when we think, in a detached way, of mental equipment, which is the part of a man that nature often makes use of to show the absurdity of racial or class distinctions, it is impossible not to view that portion of Mr. Emmons' equipment as uncommon. He was provided at birth with a mainspring which has been functioning for 67 years, and will continue to function when he is no more to be seen, except perhaps at intervals, in those places here in the East that his personality has long invested with unique and even romantic interest.

It is not essential here to give the precise date and place of Mr. Emmons' birth. He has the accent and some of the mannerisms of a typical New Englander, with more than a little of that homespun sagacity for which the Connecticut type of Yankee is noted; so I have always assumed that he was a native of Connecticut and have never deemed it necessary to verify the assumption. Moreover, I do not wish now to discover that this assumption was erroneous, for I have a favorable opinion of the state of Connecticut, because so many sturdy and useful citizens come from there, and want to leave with it the credit of having cradled George E. Emmons.

It was at the age of fourteen that the sowing of his wild oats, of which little is known, however much may be imagined, came to an end. He could read, write, and cipher about as well as the average boy of today who has reached the eighth grade, and with the modicum of education represented by those attainments, all that he ever received from any institution of learning, went to work in a grocery store. There he served an apprenticeship of seven years, receiving compensation at first of $2.00 a week, and during the final year $7.00 a week. The evidence is conclusive that he was no less frugal in those days than he afterwards proved to be as an industrial manager, for, with average earnings not exceeding $5.00 a week, he saved enough in the period of seven years to embark in the grocery business at South Bend, Indiana, in partnership with another young man. This enterprise proved to be a dismal failure, due to certain peculiarities developed by the partner, such as would have insured the failure of any enterprise similarly handicapped, and Mr. Emmons' meagre capital disappeared in a very much shorter time than it had taken him to amass it. After walking the streets of Chicago till his feet were sore, seeking in vain for a job, he returned to Connecticut and obtained a position with the American Electric Company at New Britain.

There it was that he first came into contact with two men who were destined to do work of far-reaching value in connection with the development of the electrical industry. One of them, then under thirty years of age, had been a teacher in the Philadelphia High School; the other, about ten years younger, was one of his pupils. Their names, listed now in the reference books with the names of the foremost living scientists, were respectively Elihu Thomson and E. W. Rice, Jr. These two engineers constituted the technical staff of the American Electric Company.

That pioneer corporation, it may be remarked, has more than ordinary historical interest because it was one of several industrial units that, in the course of time, and through a process of amalgamation, became the huge instrument of world-wide service now known as the General Electric Company.

It was organized in 1881, to manufacture and sell arc dynamos and lamps.

From all accounts, the American Electric Company did not flourish, but was kept alive until its work attracted the attention of a group of business men of Lynn, Massachusetts, including Charles A. Coffin, who purchased a controlling interest in the enterprise and brought about a reorganization. Out of this reorganization, which was effected in 1883, came the Thomson-Houston Electric Company, which continued at Lynn the work started at New Britain, and which, after nearly a decade of notable growth, was combined with the Edison General Electric Company which had established a plant at Schenectady.

Mr. Emmons had relinquished his job with the American Electric Company after a few months of service because the prospects of advancement there seemed to him anything but bright, and was employed elsewhere until 1886, when he was offered and accepted a position as bookkeeper and cost clerk for the Thomson-Houston Electric Company.

Reference has been made to the growth of the Thomson-Houston Electric Company to the time of its consolidation with the Edison unit. This growth continued up to the eve of the panic, a year after the consolidation. To arc dynamos and lamps as manufactured at New Britain were added several types of generators to produce current for power as well as lighting applications. Motors for operating street cars were made and sold in quantities that seemed large at that time; and with these were to be seen in production, in smaller quantities, some of the prototypes of the motors now used extensively for driving machinery in factories and mines. The manufacture of incandescent lamps was also undertaken. It was at Lynn, in fact, that the Edison Lamp Division of the General Electric Company, which now operates a dozen plants throughout the country, had part of its beginning, for one of the two major units from which that Division evolved was started there. To the technical staff, under Mr. Rice, in 1892, came the great Steinmetz, with his mathematical genius, to reveal the knowledge needed to design efficient apparatus employing alternating current. That period, in short, was one of quite as rapid progress in the electrical art as any period of like duration since, although the development of long-distance transmission, with which pioneer engineers like C. C. Chesney had much to do, and the introduction of the steam turbine, led, during a later era, to a greatly increased volume of business.

The devastating consequences of the panic that swept over the country like a blight thirty-one years ago will be vividly recalled by those affected by it, and there were few then engaged in commercial pursuits whom, in one form or other, it did not affect. That memorable crisis was the occasion for some of the most valuable service which Mr. Emmons has rendered to the electrical industry. I believe that it is in the work which he did during his stewardship of the Schenectady plant for a quarter of a century that he himself takes the keenest pride. The great value of that work is obvious. For the most part, it was constructive in character, and, therefore, Mr. Emmons must have found it enjoyable. Less pleasant, but withal of lasting usefulness, was his contribution to the enforced work of retrenchment following the panic of 1893, as well as to the work of economic rehabilitation during the ensuing period of depression. Many of the methods inaugurated by him at that time, with the help of others, to prevent needless expense and waste of every description, and to insure effective supervision of manufacturing operations, have not been improved upon fundamentally since, and are applied today, modified only in detail to suit altered conditions.

After serving for a short period as Manager of the plant at Lynn, Mr. Emmons was called to Schenectady, and in 1895 was appointed Manager of the Schenectady plant. He was made Chairman of the Manufacturing Committee in 1913, and Vice President in charge of manufacturing operations in 1916, but retained the direct management of the Schenectady plant until 1920. For the past four years his attention has been divided among the several plants of the General Electric Company's system in proportion to their size or as the local managers needed his counsel and help.

His personal monument, without question, is the Schenectady plant, with all that it means for the community in which it is located, for the General Electric Company, and for industry; with its five hundred or more acres; its upwards of three hundred factory buildings, many of them erected and equipped under his supervision; its miles of paved thoroughfares as well laid out as the streets of a modern city; its network of tracks for the economical movement of materials; its atmosphere of order and neatness; its hundreds of capable superintendents and foremen and twenty thousand other loyal workers; its capacity to produce apparatus of a selling value in excess of one hundred millions of dollars annually; and, above all, its social worth as an institution that gives to more than fifty thousand people the assurance of a decent living. In the rearing of that monument, which, without any stretch of fancy may be called magnificent, he spent the best years of his life, and during those years gave all that he had to give.

No more need be said here about Mr. Emmons' achievements; in fact, at the outset I meant to say less about them, for they speak adequately and eloquently for themselves. He has never sought to have the importance of his work emphasized. I have sometimes heard him dwell modestly on what he termed his limitations. Once, with that merry twinkle of his eye that makes conversation with him a delight, he assured me that he was old-fashioned; but as to that, it seems certain that he was in error, unless it is old-fashioned to prize realities and view untried theories with caution. The man who performs the duty of the day, and performs it well, who takes up the work in front of him and does it with dispatch and thoroughness, is more likely to be progressive than one who merely talks about being so. Mr. Emmons had little time to talk about progress; he kept busy in his own way making it.

But while the work he has done may be allowed to speak for itself, it is fitting to dwell for a moment upon the character of the man as it was revealed through what he did. When he is settled in his California home and I have occasion to say how he impressed one who knew him and worked with him from a time before the General Electric Company existed, I shall speak of him thus: Downright honesty was his outstanding trait, honesty of thought, of purpose, and of conduct. In business life a certain respectable disingenuousness, or polite deviation from a straight course within the law, is sometimes tolerated, and even looked upon as an art to be mastered. In that art Mr. Emmons was wholly unskilled. He loved the simple truth, the frank, revealing word, and nothing false or mean marred his personal relationships, or had an abiding place in his business philosophy. For him a spade was a spade—never any other kind of an implement. There was no evasion, no subterfuge, no shuffling in his intercourse either with official superiors or with those who worked with him or under him.

The men concerned with him in the upbuilding of an important branch of a great industry may not always have been able, in the discussion of plans and policies, to think precisely as he did, but different shades of opinion were welcomed by him as a help in the day's task, and one's faith in his rectitude and sense of justice was never weakened by anything he said or did. Throughout my association with him there was many a time when I saw him quick in decision, courteously firm and ready to take a short cut to attain an important end, but there was never a doubt of where he stood on any issue. In his negotiations with employees of the General Electric Company, and with all classes of individuals, he said what he could do, and what he would do; and his word, once given, was never broken or even bent.

The field of Mr. Emmons' labors was that in which attention must be focused on material things, but his impulses were beautifully human; and he had ideals, too, that gave dignity and purity to whatever he did. With his whole mind and heart he strove to make the organization that he served efficient, but he also helped to keep its moral tone high. "His life was gentle, and the elements so mix'd in him, that Nature might stand up and say to all the world, 'This was a man.!' "

John T. Broderick

The Turbine Designer's Wind Tunnel

By Loring Wirt

Turbine Engineering Department, General Electric Company

The exceptional talent and skill that is being devoted to advancing the art of turbine design is well evidenced by the fact that within the last few months we have occasion to record the results of two turbine research investigations that will have fundamental influences on the design of these prime movers. The first related to the discovery of the causes of axial vibration and the development of a manufacturing method whereby turbines can be built with certainty free from this troublesome phenomenon. (This appeared in our issues of June, July and August.) The second concerns means of improving turbine efficiency by the determination of more nearly true stream-flow passages from the boiler, through the turbine, to the condenser. To study experimentally the action of passage design upon the flow of steam, advantage was taken of the conveniently handled analogy of air flow in model passages. By means of ingeniously developed methods of test, data are secured in both numerical and graphical forms which readily furnish a visual conception of what is going on in the passage and, what is more important, a means of calculating the amounts and distribution of energy flow and losses throughout any cross-section of the passage. This article was read by the author as a paper at the Annual Meeting of the A. S. M. E., December 1 to 4, 1924.—Editor.

This article describes briefly methods developed by the General Electric Company to accelerate advancement in the art of turbine design, and to insure correct design of all the elements of a turbine that control and guide the flow of steam from the control valve through the nozzles, buckets, and exhaust hood to the condenser. The rapid improvement of the airplane is based upon an infinite amount of painstaking wind-tunnel research; and in much the same way improvements in the turbine have been pointed out by the "Turbine Air Test," which in reality is the turbine designer's wind tunnel.

The air test was started over four years ago on top of a two-inch pipe and has grown so that there are now two test stands supplied through six-inch pipes with air at 90 lb. per sq. in. pressure. The air test is run continuously—that is, days, nights, and overtime. Over 1100 different models have been tested ranging in variety from those representing turbine problems to turbine-air compressor elements, and including also the ventilation of electrical machinery. Air test methods similar to those developed could be adapted to ventilating and aerodynamical problems, in fact they are universally applicable to any problem that concerns the flow of a fluid, be it compressible or incompressible. The methods can be used to design stream-line valve passageways for water, air, or steam, or to indicate the flow around the nose of a projectile, airplane, propeller, or ship model.

The stream line and eddy flow through a passageway is clearly and beautifully indicated by flow casts that show both the flow lines and the shape that caused them. Also the issuing stream of air is explored with impact tubes, static tubes, and angle measuring devices. In particular a combined traversing, plotting, and enlarging mechanism has been devised that makes possible the quick taking of a series of accurate impact traverses covering the whole of the jet. With curve-drawing templates, these traverses are mechanically evaluated and from them the efficiency of the nozzle is found by a method of graphical triple integration. The final value of efficiency of a nozzle is the result of approximately 900 readings of impact pressure. Exhaust hoods, interstage passageways, valves, and the like are tested by measuring the volume flow through them, for any initial pressure ahead of them, and plotting pressure-flow curves.

The following condensed outline gives an idea of how thoroughly turbine elements have been tested by means of models:

- Throttle Valves
- Controlling Valves
- Intercepting Valves
- Strainers
- Elbows
- High-pressure Heads
- High-pressure Exhaust Hoods
- Crossovers from High-pressure Turbine to Low-pressure Turbine
- Low-pressure Heads
- Nozzles (for all stages and especially last stages)
- Buckets (for all stages and especially last stages)
- Exhaust Hoods

Description of Air Test

Suppose, for example, it is desired to find the relative efficiency of two proposed types of construction. A model nozzle will be made of each as shown in Fig. 1. The sides and ends are made of mahogany and the two plates of steel are let into the sides about $\frac{3}{16}$ of an inch. Three passageways only are constructed. The discharge from the first and third passageways serves to support the center jet properly. The sides and ends of the model are held together by dowels and through bolts in order that it may be taken apart readily. Model nozzles for the center stages of a turbine are made full size. Those for the first stages are enlarged two or three times, while those for the last stages are generally made ½ to ⅓ full size.

The test results are worthless unless the nozzle being tested is fed by air in the same way that the corresponding nozzle in the turbine is fed by steam. Proper feeding requires that the nozzle be preceded with a suitable guiding passageway called the "preliminary conditions" (see Figs. 2 and 3) that simulate the discharge from the previous bucket. The radial height of the preliminary conditions is made equal to the length of the active discharge portion of the preceding buckets.

The angles of discharge from the preliminary conditions into the nozzle entrance at the big and small diameter are equal to the absolute angles of discharge from the tip and root of the bucket. Angle measurements made of the steam discharge from wheels of turbines in operation indicate that the measured angle of discharge is practically equal to the angle obtained from a velocity diagram, and consequently the latter angles are used to determine the angle for the preliminary conditions.

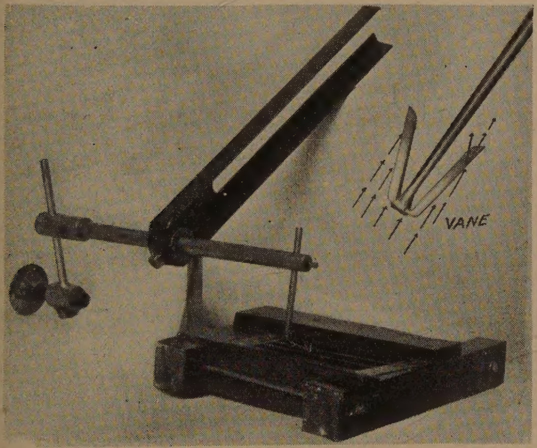

Fig. 1. Model Nozzle and Double-vane Angleometer with Telescope and Protractor

Fig. 3 shows a cast of the interior of such a nozzle and preliminary conditions. It will be seen that at the left side the approach to the nozzle is at 45 deg. while at the right side it is straight, due to the different absolute angle of discharge from the tip and root of the preceding bucket. This illustration also shows clearly the two plates of the nozzle as well as the general shape of the nozzle in the radial flow direction.

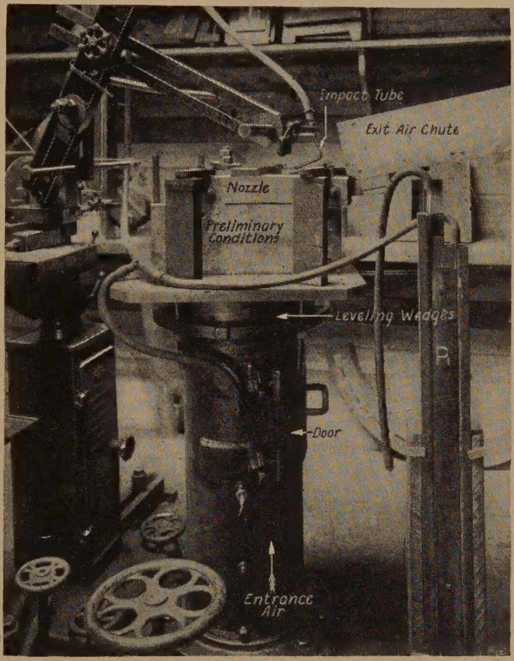

Fig. 2. Test Table Showing Part of Traversing Machine

Fig. 4 shows that a model nozzle fed in this way truly simulates turbine conditions. Figs. 4A and 4B are views of the discharge surfaces of diaphragm plates that have been in operation for two or three years and show the markings caused by boiler compound and other impurities in the steam. Fig. 4C shows similar markings obtained on the air-test model by placing dots of liquid paint on the nozzle surfaces and blowing at the proper velocity. In about a minute the paint took the form shown and the flow was stopped instantly by a clapper valve. The comparison proves several things. First, that the markings on the actual diaphragms are not due to water in the last stages of the turbine but are due to eddy flow of the steam itself, since in the air-test model there was no water. Second, the air-test markings duplicate remarkably well the turbine markings. At the side of the big diameter there is the same eddy in both cases and there is also a throat line parallel to the exit edge of each plate. The close similarity of flow indicates that the model nozzle is being fed in the correct way and that therefore turbine conditions are being duplicated. Consequently, gains shown by the air test should be realized in the turbine.

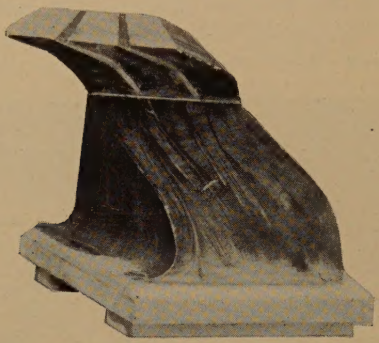

Left side view, 45 deg. approach

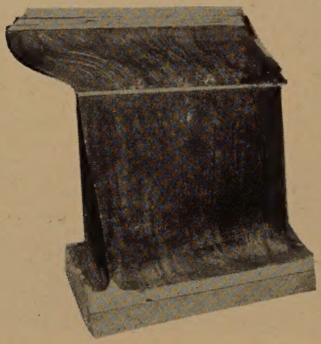

Back view, discharge into paper and up

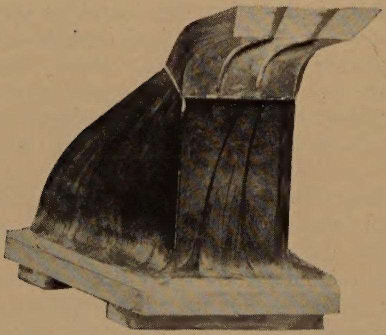

Right side view, straight approach

Fig. 3. Cast of Typical Preliminary Conditions, for Testing Last Stage Nozzles. The three white surfaces at the top of each view define the plane of exit of the actual diaphragm

The nozzle and its preliminary conditions are bolted down on the top of the test stand shown in Fig. 2. The air is controlled by the valves at the bottom so that the pressure is constant in the front of the nozzle at a value that will give a nozzle velocity corresponding to that in the turbine.

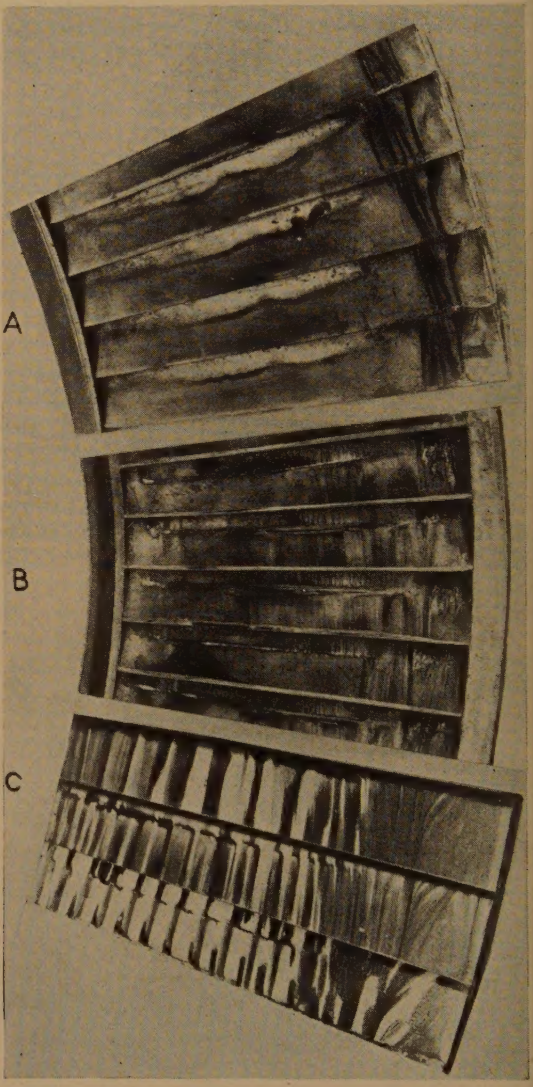

Fig. 4. (A) Turbine Diaphragm. (B) Turbine Diaphragm. (C) Air Test Model. Flow lines on exit side of nozzle prove that turbine flow conditions are duplicated in the air test models

The initial pressure is measured by an impact tube projecting into the center line of the preliminary conditions and pointing in the direction of the approaching air. Thus it reads the total initial energy, by adding the effect of the velocity of approach to the static pressure. The discharge from the nozzle escapes upward to the right (see Fig. 2) through the exit air chute.

The center jet is explored in testing, overlapping somewhat into the first and third jets by means of an impact tube held in the traversing mechanism shown in Fig. 5. This device is a combined traversing, plotting, and enlarging machine improvised from a grinding machine. The three feeds are used to move the impact tube in three rectilinear directions. The location along the path of the traverse of the point of the tube is known at all times by the position of the edge of the ruler on a flat table or by the edge of the tool rest which rubs on the revolving drum. By means of a steel wire and ratio wheel this drum can be made to revolve at any enlarged ratio up to 20 times full size. The impact tube is connected to both a simple U-tube and differential U-tube that are immediately in front of the operator. These tubes are selected so as to have uniform bore in order that it may be sufficient to read only one side of the U-tube and plot this value to the proper double scale.

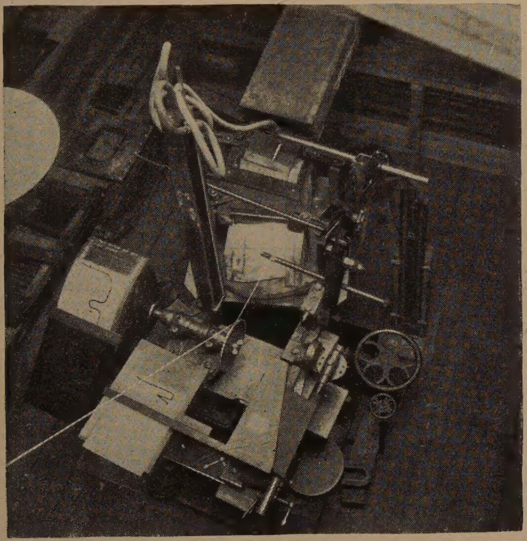

Fig. 5. Top View of Combined Traversing, Plotting, and Enlarging Machine, Improvised from a Grinder

In using the traversing machine, the operator with his right hand moves the impact tube in small increments and with his left plots the value of impact pressure on the revolving drum. The points when connected give a curve like any one of the solid heavy curves on Figs. 6 and 7. It is clear that as the point of the impact tube moves along on a circumferential traverse from a region of high velocity in the center line of the first nozzle to a point in line with the partition exit edge it will move into a region of lower velocity due to the loss caused by the plate and the eddies following it. This will produce a dip in the impact curve, the two dips corresponding to the two plate edges. Fig. 6 shows most of the traverses of the set for one type of nozzle. The traverses are spaced further apart in the center of the nozzle where there is little difference from one traverse to another, while at the sides where the difference between traverses is great the spacing is reduced to 1/8 of an inch or less.

The process of taking data is so simple and automatic that very accurate curves can be taken quickly and points on them checked if necessary. In testing models of last-stage diaphragms, it is customary to run about 30 traverses and as each traverse contains about 35 points, some thousand values of impact pressure are read and plotted in order to obtain the efficiency of each nozzle tested. The model for a 16th-stage nozzle discharges 7000 cu. ft. of free air per minute which is expending energy at the rate of 358 horse power, so it will be seen why such a model nozzle is made 1/2 size and limited to only three active passageways and why the method of taking data must be accurate and quick. The whole set of impact traverses on one nozzle can be run off in one night. Tests requiring large flows of air are run at night because more air is then available. In fact, some very large models have been tested on Sunday when exclusive use could be made of 14,000 cu. ft. of free air per minute at 90 lb. per sq. in. pressure, the entire air compressor capacity of the Schenectady Works.

Fig. 7 shows a set of traverses on a second type of nozzle. The better performance is self evident since the dips are small and the impact pressure comes up to maximum between them. Before describing how to evaluate impact pressures, it will be well to discuss flow or paint casts and how they are made.

Flow Casts

The best way that has been found to indicate stream-line flow through a model is to paint the interior surfaces with a mixture of lamp black and neatsfoot oil. The model

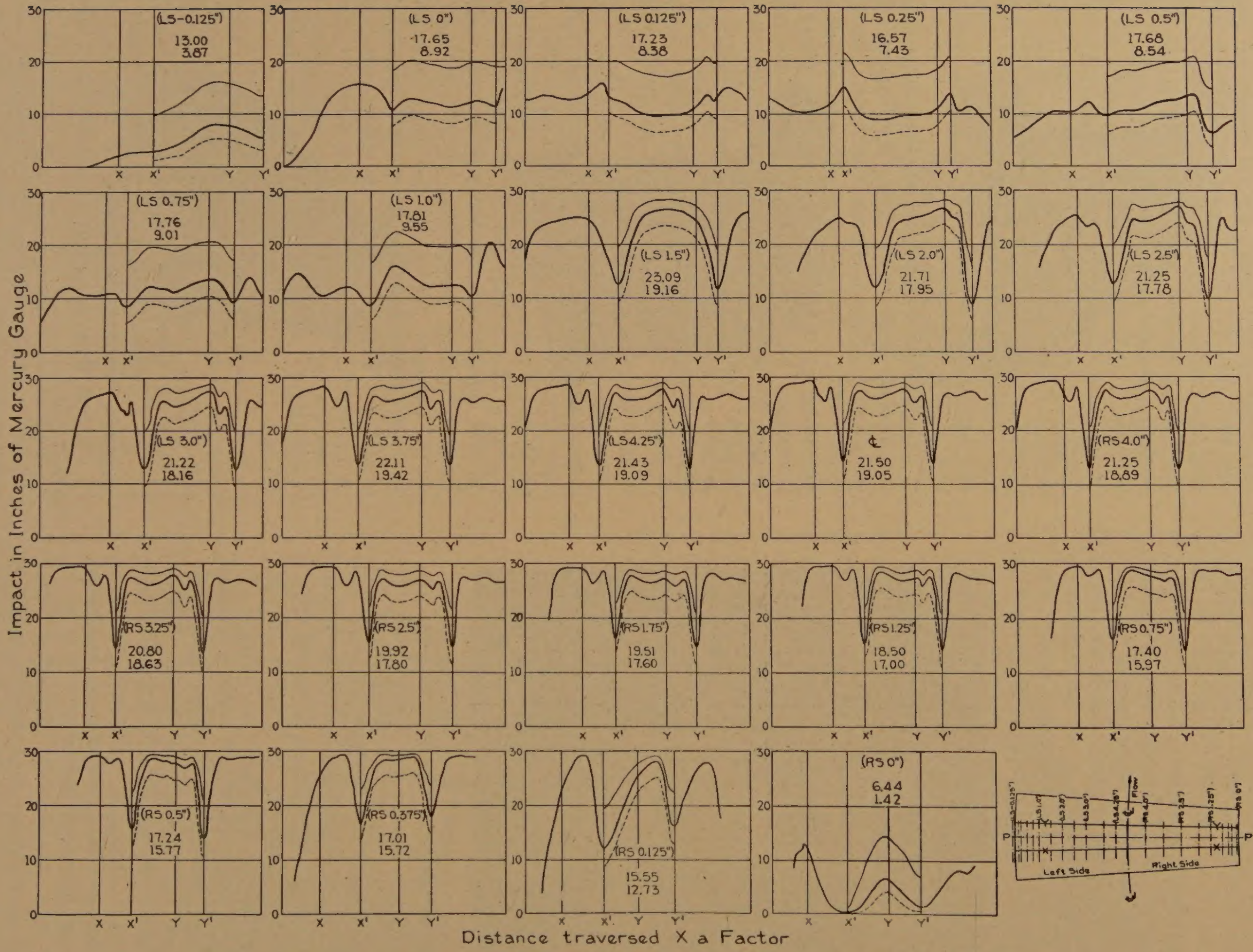

Fig. 6. SET OF IMPACT TRAVERSES ON AN INEFFICIENT TYPE OF NOZZLE

The heavy or middle curves are curves of impact pressure as obtained on the plotting machine The dotted or lower curves represent the actual energy and the lower number gives its value; the upper curves represent 100 per cent energy and the upper number gives its value. The ratio of these values gives the efficiency of any particular traverse. The dimensions in parentheses give the distance of the traverses from the nearest side of the nozzle as indicated in the key at the bottom right

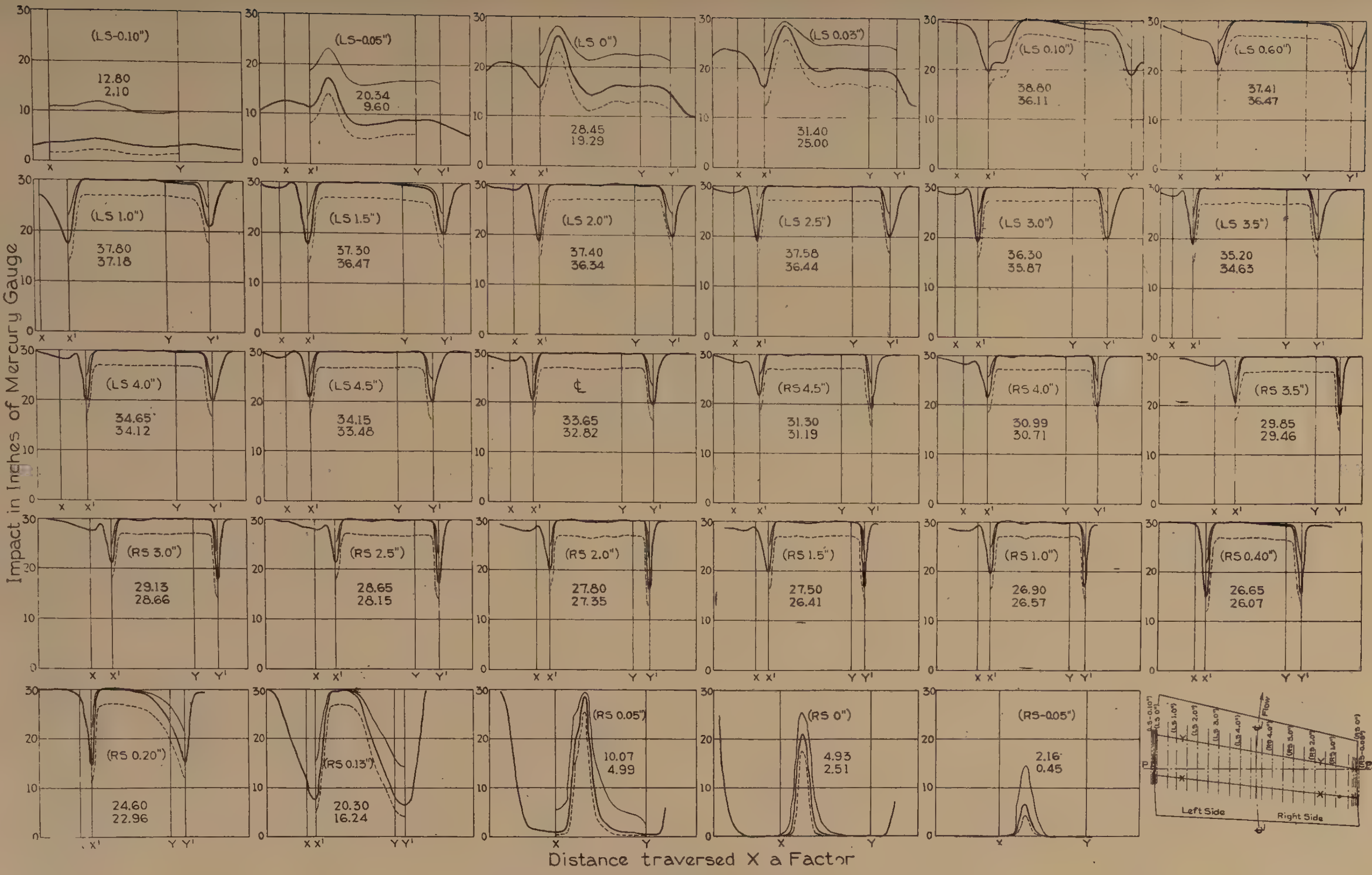

Fig. 7. SET OF IMPACT TRAVERSES ON AN EFFICIENT TYPE OF NOZZLE

The heavy or middle curves are curves of impact pressure as obtained on the plotting machine. The dotted or lower curves represent the actual energy and the lower number gives its value; the upper curves represent 100 per cent energy and the upper number gives its value. The ratio of these values gives the efficiency of any particular traverse. The dimensions in parentheses give the distance of the traverses from the nearest side of the nozzle as indicated in the key at the bottom right is then clamped on the test stand and blown at the proper velocity, generally about 1200 ft. a second. The air blows away most of the paint and streaks the remainder out into fine lines in the direction of flow with clear places in between. In about a minute when the desired consistency of lines is obtained, the flow is stopped instantly with a clapper valve. The model is removed and the interior filled with plaster of paris which, when it hardens, absorbs the lines. By taking the model apart the cast can be removed and lacquered, thereby obtaining a permanent record of the stream-line flow through the model as well as the shape that produced that flow. Ever since turbines were first designed, stream-line flow and eddies have been talked about a great deal; consequently, this method is of immense value in showing what and where the eddies actually are, thereby eliminating guess-work and much loose talking and enabling real improvement in design to be made.

The flow casts of the first type nozzle show that the flow is actually backward in places and that in general the big diameter side of the nozzle is filled with a large spiral eddy. The impact traverses over the portion of discharge fed by this eddy come up to less than 50 per cent of their full value. This is significant since an impact traverse is run throughout the interior of the jet while the flow cast shows only the flow on the surface of the plates and walls. Therefore the traverses prove that when this flow, as indicated by lines on the flow cast, is properly analyzed it can be interpreted as indicating the flow conditions throughout the center of the jet.

Fig. 8 is a photograph of the impact traverses on the first nozzle cut out of cardboard and mounted in their proper relative positions and lined up with their flow cast. Threads indicate the 100 per cent value of impact pressure. In general, it will be seen that the traverses do not come up to maximum, that the partition dips are wide and deep, and that there are secondary dips in the maximum portion of the traverses. Also, toward the back in the region occupied by the big eddy, the traverses make no pretense of coming up to maximum.

Comparison of Two Nozzles

Contrasting with the first nozzle is the second nozzle whose traverses are shown in Fig. 7. The flow casts in Figs. 11 and 13 show that the good traverses are due to perfect stream-line flow in the nozzle.

Fig. 9 shows the flow cast lined up with its set of impact traverses. The dips are narrow and no threads are needed to show the maximums.

From the foregoing it is evident that the second nozzle is a considerable improvement over the first, but the question to be answered is: "How much is this improvement in per cent?" The answer is obtained by applying a method of graphical triple integration to the impact traverses. Briefly, the initial temperature and pressure are known and the final static pressure is atmospheric. If the impact pressure equals the initial pressure or in other words comes up to maximum, the usual equations for the discharge of an elastic fluid from an orifice can be used to compute the mass and energy discharged per unit area. If the impact pressure is less than maximum, a similar solution for mass and energy is possible if it is assumed that all of the initial energy that fails to show up as observed energy has been used to reheat the discharging air at atmospheric pressure. Therefore, in a region of low impact pressure there will be less mass and less energy per unit area per second for two reasons. The velocity of flow is less and the density is less.

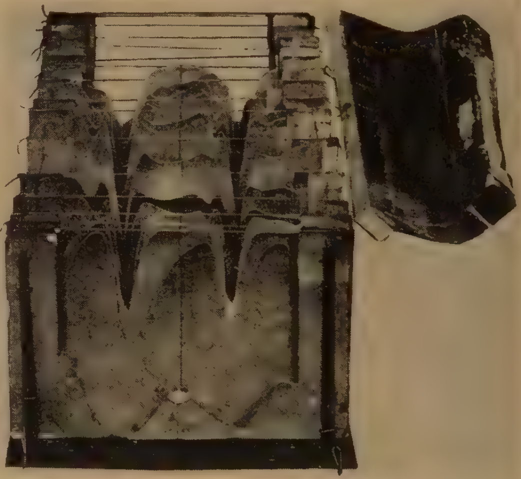

Fig. 8. Inefficient Type of Nozzle, Set of Traverses Cut Out and Assembled, and Lined up with Their Stream-line Cast. Threads show 100 per cent values of impact pressure

Celluloid templates with impact pressure as an argument are used to draw in curves of mass and energy that are roughly parallel to the curve of impact pressure. These curves can be seen in Figs. 6 and 7. The mass curve is the light line and the energy curve the dotted line. The area of the mass curve when multiplied by scale factors gives the total mass discharged per unit width. If this mass of air had expanded from its original pressure and temperature to the final atmospheric pressure with an efficiency of 100 per cent, it would have set free an amount of energy that is called the 100 per cent energy. Consequently, the mass is multiplied by the 100 per cent energy per unit mass to obtain the 100 per cent energy. The area of the energy curve when multiplied by scale factors is the actual energy. Then the ratio of the two, the actual energy divided by the 100 per cent energy, is the efficiency of the traverse.

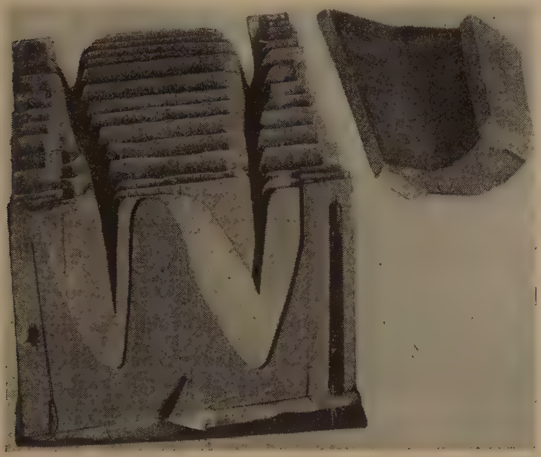

Fig. 9. Efficient Type of Nozzle, Set of Traverses Cut Out and Assembled, and Lined up with Their Stream-line Cast

The efficiency of the nozzle is found by plotting the values of actual energy and 100 per cent energy found from each traverse as ordinates and the traverse spacing as abscissas, thereby making a loss diagram as shown in Fig. 14. The area under the lower curve is the actual energy and the area under the top curve is the 100 per cent energy, and the ratio of the two is the efficiency of the nozzle. The area between the two curves, therefore, is the loss. A comparison of the loss diagram in Fig. 14 with the lower flow cast in Fig. 10 shows that the excessive loss near the left side is due to the eddy. The loss diagram for the second nozzle has no excessive loss at this place (see Fig. 15) and the cast also shows no eddy (see Fig. 11). A comparison of the efficiencies of the two nozzles shows that the first nozzle had a total efficiency of 82.9 per cent and the second nozzle a total efficiency of 96.6 per cent, a gain of 13.7 per cent.

Other Typical Tests

Fig. 16 shows flow casts of two additional nozzles lined up with their loss diagrams and again proves that the side eddy causes loss and that certain lines on the surface of the cast can be interpreted as showing loss throughout the jet.

Figs. 17 and 18 show flow casts of long buckets and indicate the disturbed character of flow through a bucket. The flow is backward in many places and the ends of the bucket are filled with large eddies.

Fig. 1 shows the set-up for measuring the angle of discharge. The design of the double-vane angleometer is the result of much experimenting with various shapes of vane, and the vane shown has been the only type that has been found to work properly at high velocity. Flat vanes shaped like a flag split a high-velocity jet and read the angle of one current of flow or the other current of flow. A double-vane angleometer has its active edge inclined to the impinging jet so that each increment of edge has an undisturbed stream striking it. Sufficient torque is developed along the line of the active edge to turn the vane and so indicate the angle. The angle is read by means of a telescope with cross hairs.

Valves, right-angle turns, exhaust hoods, and the like are tested by measuring the flow through them for any pressure ahead of them and comparing their flow curves with the flow curve of an orifice of equal area. Fig. 19 shows two views of a model 30,000-kw. exhaust hood. The view at the left directly into the preliminary conditions or annular opening is a reflection in a mirror. The struts are removable so that their effect on exhaust hood loss can be determined.

From the foregoing it will be seen that these methods of investigation have many advantages which previous methods have lacked.

Advantages of Air Test Method

(1) The performance of each part of the nozzle is observed in detail, and so cause and effect can be isolated in a way that is impossible in any nozzle-testing machine which gives only the final result and from

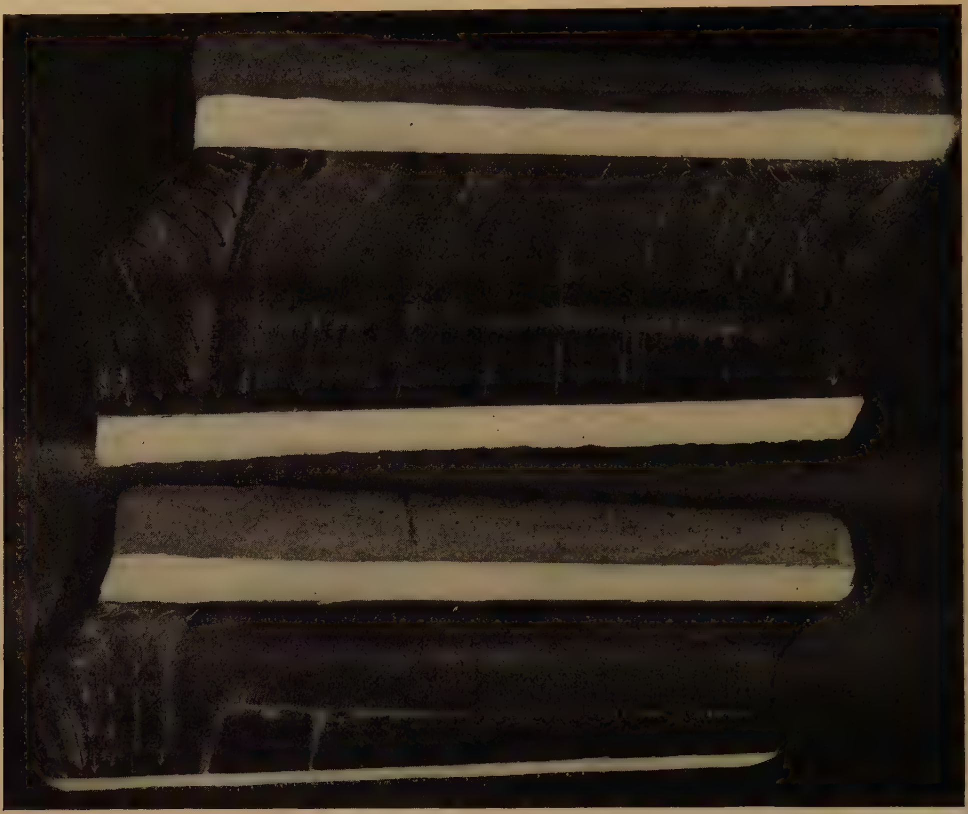

Fig. 10. Flow Casts of Inefficient Nozzles

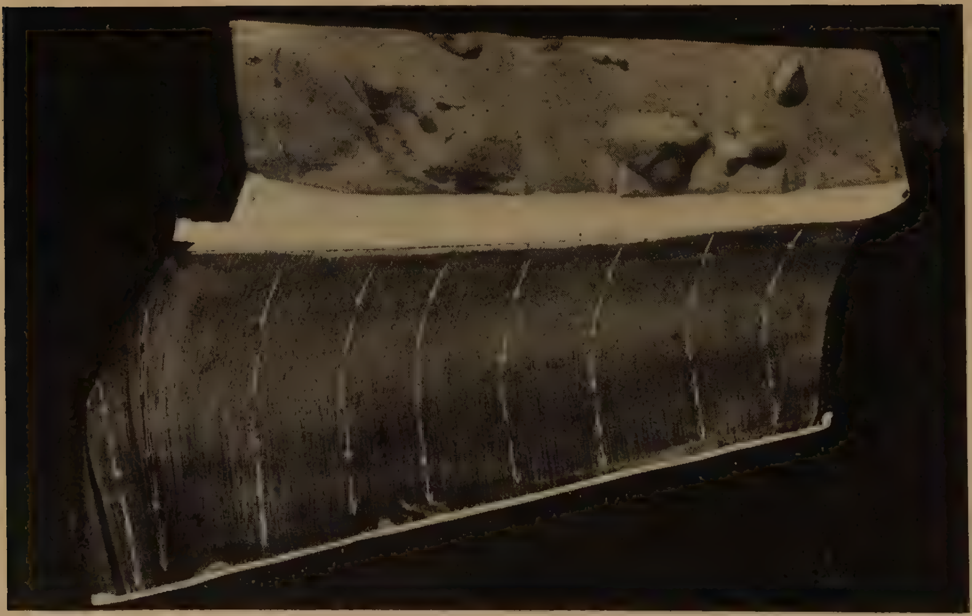

Fig 11. Flow Cast of Efficient Nozzle

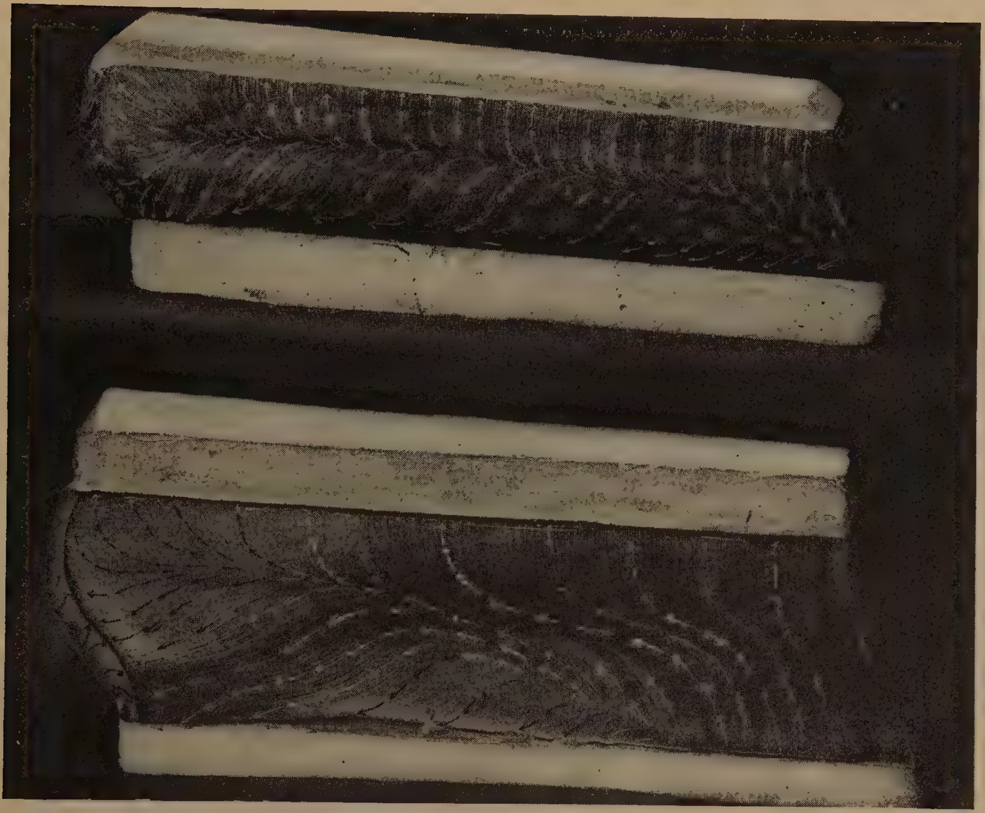

Fig. 12. Flow Casts of Inefficient Nozzles

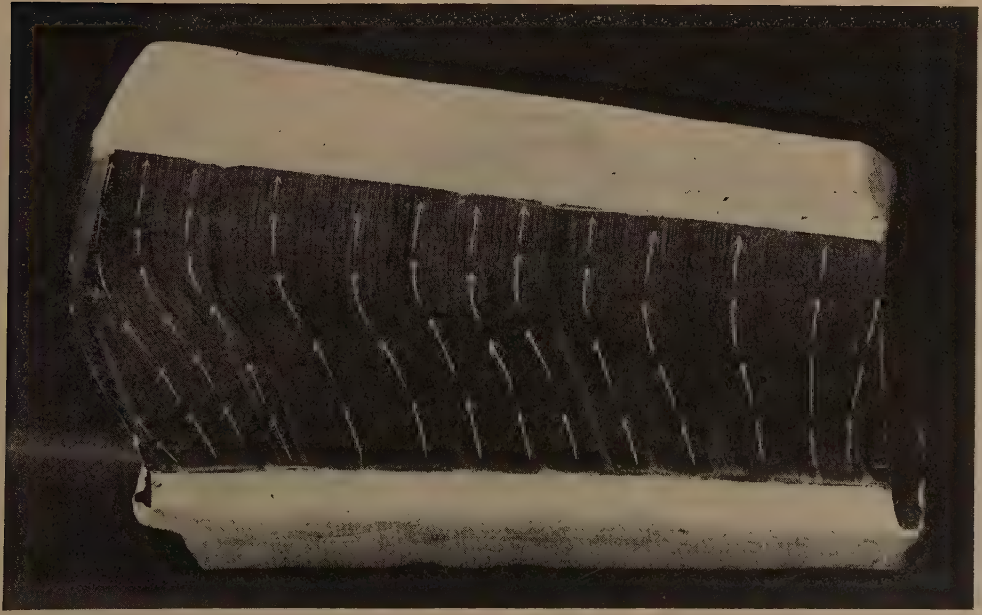

Fig. 13. Flow Cast of Efficient Nozzle

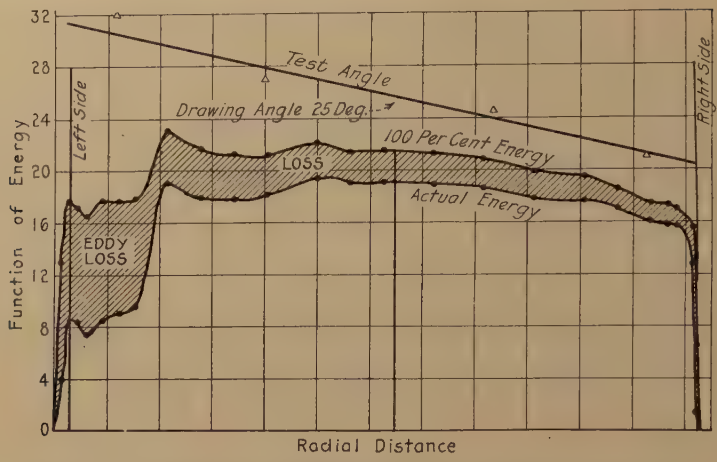

Fig. 14. Loss Diagram of Inefficient Nozzle. Total efficiency 82.9 per cent

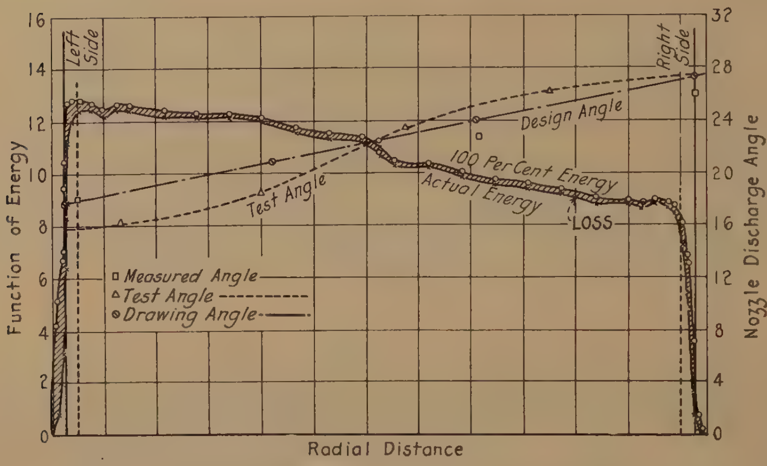

Fig. 15. Loss Diagram of Efficient Nozzle. Total efficiency 96.6 per cent

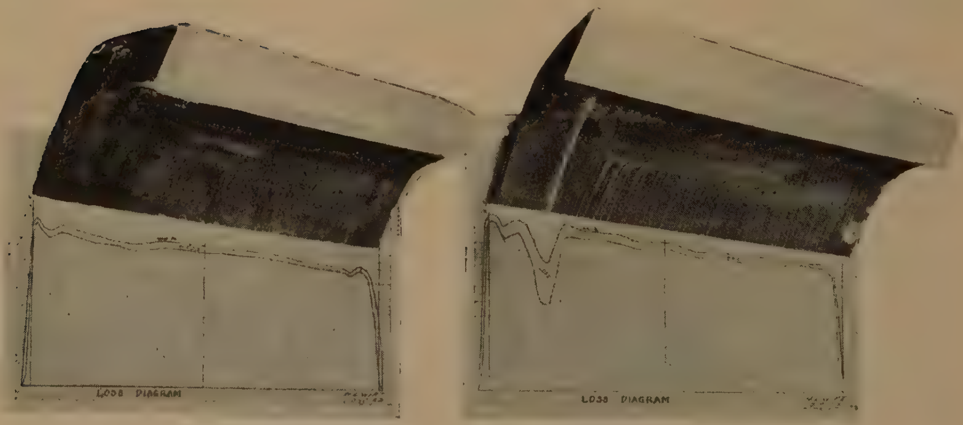

Fig. 16. Flow Casts and Loss Diagrams without and with Side Eddy

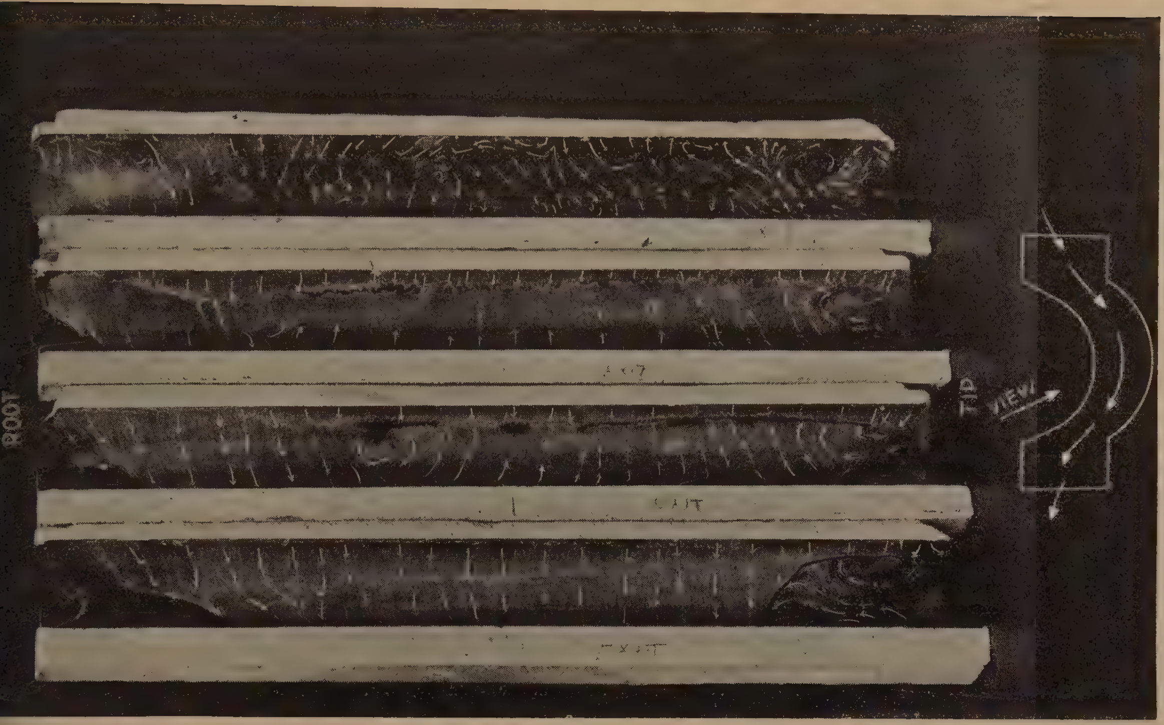

Fig. 17. Flow Casts of Buckets Showing View of Entrance Flats

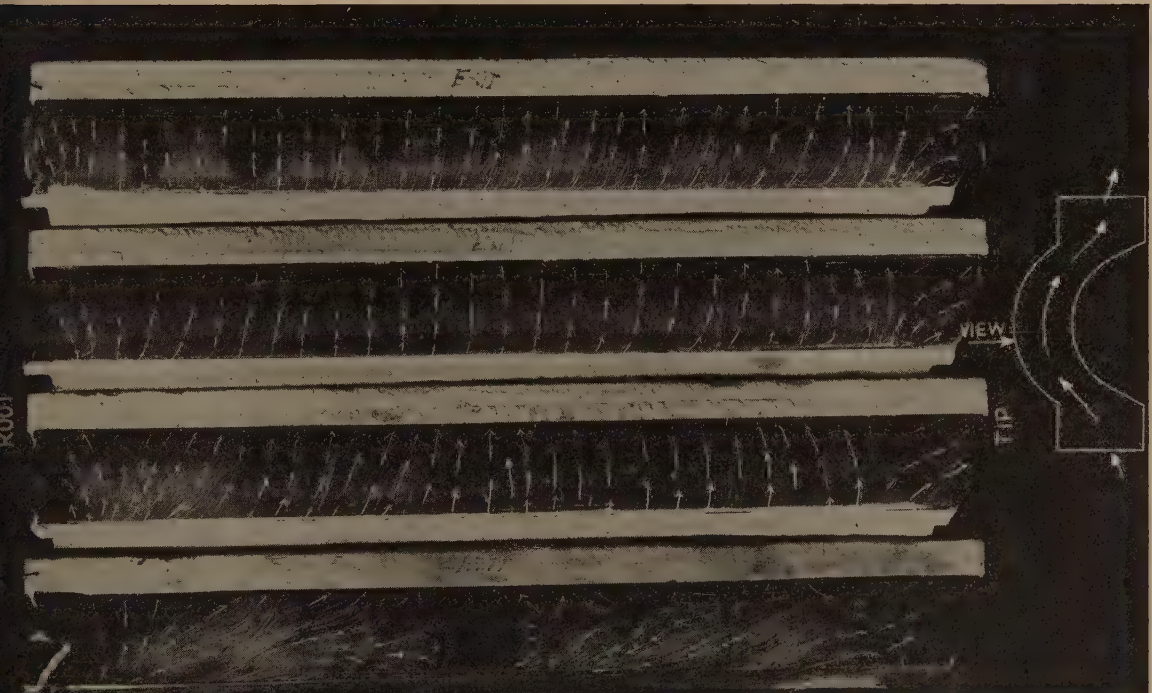

Fig. 18. Flow Casts of Buckets Showing View of Concave Surface or Convex Cast Surface

the nature of its operation cannot differentiate between the good and bad features that contribute to that result.

(2) Actual diaphragms of a turbine under construction can be tested and their relative performance in the turbine predicted. The diaphragms are tested by blowing three or five nozzle passageways preceded by their proper preliminary conditions. Diaphragms set up in this way have had changes made in the nozzles while on the test stand and efficiency tests made after each change. The whole diaphragm was then altered to the most efficient condition and the gains indicated were confirmed by water rates on the turbine.

(3) Nozzles, buckets, etc., are tested by measuring the loss directly, that is, the distance between 95 and 100 per cent. Other methods measure the effect from 0 to 95 per cent and take the result from 100 per cent to find the loss. Consequently, the air test gives highly accurate differentials of values of efficiency that are near 100 per cent.

(4) The models for test can be made cheaply and quickly from easily worked materials like wood, plaster, and white metal, and slight alterations can be made with solder or plaster. With a new feature of design, it is no longer necessary to follow a "hunch," but instead a model can be constructed and tested within a week and in almost all cases a definite answer can be given as to how much gain or loss will be caused by the change. This feature is of immense value in developing an art like turbine design where considerable time separates conceived ideas and test results, and where in most cases there could be no comparable test results because of the many new features in every succeeding design.

(5) The performance of large parts of a turbine, for instance exhaust hoods, may be investigated in small-size models where it is both impracticable and expensive to experiment with the actual turbine.

(6) The air-test method gives an independent check on results obtained by other methods of testing such as steam-reaction nozzle tests and water-rate tests on turbines.

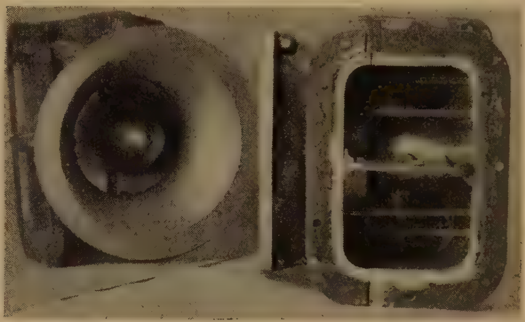

Fig. 19. Model of 30,000-kw. Exhaust Hood

When properly controlled, the three methods have been found to give remarkably interchangeable results. Thus a gain indicated by the turbine air test can be confirmed by a steam-reaction nozzle test and definitely proved by a turbine water-rate test. Thus, if the air test shows a gain of say 3 per cent, a gain of about 3 per cent will be shown by the other two independent methods of testing.

In conclusion, all of the foregoing appears so simple and straightforward that it would be well to point out that a few isolated experiments are misleading and dangerous. For instance, nozzle and bucket action are so interrelated that tests of either one alone may give wrong conclusions. Therefore, the background of all the previous work done, the 1100 models tested, has to be freely drawn upon in order to design models properly for test and to interpret test results correctly.

Electric Trucks for Store Door Delivery of Freight

By R. Macrae

Electric Vehicle Engineer, Commonwealth Edison Company, Chicago

Most of us have at some time received a freight shipment and, in making the necessary special arrangements for its delivery from the freight depot, have experienced an annoyance and cost all out of proportion to these last few miles of transportation. Thus it is with merchants, though they naturally fare somewhat better because their demands for service are regular. How much better it would be if it were only necessary to engage one carrier to bring the goods first miles by rail then blocks by truck to the store door. For this service the railroad is the logical operator, and in the following article Mr. Macrae explains how attractive is the electric truck proposition as the adjunct of the freight train.—Editor.

The railroad companies have been considering the matter of store door delivery of freight for some time but nothing has been done so far to put it into effect. It is generally conceded, however, that such an arrangement is the only satisfactory solution of one of the most important transportation problems.

No one seems to be entirely satisfied with the present way in which freight passes through railway depots. Many merchants who formerly hired teams to carry their goods to the railways now ship direct to destination by motor trucks. Sometimes it costs more to make shipments in this way, but delays are avoided and also the inconvenience of having to deal with two or three different carriers.

There is a limit, however, to the distance over which heavy loads can be carried economically on rubber tires. What the limiting distance is depends on circumstances. It is undoubtedly less than it is now generally supposed to be.

When merchandise is shipped by rail, the railroad companies carry it part way to its destination and then notify the customer to carry it the remainder of the way himself. The result is that the owner of the merchandise frequently has to pay more for carrying it a few blocks from the railroad depot to his place of business than he has to pay for carrying it several hundred miles by rail. Besides, there are always delays. Even when the shipper has a railway spur to his warehouse, it often takes a day or two to get a car switched to his loading platform.

It cannot be said, however, that those who are now engaged in hauling freight in cities are getting too much for their services. On the contrary, many of them are being forced out of business. They cannot get work for their horse-drawn equipment because the horses are too slow, obstruct traffic, and are in other ways objectionable on city streets. When they try to do the work with motor trucks they generally find out, after they have bought two or three trucks, that they do not know how to keep them in working order. Repairs which would amount to comparatively little, if made with an equipment capable of taking care of a large number of cars, often amount to more than the trucks can earn when only a few trucks are operated. In other words, the demands of transportation have outgrown not only the capacity of the horse-drawn equipment but have also outgrown the methods of operation that were successfully employed when horses were able to take care of the work.

When horse-drawn trucks were the only trucks available for what is called depot work, there was some excuse for having to deal with two different carriers with regard to the transportation of the same load of merchandise. The operation of two or three teams has nothing in common with the operation of a railroad; and it was obviously to the advantage of the men who paid the freight that the different carriers should confine themselves to the work with which they were familiar.

The development of motor trucks, however, has changed the situation. Team owners who are now operating motor equipment are doing but little to reduce the cost of transportation to the public. The reason is that they have neither the experience nor the organization necessary to get the best results from motor equipment.

It is to the railroads, therefore, that we must look for the economical operation of motor trucks and for improved methods of transporting merchandise. The railroads have the organization, the equipment and the necessary experience, and it is only natural that they should carry to its destination the freight that has passed over their lines. By collecting and delivering freight at the store door, they can add to their revenue and at the same time give better service to their customers.

One of the reasons that the railroad companies have not before undertaken to deliver freight in the cities was, no doubt, a difference of opinion as to the best type of equipment to use. Until quite recently, every truck manufacturer claimed that his truck was the only one suitable for depot work. It is now generally admitted, however, that electric trucks are not only the most economical to use for all work of this kind but that they are also the most desirable in other ways. To support this claim, it is only necessary to point to the fact that some of the most progressive manufacturers of gasoline trucks are now making electric trucks for city use while continuing to make gasoline trucks for long-distance work.

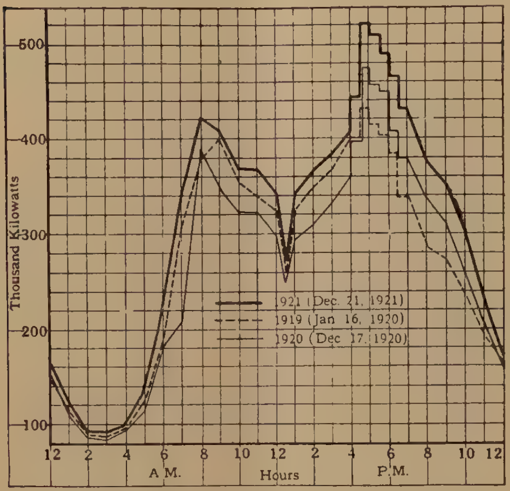

Fig. 1. Diagram Showing Energy to Spare for Charging Electric Trucks, about 1,800,000 kw-hr. from 12 to 6 a. m.

The transportation manager of a company using a large number of motor trucks says with reference to electrics: "I used to think that horse-drawn trucks were more economical for depot and short-haul work, but experience has changed my opinion."

A favorite argument with those who claim that horse-drawn trucks should be used for depot work is that the investment standing idle, when waiting at the depot, is less for horse-drawn trucks than for motor trucks. A simple calculation however will show, when the maintenance of the horses is taken into consideration as well as the interest on the investment, that we could better afford to have two electric trucks standing idle than one horse-drawn truck, even if we got the horses for nothing.

Electric trucks are especially adapted for the work that the railroad companies have to do because the electrics may be charged at the loading platforms of the freight depots while left standing there overnight. The only equipment necessary is the apparatus which many railroad companies already have for charging electric platform trucks. Repair shops would of course be needed, but in some places the electric trucks could be taken care of in the railroad repair shops.

Any outside organizations that started to do inter-terminal and store door delivery of freight would have to maintain their own garages.

In every large city there are miles of space at the loading platforms in the freight yards that could be used to accommodate electric trucks. Chicago, for example, has twenty-five different railroad freight depots. A rough estimate of the value of this space at the usual garage space rates would be between one and two million dollars per year.

During the night, the loading space at the freight depots in the different cities is bringing in no return to the railroad companies; while the electric central stations in these cities have enough power to spare at night to take care of any demand that the operation of electric trucks could possibly make on them.

The central station, whose load curve is shown in Fig. 1, could for example supply 1,800 000 kw-hr. of energy for charging batteries between midnight and 6 a. m. This amount would be sufficient to charge more than 70,000 trucks taking an average of 25 kw-hr. each.

There are several large electric trucks now on the market suitable for inter-terminal and store door delivery of freight, including those of short turning radius which insures easy maneuvering in congested quarters. If other features are needed to fill local requirements, they can readily be incorporated in the design of special electric trucks.

Study of Crystal Structure and Its Applications

PART II

CRYSTAL LATTICES

By Dr. Wheeler P. Davey

Research Laboratory, General Electric Company

In this second installment of a series of articles on crystal structure analysis and its applications in theoretical and industrial fields, the author describes and illustrates the different ways in which crystal lattices are built up. By means of relationships between the characteristic equations for the different types of crystals, the connections between the crystal families are shown. The author explains the ways in which the complete lattices are built up from the small units, and shows how each of these units has its effect on the properties of the entire structure. An idea of the applications of crystal analysis is given in the calculation of density from measurements determined by x-ray methods.—Editor.

Cubic Lattices

If a crystal such as rock salt (Na Cl) is crushed, it is found that the fragments have the same angles between their faces that the original crystal had. Experiments of this sort indicate that the external form of a crystal results from a systematic arrangement of the atoms of which the crystal is composed. As a result of studies on x-ray diffraction patterns of crystals, this assumption is now universally accepted. If the crystal is cubic in exterior form, or if it is bounded by a geometrical figure which may be derived from a cube, the simplest atomic arrangement would be to have atoms at the intersections of an imaginary cubic lattice work, as in Fig. 3. Such a crystal might be thought of as built up of unit-cubes, so placed together that each one shares its corners, edges, and faces with its neighbors. It is at once evident that this structure requires each atom in the interior of the crystal to belong to eight unit-cubes at once, so that, if the lattice were of infinite extent, it would require one atom per unit-cube.

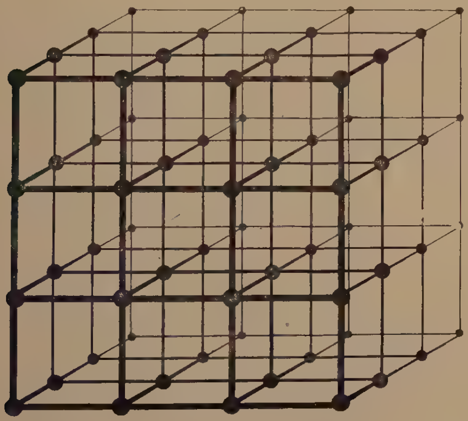

Fig. 3. Simple Cubic Lattices

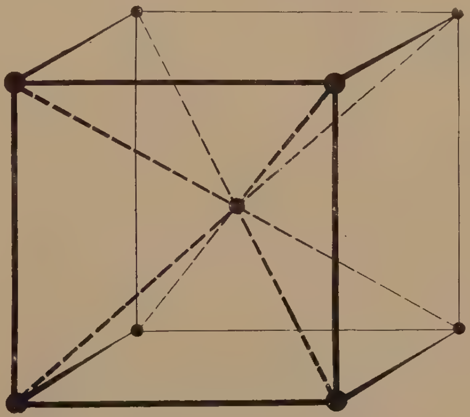

Fig. 4. Unit-cube of Body-centered Cubic Lattice

Not all "cubic" crystals have this simple structure. Additional atoms may be placed in symmetrical positions in the lattice to give more or less complicated structures which still retain many of the cubic characteristics of the simple cubic crystal. For instance, an additional atom may be placed at the center of each unit-cube. Such a unit-cube, shown in Fig. 4, is called a "body-centered" cube. It is evident that, if this lattice were of infinite extent, it would require two atoms per unit-cube. A body-centered cubic lattice may be thought of as composed of two interpenetrating simple cubic lattices so placed with respect to each other that the corners of the unit-cubes of one lattice lie at the centers of the unit-cubes of the other lattice.

A more complicated form is the "face-centered" cubic lattice, shown in Fig. 5. The unit-cube has an atom at each corner as in the simple cube, and in addition has an atom at the center of each face. As before, the eight atoms at the corners contribute a total of one atom to the unit-cube. The atoms at the centers of the faces each belong to two unit-cubes, so that these six atoms contribute a total of three atoms to the unit-cube. The face-centered cubic lattice therefore has a grand total of four atoms per unit-cube. Such a lattice may be thought of as composed of four interpenetrating simple cubic lattices.

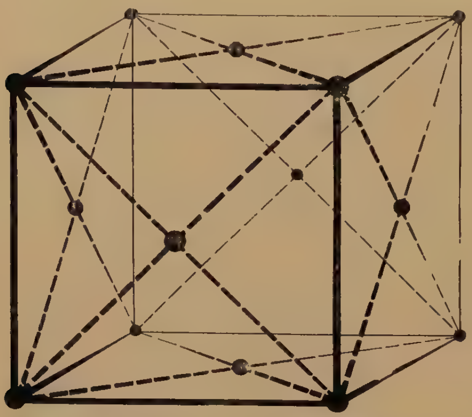

Fig. 5. Unit-cube of Face-centered Cubic Lattice

A still more complicated structure is the "diamond" cubic lattice—so called because it represents the arrangement of the carbon atoms in the diamond. This lattice is most easily described as composed of two interpenetrating face-centered cubic lattices of equal size, placed so that the corners of the unit-cubes of one lattice lie on the body-diagonals of the other lattice, at a distance from the end of the diagonal equal to one-fourth the length of the diagonal. The effect is that of putting four additional atoms inside a face-centered cube. These additional atoms are shown in Fig. 6, but for the sake of clearness only the corners of the unit face-centered cube are shown. The complete unit diamond cube is shown in Fig. 7, which is a superposition of Figs. 5 and 6.

All dimensions of a cubic crystal are expressed in terms of the length of the side of its unit-cube. The origin of co-ordinates is put at the center of one atom and the co-ordinate axes are chosen so as to pass through the edges of the unit-cubes. Then the position of any atom in a simple cubic lattice is given by the general co-ordinates:

$$m,\ n,\ p$$

each of which may be any exact multiple (indicating zero) of the side of the unit-cube.

The corresponding general co-ordinates for the atoms of a body-centered cube are:

$$\begin{array}{lll} m, & n & p \\ m+\frac{1}{2}, & n+\frac{1}{2}, & p+\frac{1}{2} \end{array}$$

For a face-centered cube they are:

$$\begin{array}{lll} m, & n, & p \\ m+\frac{1}{2}, & n+\frac{1}{2}, & p \\ m+\frac{1}{2}, & n, & p+\frac{1}{2} \\ m, & n+\frac{1}{2}, & p+\frac{1}{2} \end{array}$$

For a diamond cube they are:

$$\begin{array}{lll} m, & n, & p \\ m+\frac{1}{2}, & n+\frac{1}{2}, & p \\ m+\frac{1}{2}, & n, & p+\frac{1}{2} \\ m, & n+\frac{1}{2}, & p+\frac{1}{2} \\ m+\frac{1}{4}, & n+\frac{1}{4}, & p+\frac{1}{4} \\ m+\frac{3}{4}, & n+\frac{3}{4}, & p+\frac{1}{4} \\ m+\frac{3}{4}, & n+\frac{1}{4}, & p+\frac{3}{4} \\ m+\frac{1}{4}, & n+\frac{3}{4}, & p+\frac{3}{4} \end{array}$$

Interplanar Distances in Cubic Crystals

It is evident from Fig. 3 that the atoms in a crystal may be regarded as lying in planes. If a model of a simple cubic crystal is viewed in a direction parallel to the cube face, all the atoms are seen in parallel planes (the 1 0 0 planes). The distance between the planes is equal to the length of the side of the unit-cube. If the same model is rotated 45 deg., using one edge of the cube as an axis, these same atoms appear to lie in parallel planes (the 1 1 0 planes) whose distance apart is $1/\sqrt{2}$ times the side of the unit-cube. Still other orientations of the crystal show other families of planes. Since the number of atoms involved is necessarily the same in all orientations of the same crystal, we have the general rule that "*in a given crystal, the atomic population of a plane is directly proportional to the interplanar distance.*"

The intercepts of a family of parallel planes are all multiples of the intercepts of some one plane in that family. For instance, the planes whose intercepts are:

1	$\frac{1}{3}$	$\frac{1}{5}$
2	$\frac{2}{3}$	$\frac{2}{5}$
3	1	$\frac{3}{5}$
4	$1\frac{1}{3}$	$\frac{4}{5}$
—	—	—
—	—	—

are all parallel to each other. The Miller indices⁽²²⁾ of a family of planes are always expressed in terms of the reciprocals of the simplest indices in the whole family. Thus all the planes whose intercepts were just given are called 1 3 5 planes.

In a cubic crystal, the distance from an atom whose co-ordinates are x_1, y_1, z_1, to a plane whose Miller indices are h, k, l, is given by⁽²³⁾

$$d_1=\frac{hx_1+ky_1+lz_1-1}{\sqrt{h^2+k^2+l^2}} \tag{17}$$

The interplanar distance between members of the same family is the smallest value of d_1 that regularly repeats itself. This may be found by systematically substituting numerical values for x_1, y_1, z_1, and observing the differences between successive values of the numerator and the periodicity of these differences. If these differences are represented by s, and if d is the interplanar spacing, we have from equation (17)

$$d=\frac{s}{\sqrt{h^2+k^2+l^2}} \tag{18}$$

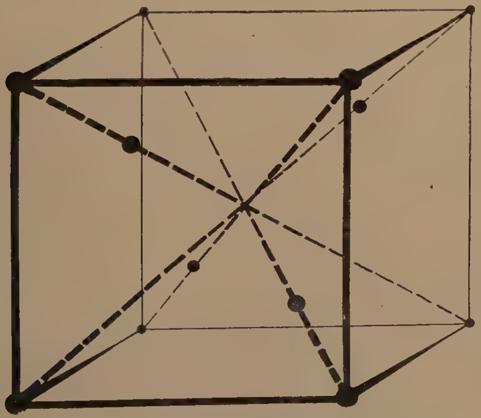

Fig. 6. Structure of the Interior of the Unit-cube of a Diamond Cubic Lattice

Since the co-ordinates of the atoms of a simple cubic lattice are all integers, and since h, k, and l are necessarily integers, it is evident that the successive numerators will differ from each other by unity for all planes of a simple cubic lattice. The co-ordinates of the atoms in a body-centered cubic lattice may be either integers, or integers increased by ½. For the cube faces (1 0 0 planes) $h=1$, $k=0$, $l=0$, and the successive numerators of equation (17) differ from each other by ½. For the 1 1 0 planes, the successive numerators differ by unity. Considerations of this sort lead to the following rules for the value of s in equation (18).

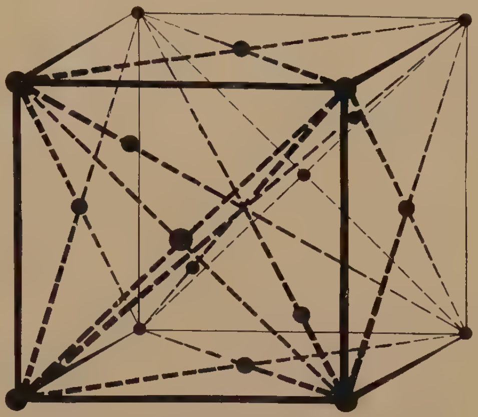

Fig. 7. Unit-cube of Diamond Cubic Lattice

Simple cube: s always $=1$.

Body-centered cube: If all the indices are odd or if only one index is odd, $s=\frac{1}{2}$; otherwise $s=1$.

Face-centered cube: If only one or two indices are odd, $s=\frac{1}{2}$; otherwise $s=1$.

Diamond cube: If only one index is odd, $s=\frac{1}{4}$; if only two indices are odd, or if the indices are even but not divisible by 4, $s=\frac{1}{2}$; otherwise $s=1$.

It has been stated that the interplanar distance could be found by studying the *differences and periodicity* in the values for d_1 in equation (17). This is well illustrated in the case of the 1 1 1 plane in the diamond cube. If the indices of a family of planes are all multiplied by 2, so as to give indices $2h$ $2k$ $2l$, then equation (17) gives an interplanar spacing of half that found for the planes h k l. The interplanar spacing of planes h k l would give, with a given wavelength of x-rays, a diffraction pattern of the second order at the same angle as the first-order pattern of the $2h$ $2k$ $2l$ planes. The third-order pattern of h k l is at the same angle as the first order of $3h$ $3k$ $3l$, etc. Planes whose indices contain a common

---

(22) Part I (Nov., 1924). See page 744.
(23) A. W. Hull, *Phys. Rev.*, *10*, 661 (1917).

factor may or may not be present in a crystal. For instance, the 2 0 0 plane is present in body-centered, face-centered, and diamond cubic lattices, but not in the simple cubic lattices. When actually present, such a plane is commonly called by the simpler indices; thus the 4 4 4 plane is called merely the 1 1 1 plane except when, for some reason, it is necessary to distinguish between the two.

It is evident from the co-ordinates of the atoms in the diamond cubic lattice that the distances from a given atom to successive 1 1 1 planes are

$$\frac{0}{\sqrt{3}},\ \frac{\frac{3}{4}}{\sqrt{3}},\ \frac{1}{\sqrt{3}},\ \frac{1\frac{3}{4}}{\sqrt{3}},\ \frac{2}{\sqrt{3}},\ \frac{2\frac{3}{4}}{\sqrt{3}},\ \text{etc.}$$

This means that 1 1 1 planes in a diamond cube show a periodicity such that the spacings are alternately $\frac{\frac{3}{4}}{\sqrt{3}}$ and $\frac{1}{\sqrt{3}}$. Such a structure may be thought of as being composed of two families of 1 1 1 planes, the members of each family having an interplanar distance of $\frac{1}{\sqrt{3}}$. If x-rays of a given wavelength strike the 1 1 1 planes at the appropriate angle of incidence, diffraction of the first order will occur from both these two families of planes. The two diffracted beams will not be exactly in phase with each other, but they will be nearly enough in phase to give a resultant of considerable intensity. The rule for s as given for the diamond cubic lattice is therefore worded so that $s=1$ for the 1 1 1 plane. Hence the interplanar spacing agrees with that found from the experimental diffraction pattern with the aid of equation (1).*

In the case of the diffracted beam of the second order, the periodicity of the 1 1 1 planes in the diamond cube is such as to present interesting complications. The two families of 1 1 1 planes are so spaced with respect to each other that the distance between adjacent members of the two families is ¼ $\left(\frac{1}{\sqrt{3}}\right)$, thus giving the effect of a family of 4 4 4 planes (see Fig. 8). The diffracted beam of the second order from the 1 1 1 planes (first order from a fictitious family of 2 2 2 planes) is destroyed by interference with the first-order beam from these 4 4 4 planes, so that this beam is absent from the diffraction pattern of a diamond cube. The effect is the same as if the spacing of these fictitious 2 2 2 planes had been made half as great. The rule for s is therefore so worded as to make $s = \frac{1}{2}$ for the 2 2 2 plane.

Tetragonal and Orthorhombic Lattices

Just as the structure of a crystal having cubic symmetry is accounted for by assuming that the atoms lie on some sort of an imaginary cubic framework, in the same way it is assumed that in crystals belonging to the tetragonal system the atoms lie on an imaginary tetragonal framework. The bases of the prisms of which this framework is composed are squares. The vertical sides (direction of the Z-axis) may be either longer or shorter than the sides of the base, depending upon the material of which the crystal is composed.

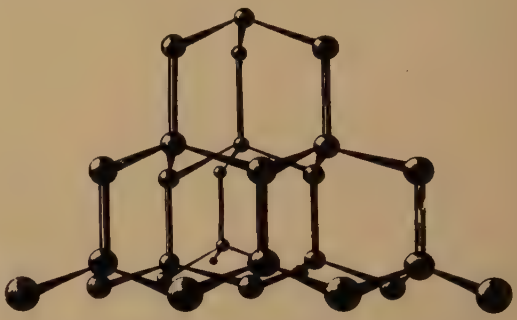

Fig. 8. Diamond Cubic Lattice Showing 1 1 1 Planes

The dimensions of a tetragonal crystal are expressed in terms of the lengths of the sides of the unit tetragonal prism. If the sides of the base of the unit-prism are called a and b, and if the altitude is c, then $a=b\neq c$. The unit of length along the Z-axis is therefore different from the unit of length along the X- and Y-axes. The ratio of these two units of length $\left(\frac{c}{a}=C\right)$ is called the "axial ratio." The advantage of this sort of units of length is that it permits the use of equations for calculating interplanar distances which closely resemble those used in the cubic lattices. Corresponding to equation (17) for a cubic lattice, we have for the distance from any atom to the plane $h\ k\ l$:

$$d_1=\frac{hx_1+ky_1+lz_1-1}{\sqrt{h^2+k^2+(l/C)^2}} \qquad (19)$$

---

* For convenience of reference, equations (1) to (16) will be found in Part I (Nov., 1924, p. 742).

Similarly, equation (18) is replaced by

$$d=\frac{s}{\sqrt{h^2+k^2+(l/C)^2}} \tag{20}$$

Crystals belonging to the orthorhombic system are assumed to have their atoms arranged on an imaginary framework such that the unit-prism has rectangles for bases and sides. The edges of this unit-prism along the X-, Y-, and Z-axes are a, b, and c respectively, and $a \neq b \neq c$. Such crystals have two axial ratios, $a/b=A$ and $c/b=C$, and equations (17) and (18) become

$$d_1=\frac{hx_1+ky_1+lz_1-1}{\sqrt{(h/A)^2+k^2+(l/C)^2}} \tag{21}$$

$$d=\frac{s}{\sqrt{(h/A)^2+k^2+(l/C)^2}} \tag{22}$$

Monoclinic and Triclinic Lattices

In the three crystal systems so far considered, the X-, Y-, and Z-axes were mutually perpendicular to each other. In crystals which, because of the symmetry of their exterior, are assigned to the hexagonal, monoclinic, or triclinic systems, this restriction no longer holds. If we call the angles between the YZ-, XZ-, and XY-axes λ, μ, and ν respectively, then:

In the hexagonal system, $\lambda=\mu=90$ deg., $\nu=120$ deg., and $a=b=c$

In the monoclinic system, $\lambda=\nu=90$ deg. but μ may have any value and $a \neq b \neq c$

In the triclinic system, $\lambda \neq \mu \neq \nu$, and $a \neq b \neq c$.

Let p be the length of the perpendicular from the origin of co-ordinates to the plane $h\ k\ l$; let l, m, n be its direction ratios; and $\cos\alpha$, $\cos\beta$, $\cos\gamma$ its direction cosines. Then

$$\begin{aligned} \cos\alpha &= hp = l'+m\cos\nu+n\cos\mu \\ \cos\beta &= kp = l'\cos\nu+m+n\cos\lambda \\ \cos\gamma &= lp = l'\cos\mu+m\cos\lambda+n \\ l'\cos\alpha &+ m\cos\beta+n\cos\gamma=1 \end{aligned} \tag{23}$$

but

$$d_1=x_1\cos\alpha+y_1\cos\beta+z_1\cos\gamma-p \tag{24}$$

where d_1 is as before the distance from any atom in the crystal to the plane $h\ k\ l$. Equations (23) and (24) give equation (25):

$$d_1=\frac{hx_1+ky_1+lz_1-1}{\left[\dfrac{h/A\begin{vmatrix} h/A & \cos\nu & \cos\mu \\ k & 1 & \cos\lambda \\ l/C & \cos\lambda & 1 \end{vmatrix}+k\begin{vmatrix} 1 & h/A & \cos\mu \\ \cos\nu & k & \cos\lambda \\ \cos\mu & l/C & 1 \end{vmatrix}+l/C\begin{vmatrix} 1 & \cos\nu & h/A \\ \cos\nu & 1 & k \\ \cos\mu & \cos\lambda & l/C \end{vmatrix}}{\begin{vmatrix} 1 & \cos\nu & \cos\mu \\ \cos\nu & 1 & \cos\lambda \\ \cos\mu & \cos\lambda & 1 \end{vmatrix}}\right]^{1/2}} \tag{25}$$

No simplification of equation (25) is possible for the triclinic lattice. For the monoclinic lattice, equation (25) becomes

$$d_1=\frac{hx_1+ky_1+lz_1-1}{\sqrt{\dfrac{(h/A)^2+(l/C)^2-2\dfrac{hl}{AC}\cos\mu}{\sin^2\mu}+k^2}} \tag{26}$$

For the cubic lattice $\lambda=\mu=\nu=90$ deg. and $a=b=c$ so that equation (25) simplifies at once to equation (17). Similarly equations (19) and (21) may be obtained for the tetragonal and orthorhombic lattices. For the hexagonal system of lattices equation (25) becomes:

$$d_1=\frac{hx_1+ky_1+lz_1-1}{\sqrt{4/3(h^2+hk+k^2)+(l/C)^2}} \tag{27}$$

Corresponding to equation (18), we have

$$d=\frac{s}{\sqrt{4/3(h^2+hk+k^2)+(l/C)^2}} \tag{28}$$

Triangular or Hexagonal Lattices

The triangular or hexagonal lattice system received the name "hexagonal" from the fact that certain crystals of this group have the exterior form of a hexagonal prism. However, this name is not sufficiently inclusive because the system is really built up of unit-prisms whose bases are equilateral triangles. If the original name had not the sanction of long usage, it would have been long ago replaced by the more appropriate name "triangular system." Fig. 9 shows how the triangular bases of the unit-prisms (shaded in the figure) fit together so that, under the proper conditions, a hexagonal outline may be obtained. The prisms whose bases are unshaded in Fig. 9 are not regarded as contributing to the structure and are therefore ordinarily omitted from any discussion of the structure of the lattice. This precedent will be followed and only the prisms with shaded bases will be considered.

In the simple triangular lattice the atoms are at the corners of the triangular prisms only. The co-ordinates of the atoms in terms of "hexagonal co-ordinates" (in which the x- and y-axes are 120 deg. apart) are:

$$m, n, p\,C$$

Each atom is shared by six prisms, so that each prism whose base is shaded in Fig. 9 contains a total of one atom. Since, however, in a simple triangular lattice the prisms occupy only half the total volume of the crystal, the net result is as if each unit-prism contributed one-half an atom to the whole structure.

If an additional atom is placed at the body-center of each prism, we have the "hexagonal close-packed" lattice; sometimes called the "triangular close-packed" lattice (Fig. 10). The name comes from the fact that when the axial ratio is 1.633, this structure is one of the two alternative closest packings for spheres of equal size. (The other alternative is the face-centered cube.) The atomic co-ordinates are:

$$m, n, p\,C$$
$$m+\tfrac{1}{3}, n+\tfrac{2}{3}, (p+\tfrac{1}{2})\,C$$

Each unit-prism contributes one atom to the whole lattice.

This lattice may be regarded as being composed of two interpenetrating simple triangular lattices, so placed with respect to each other that a corner of the unit-prism of one lattice lies at the body-center of the unit-prism of the other lattice. It is sometimes convenient to regard this structure as being composed of layers of atoms, each layer corresponding to Fig. 9. These layers are then placed above each other at distances of $\frac{1}{2}\,C$, in such a way that the sides of the shaded triangles in the second layer are parallel to those in the first layer, but so that the corners of each shaded triangle of the second layer come directly above the centers of the shaded triangles of the first layer. The third layer is placed directly above the first, the fourth directly above the second, and so on. From this viewpoint, a triangular close-packed lattice is a two-story structure of equilateral triangles.

If the layers of triangles are placed so that the corners of the shaded triangles of any layer are above the centers of the shaded triangles of the next lower layer, the sides of the triangles being parallel as before, a rhombohedron is obtained. It is evident that in such a structure the triangles of the fourth layer must come directly above the triangles of the first layer so that a rhombohedron may be thought of as a three-story structure of equilateral triangles. The atomic co-ordinates are

$$m, \quad n, \quad p\,C$$
$$m+\tfrac{1}{3}, n+\tfrac{2}{3}, (p+\tfrac{1}{3})\,C$$
$$m+\tfrac{2}{3}, n+\tfrac{1}{3}, (p+\tfrac{2}{3})\,C$$

and the unit-rhombohedron contributes $1\frac{1}{2}$ atoms to the lattice.

A consideration of the atomic co-ordinates gives the following rules for the value of s of equation (28).

Simple triangular lattice: s is always unity.

Triangular close-packed lattice: If the difference between h and k is a multiple of 3, then if l is odd, $s=\frac{1}{2}$; otherwise $s=1$.

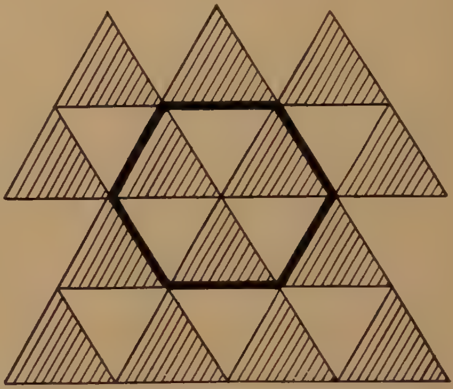

Fig. 9. Bases of Triangular Prisms in the Hexagonal System

Rhombohedral lattice: If the difference between h and k is a multiple of 3, then if l is a multiple of 3, $s=1$, but if l is not a multiple of 3, $s=\frac{1}{3}$; if the difference between h and k is not a multiple of 3, then if l is a multiple of 3, $s=\frac{1}{3}$, but if l is not a multiple of 3, then $s=1$.

Text-books of crystallography usually assign four co-ordinate axes instead of three to the hexagonal system. This is done by having an extra axis in the plane of the X- and Y-axes at an angle of 120 deg. to each of them. Miller indices for this extra axis are always equal to the sum of the indices for the X- and Y-axes, but are measured in the negative direction along this axis. Thus the prismatic face of a hexagonal prism is the $1\ 1\ \bar{2}\ 0$ plane. Since this extra axis serves no useful purpose, it is disregarded in x-ray crystal analysis; and the third index is replaced by a dot, so that the prismatic face is written $1\ 1 \cdot 0$. The dot serves to set off the l index from the h and k indices. This is a considerable convenience, especially in applying the rules of the rhombohedral lattice for the values of s in equation (28).

Since a rhombohedron may be regarded as a distorted cube, it is often referred to three trigonal axes, each of which is parallel to an edge of the unit rhombohedron. Table III(24) gives the indices of planes referred to the trigonal axes in terms of indices referred to the hexagonal axes. For the trigonal axes, since $\lambda=\mu=\nu$, equation (25) becomes:

$$d_1=\frac{(hx_1+ky_1+lz_1-1)\sqrt{1+2\cos^3\lambda-3\cos^2\lambda}}{\sqrt{(h^2+k^2+l^2)\sin^2\lambda+2(hk+hl+kl)(\cos^2\lambda-\cos\lambda)}} \tag{29}$$

A second set of trigonal axes may be used which have the directions of the face-diagonals of the original rhombohedron. Indices h' k' l' for the new axes may be calculated from the indices for the ordinary trigonal axes by means of the following equations (25):

$$h=k'+l'$$
$$k=h'+l'$$
$$l=h'+k'$$

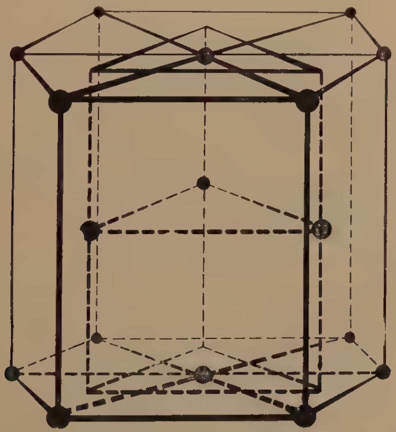

Fig. 10. Unit Triangular Close-packed Prism

Inter-relations Between Lattices

There are certain crystal forms of especial interest in that they may be regarded as belonging to either of two crystal systems. For instance, if a model of a face-centered cube is held so that one of its body-diagonals is vertical, a triangular arrangement of the "atoms" is at once evident, and it is seen that the structure may be regarded as a rhombohedron whose axial ratio is 2.45. Similarly a simple cube is a rhombohedron of axial ratio 1.225, and a body-centered cube is a rhombohedron of axial ratio 0.612. A body-centered cube is a face-centered tetragonal prism of axial ratio $1/\sqrt{2}$ and a face-centered cube is a body-centered tetragonal prism of axial ratio $\sqrt{2}$. Any body-

TABLE III

INDICES OF PLANES IN RHOMBOHEDRA

Indices Referred to Trigonal Axes	Indices Referred to Hexagonal Axes	Indices Referred to Trigonal Axes	Indices Referred to Hexagonal Axes
100	10·1	403	13·7
110	01·2	$40\bar{3}$	43·1
$10\bar{1}$	11·0	322	10·7
111	00·1	$32\bar{2}$	14·3
$11\bar{1}$	02·1	$3\bar{2}\bar{2}$	05·1
201	11·3	421	21·7
$20\bar{1}$	21·1	$42\bar{1}$	23·5
211	10·4	$4\bar{2}1$	11·1
$21\bar{1}$	12·2	$4\bar{2}\bar{1}$	51·1
$2\bar{1}\bar{1}$	10·0	332	01·8
301	21·4	$33\bar{2}$	05·4
$30\bar{1}$	31·2	$3\bar{3}2$	15·2
311	20·5	431	12·8
$31\bar{1}$	22·3	$43\bar{1}$	14·6
$3\bar{1}\bar{1}$	40·1	$4\bar{3}1$	34·2
302	12·5	$4\bar{3}\bar{1}$	$7\bar{2}\cdot0$
$30\bar{2}$	32·1	441	01·3
221	01·5	$44\bar{1}$	05·7
$22\bar{1}$	01·1	$4\bar{4}1$	35·1
$2\bar{2}1$	13·1	432	11·9
401	31·5	$43\bar{2}$	15·5
$40\bar{1}$	41·3	$4\bar{3}2$	25·3
411	10·2	$4\bar{3}\bar{2}$	16·1
$41\bar{1}$	32·4	433	10·10
$4\bar{1}\bar{1}$	50·2	$43\bar{3}$	16·4
321	11·6	$4\bar{3}\bar{3}$	07·2
$32\bar{1}$	13·4	443	01·11
$3\bar{2}1$	23·2	$44\bar{3}$	07·5
$3\bar{2}\bar{1}$	$5\bar{4}\cdot0$	$4\bar{4}3$	17·3
331	02·7		
$33\bar{1}$	04·5		
$3\bar{3}1$	24·1		

---

(24) P. Groth, *Physikalische Krystallographic*, pp. 454–455 (1905).

(25) W. W. G. Wyckoff, *Am. Jour. Sci.*, *50*, 317 (1920).

centered tetragonal prism of axial ratio C may be considered as being a face-centered tetragonal prism of axial ratio $C/\sqrt{2}$, or a face-centered tetragonal prism of axial ratio C may be called a body-centered tetragonal prism of axial ratio $\sqrt{2}\,C$. A simple triangular lattice of axial ratio C may be regarded as an orthorhombic lattice of a special sort (base-centered) whose axes are $\sqrt{3}$ and C. A large number of crystals have their axial ratios at or near some of these critical values.

Densities of Crystals

Since the determinations of the standard grating spaces of calcite and rock-salt are made in terms of the densities of single crystals and the mass in grams of the unit of structure(26), it is evident that a density for crystalline materials may be calculated in terms of the grating space as determined by x-ray methods. Such calculated values are subject to whatever errors there may be in the determination of the standard substances. This error seems to be considerably greater than is usually supposed, not because of an inability to make more refined x-ray measurements, but because the crystals of the same substance do not exactly duplicate each other, due to the effect of traces of impurities on the interplanar distances, and due to strains in the crystal. Measurements of the size of the unit of structure may be easily duplicated for the crystals of most materials to within one-tenth per cent, using different crystals of the same substance from different sources. This gives a limit of duplicatability to all density measurements from x-ray data of three-tenths per cent. Although densities calculated in this way agree in a general way with those found by direct measurement, they rarely agree exactly, probably because the material used for direct measurement contains a small amount of amorphous material whose density can hardly be expected to be that of the crystal. This is especially well illustrated by the case of CsI as measured by Clark and Duane.(20) The salt was of atomic weight purity, yet the density of one of the crystals, as calculated from x-ray measurements was 4.513, while the density of the whole sample was found by Baxter and Wallace(27) to be 4.509. The difference between these two values is within the limits of the estimate given for the accuracy of densities calculated from x-ray measurements.

In the cubic system the density of the crystal may be calculated from the formula:

$$\rho = n\,\frac{M\times 1.649\times 10^{-24}}{a^3} \qquad (30)$$

where

M is the mass of the unit of structure in terms of "atomic weight"

a is the side of the unit cube in centimeters

n is the number of points associated with a unit cube in the crystal lattice.

n is

1 for a simple cube
2 for a body-centered cube
4 for a face-centered cube
8 for a diamond cube.

In the tetragonal system the density is obviously

$$\rho = \frac{M\times 1.649\times 10^{-24}}{C\;(a^3)}\,n \qquad (31)$$

In the hexagonal system the density is

$$\rho = \frac{M\times 1.649\times 10^{-24}}{\frac{3}{4}\,C\;(a^3)}\,n \qquad (32)$$

where

ρ is the density
a is the side of the unit triangle
n is ½ for a simple triangular lattice
  1 for a triangular close-packed lattice
  1½ for a rhombohedral lattice.

The value of a in formula (32) is most easily found as $2d/\sqrt{3}$ for the 1 0 · 0 planes or as 2 d for the 1 1 · 0 planes.

(*To be continued*)

---

(20) Clark and Duane, *Proc. Nat. Acad. Sci.*, *9*, 117, 126, 131, 398 (1923); *Jour. Opt. Soc. Am.*, *7*, 455 (1923); *Science*, *58*, 398 (1923).

(26) Part I (Nov., 1924). See page 745.

(27) Baxter and Wallace, *J. Am. Chem. Soc.*, *38*, 96 (1916).

Relighting Atlantic City's Boardwalk

By T. P. Brown

Lighting Service Department, Edison Lamp Works

When a really difficult task has been accomplished particularly well, it is desirable to review the problem and make known the solution, for this furnishes a means of advancing the art, in this case, illumination. The especially notable feature of the new lighting installation for America's playground is its fulfillment of a wide variety of requirements. The equipment furnishes the choice of three lighting intensities from a spectacular blaze of light to a purely utilitarian amount, for use to suit the occasion and the time of night. By a special design and arrangement of reflectors, an asymmetric distribution of light is obtained which proportions the light going to the beach and the boardwalk in accordance with their respective needs. The new installation meets the requirements of a moderate first cost, and is several times more effective than the installation it replaces.—Editor.

Atlantic City, "America's Playground," the place of piers, magnificent hotels, boardwalk shops, tremendous crowds, conventions, and the like has long felt the need of boardwalk lighting that would be more in keeping with the surroundings—a system that would be flexible enough to meet the widely varying requirements. Such a system must serve a summer population of 400,000 to 500,000 as well a winter population of 80,000. A system was needed that would bring out the boardwalk in all its glory on the occasion of some national convention, yet be economical and adequate for ordinary periods. After the early hours of the evening when practically the entire population turns out en masse to stroll, a certain degree of illumination is still needed although the traffic is almost nil. Atlantic City needs on occasions to have a uniform light of high intensity over the whole boardwalk area. High-intensity lighting permits easy recognition of people and objects at some little distance, and gives the much desired effect of sparkle, vivacity, and prosperity to the scene. Uniformity eliminates the depressing effect produced by splotches of light separated by areas of comparative darkness. While illuminating the beach properly, the ideal system would put no more light there than necessary, thus allowing the building up of the intensity on the boardwalk. The equipment must withstand the severe ravages of the weather, including the moist and salty air. Finally, as it was necessary to light approximately eight miles of boardwalk, the cost of installation had to be as low as possible, consistent with other exacting requirements.

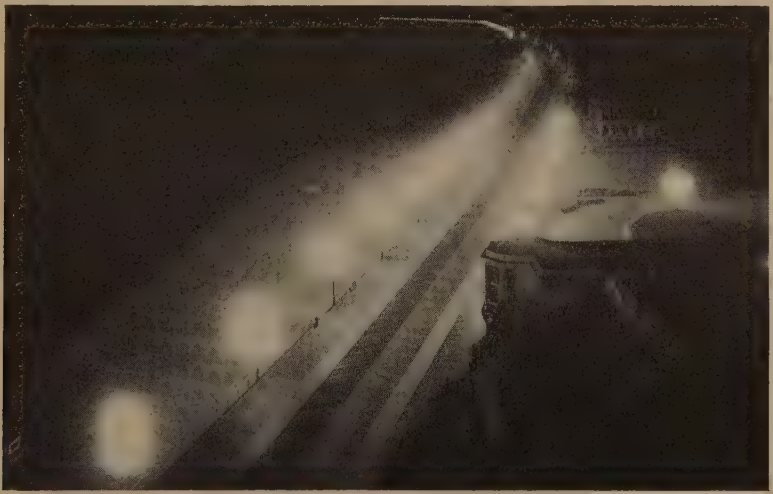

Fig. 1. A Comparative View of the Old and New Systems, the New System Having One Globe Per Standard and the Old System Five Per Standard. This photograph shows how much more effectively the boardwalk and the beach are lighted by the new system

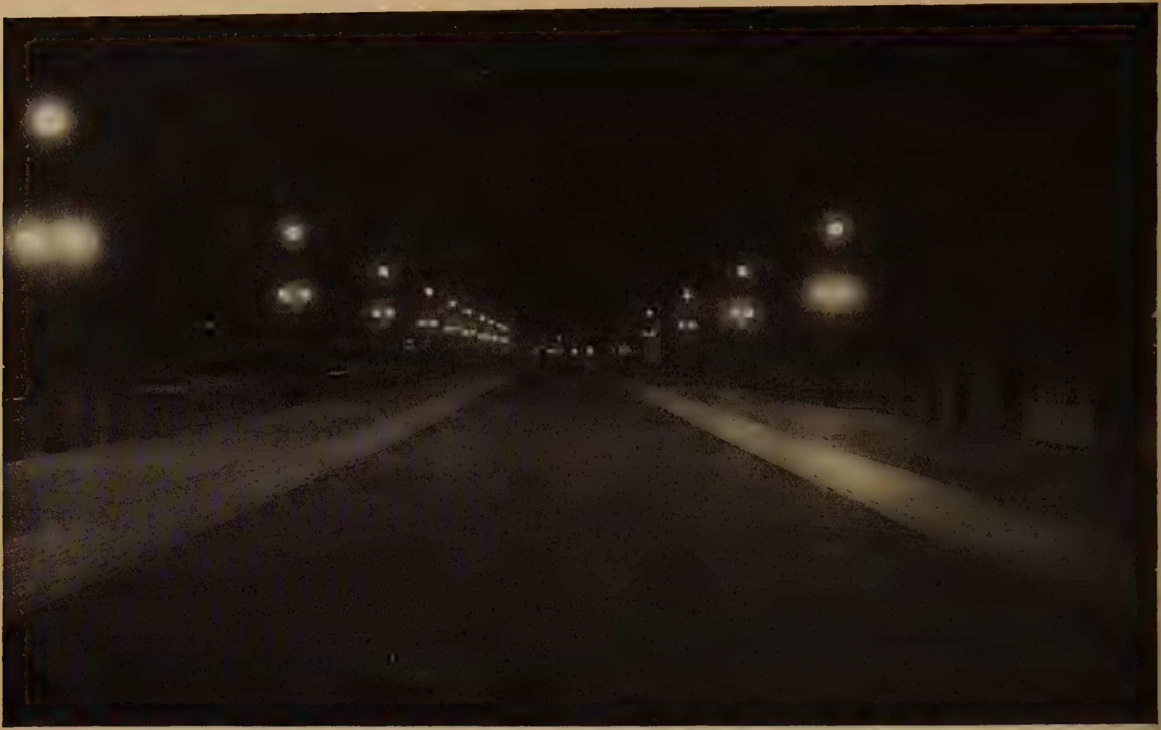

Fig. 2. Boardwalk, Atlantic City, Lighted by the Old System

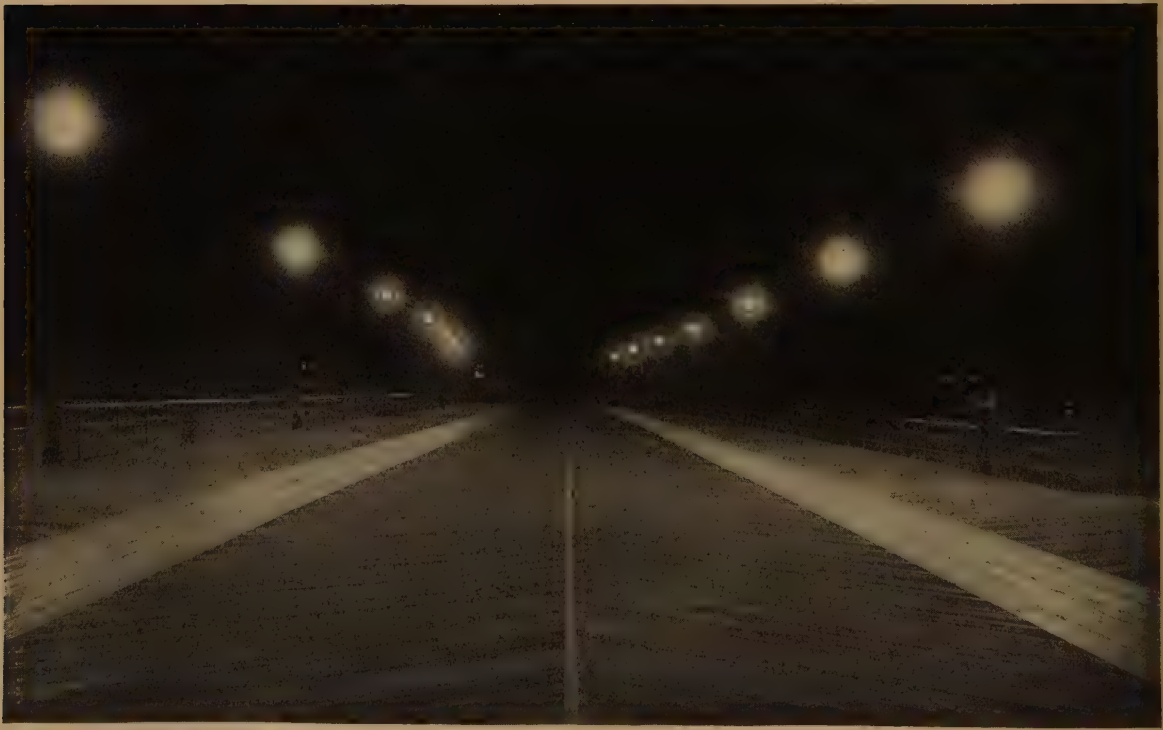

Fig. 3. Boardwalk Lighted by the New System, Showing the even distribution of light across the walk and the absence of dark spots

The superseded installation on the walk, Fig. 2, consisted of two rows of standards mounted along the railings and spaced approximately 65 ft. apart. Each standard had a 150-watt Mazda C lamp enclosed in a diffusing globe and mounted at a height of 19 ft. 5 in. with a cluster of four brackets mounted on the same pole at a height of 12 ft. 6 in. Each bracket supported a 100-watt Mazda C lamp enclosed in a diffusing globe. There was thus a total of 550 watts per standard; one-fourth of which went to the boardwalk, a fourth to the beach, and a half to the upper atmosphere (most of which was wasted). The plan of operation was to burn the top lamp (150 watts) all night, and the four cluster lamps (100 watts each) only during the early part of the night. Facilities were not available whereby more light could be put on the boardwalk on gala occasions. Furthermore, the use of opal diffusing globes gave the appearance of a "flat" light source —no sparkle, no life, no vivacity.

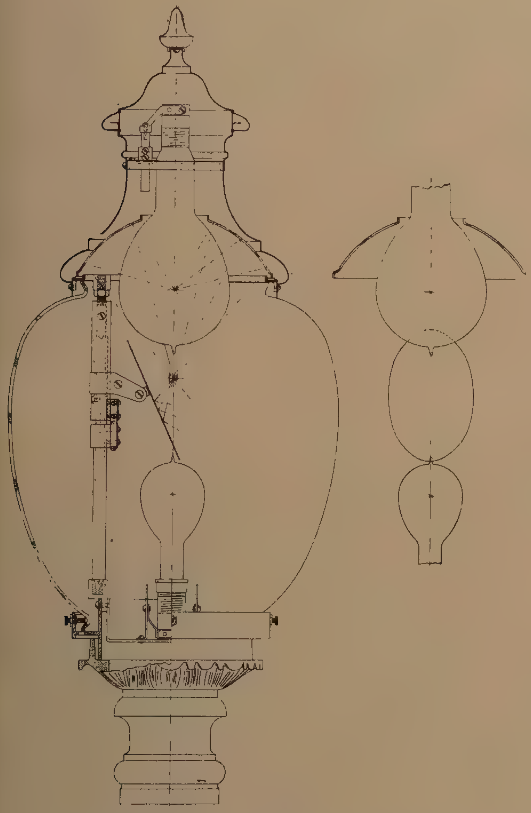
Fig. 4. **Sectional Assembly of the Ornamental Novalux Unit with Ellipsoidal Asymmetric Target Reflector**

After an extensive study of the relighting problem, it was determined that the new system should embody all the features outlined in the first paragraph. This would call for an asymmetric distribution of light, allowing just enough to go to the beach and directing the greater part onto the boardwalk where it would be appreciated. Such a distribution meant quite a radical departure from the old system and in fact from the general trend of present-day street lighting practice. It meant calling upon the knowledge gained during the past few years by many lighting developments; and it is worthy of note that the new system meets all the requirements even better than was anticipated.

The new system is flexible and is economical; three different intensities can be put on the boardwalk to serve the widely varying requirements for light from time to time. Also, the beach is served amply without sacrificing the high intensity on the boardwalk. That the intensity is uniform and high is shown by Fig. 3 and the tests described later. The first cost of the system is relatively low as compared with the results produced, and the system will be able to endure the rigors of the weather.

This installation and the methods used for solving this problem are particularly interesting in that they illustrate the flexibility of modern street lighting equipment and the ability of illuminating and designing engineers to meet unusual conditions. The familiar problem of lighting streets and boulevards does not present the same difficulties and as a result is more simply solved by the use of other standard forms of street lighting units.

The new units were of course especially designed and are extremely novel in their construction. The existing standards are utilized but the brackets forming the cluster were removed. At the top of the pole is a rippled alabaster globe seated and fastened in a casing, and surmounted by a metal canopy. Within the globe are two lamps: a 200-watt Mazda C lamp, 19 ft. 3 in. above the boardwalk, mounted on the casing in the tip-up burning position; and a 750-watt Mazda C lamp mounted in the tip-down burning position. The 750-watt lamp is located 20 ft. 5 in. above the walk in the metal canopy which seats on the top of the globe. Surrounding this large lamp is an elliptical reflector arranged with its primary focus at the lamp filament as shown in Fig. 4. Practically one half of the upward light of the lamp is gathered by this reflector and

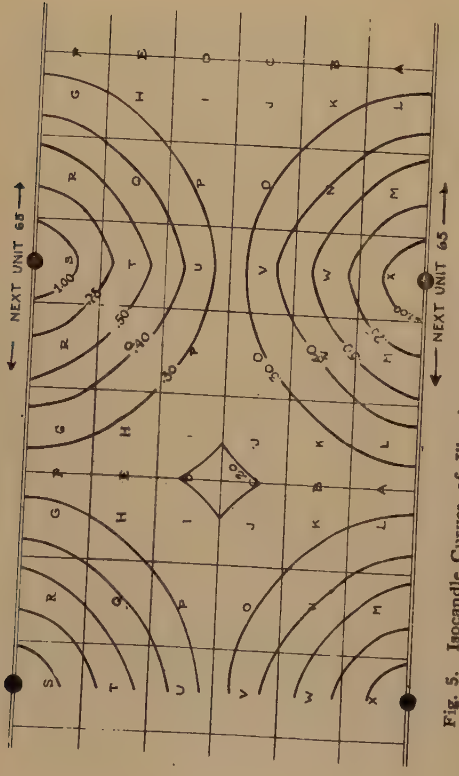

Fig. 5. Isocandle Curves of Illumination by Old System on Boardwalk Using All Lamps on Both Sides. (See Table I)

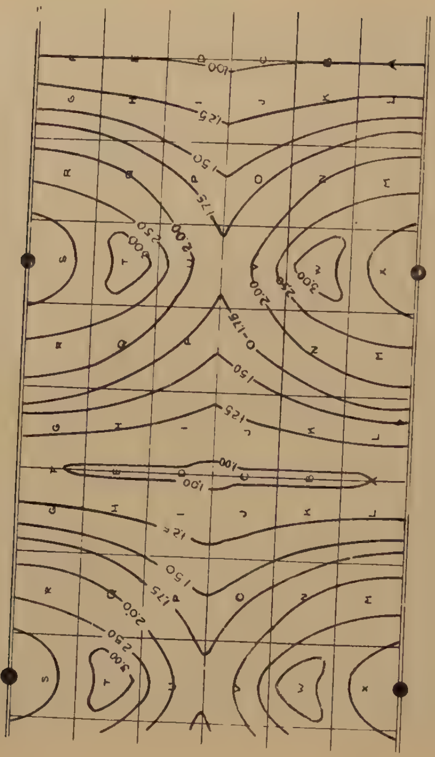

Fig. 6. Illumination by New System on Boardwalk Using All Lamps on Both Sides. (See Table II)

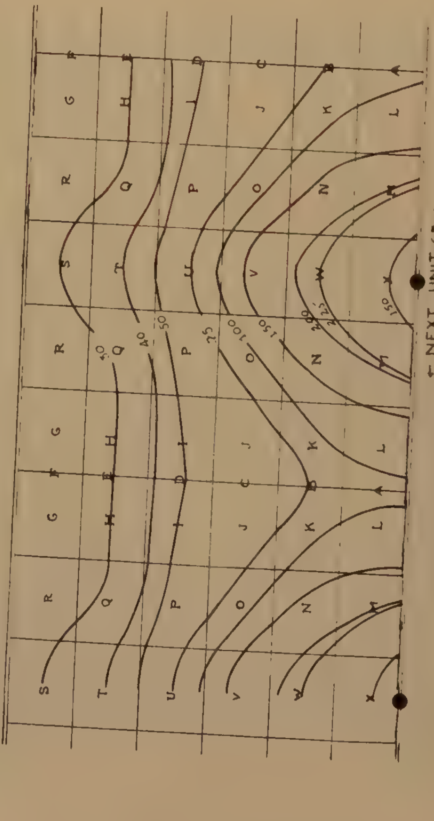

Fig. 7. Illumination by New System on Boardwalk Using All Lamps on One Side Only. (See Table III)

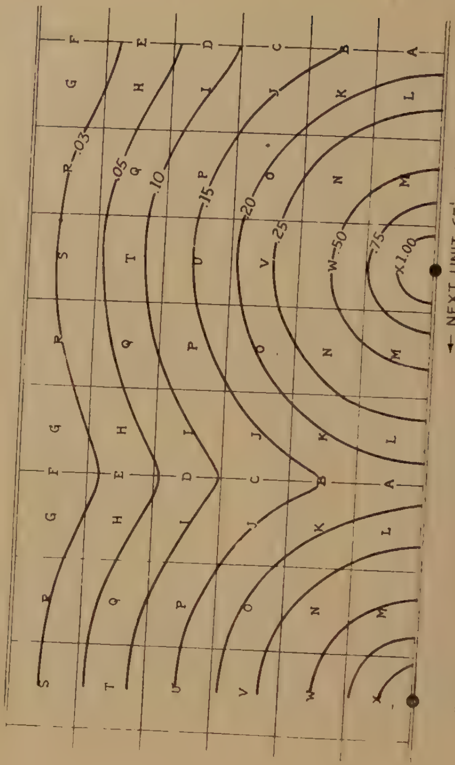

Fig. 8. Illumination by Old System on Boardwalk Using All Lamps on One Side Only. (See Table IV)

TABLES I-VI

FOOT-CANDLE INTENSITIES

Stations	TABLE I	TABLE II	TABLE III	TABLE IV	TABLE V	TABLE VI
	Fig. 5	Fig. 6	Fig. 7	Fig. 8	Fig. 9	Fig. 10
A	0.26	1.01	0.85	0.19	0.27	0.96
B	0.23	0.98	0.74	0.15	0.24	0.83
C	0.19	0.97	0.59	0.12	0.21	0.79
D	0.19	0.97	0.47	0.07	0.13	0.61
E	0.23	0.98	0.30	0.04	0.09	0.45
F	0.26	1.01	0.22	0.02		0.30
G	0.29	1.29	0.26	0.02		0.26
H	0.36	1.24	0.31	0.04		0.15
I	0.27	1.10	0.50	0.08		0.17
J	0.27	1.10	0.69	0.15		0.21
K	0.36	1.24	0.83	0.19		0.28
L	0.29	1.29	1.14	0.21	0.12	0.42
M	0.68	2.41	2.24	0.55	0.20	0.58
N	0.40	2.17	1.77	0.33	0.31	0.76
O	0.29	1.73	0.96	0.20	0.73	0.73
P	0.29	1.73	0.60	0.14	1.24	0.62
Q	0.40	2.17	0.30	0.08		
R	0.68	2.41	0.23	0.03		
S	1.14	2.04	0.30	0.03		
T	0.59	3.08	0.40	0.08		
U	0.38	2.09	0.72	0.16		
V	0.38	2.09	1.63	0.23		
W	0.59	3.08	2.25	0.52		
X	1.14	2.04	1.65	1.00		

TABLE VII

FOOT-CANDLE INTENSITIES

Both Sides Lighted	Old System	New System	Ratio of New to Old
Average over whole area	0.38	1.57	4.1
Average in line of standards across boardwalk	0.70	2.40	3.4
Average midway between standards across boardwalk	0.23	0.99	4.4
Ratio $\frac{\text{min.}}{\text{max.}}$ on line of standards across boardwalk	0.32	0.66	
Ratio $\frac{\text{min.}}{\text{max.}}$ midway between standards across boardwalk	0.73	0.96	
Ratio $\frac{\text{lowest reading}}{\text{highest reading}}$	0.17	0.31	
Total wattage per standard	550	950	1.72
One Side Only Lighted			
Average over whole area	0.19	0.83	4.4
Average in line of standards across boardwalk	0.33	1.16	3.5
Average midway between standards across boardwalk	0.10	0.53	5.3
Ratio $\frac{\text{min.}}{\text{max.}}$ on line of standards across boardwalk	0.03	0.13	
Ratio $\frac{\text{min.}}{\text{max.}}$ midway between standards across boardwalk	0.10	0.26	
Ratio $\frac{\text{lowest reading}}{\text{highest reading}}$	0.02	0.13	

concentrated at the conjugate focus several inches below. Attached to an upright is a small plane reflector so placed that it intercepts the concentrated light from the elliptical reflector and redirects it toward the boardwalk. The lamps are wired to separate circuits, the 200-watt lamps to one circuit and the 750-watt lamps to a second circuit, so that either or both may be used, giving three combinations and intensities of illumination. Under ordinary conditions, the 750-watt lamps will be lighted from sunset until 1:00 a.m., when they will be turned off and replaced by the 200-watt lamps which will burn until sunrise.

Illumination tests were run to determine the amount of light reaching the boardwalk, its distribution, and how the new system compares with the old. All readings were corrected to 115 volts, the rated voltage of the lamps. All readings in any one test were taken in symmetrical positions and were averaged to compensate for any errors caused by a possible inaccurate placing of the lamps. Six tests were run as follows:

(1) On boardwalk, old system, using all lamps on both sides.
(2) On boardwalk, new system, using all lamps on both sides.
(3) On boardwalk, new system, using all lamps on one side only.
(4) On boardwalk, old system, using all lamps on one side only.
(5) On beach, old system, using all lamps on both sides.
(6) On beach, new system, using all lamps on both sides.

Isocandle curves have been drawn for each of the tests and are shown in Figs. 5 to 10. Tables I to VI give the average readings for each of the tests. Table VII gives a summary, and furnishes a comparison between the old and new systems.

Comparison of Results with Both Sides Lighted

The average intensity over the whole area of the boardwalk was increased from 0.38 foot-candles to 1.57 foot-candles. In other words, the new system furnishes more than four times as much light as the old.

The intensity in the line of the standards across the boardwalk is about two and a half times higher in the new than in the old system.

The average intensity of the new system on a line across the boardwalk midway between the standards, that is a line of minimum points, is almost four and a half times that of the old.

Comparison of Results with Only One Side Lighted

There are sections along the boardwalk where it is possible to place lighting units on the ocean side only, because of buildings on the land side. The new installation proves its superiority here also.

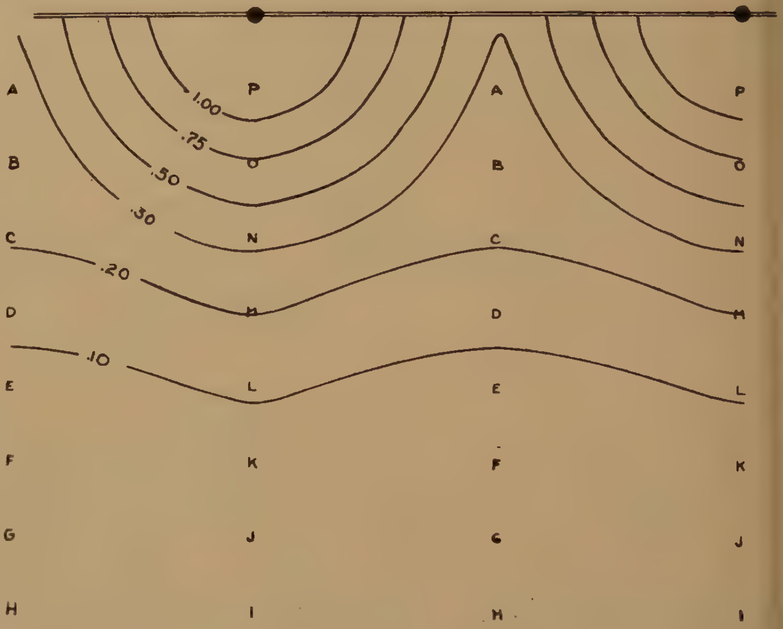

Fig. 9. Illumination by Old System on Beach Using All Lamps on Both Sides. (See Table V)

Over the entire area of the boardwalk, the average intensity with the old system was 0.19 foot-candles and with the new system it is 0.83 foot-candles, an increase of about 340 per cent.

A comparison of the intensity in the line of standards across the boardwalk shows that the new system delivers three and a half times as much light as the old system.

On a line across the boardwalk midway between standards, where the light is least intense, the new system shows a brightness 5.3 times greater than the old system.

While the new system would naturally be expected to deliver more light because of its higher wattage per standard—950 for the new as against 550 for the old—this increase in current consumption only partially accounts for the gain in illumination. Greater efficiency accounts for the major share of the gain. The increase in light obtained is several times the increase in wattage; for an increase of 72 per cent in the power used, the boardwalk receives 310 per cent more light.

Effect of Directional Device

The effect of the directional device used in the new system is apparent from a study of the ratio of minimum to maximum readings.

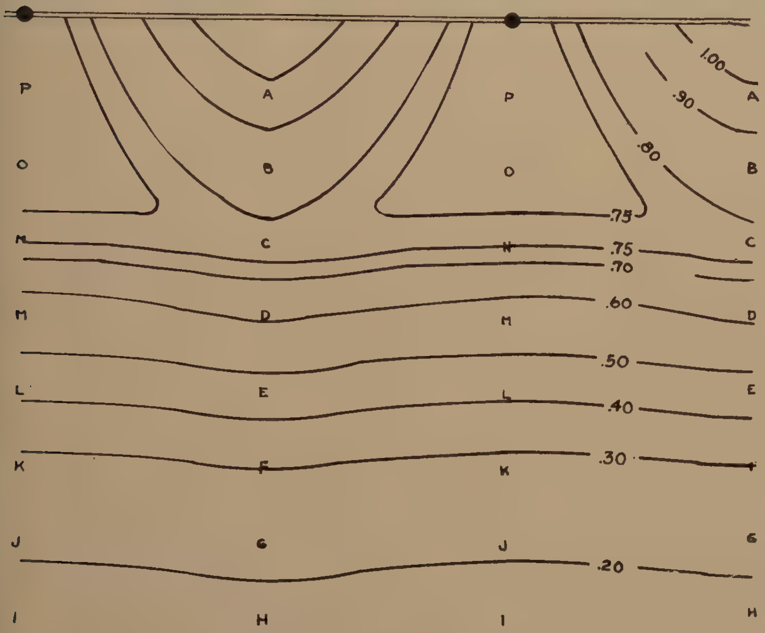

Fig. 10. Illumination by New System on Beach Using All Lamps on Both Sides. (See Table VI)

It may be stated that the ideal system would have no minimum or maximum points; in other words, the nearer the ratio of these two readings approaches unity, the more evenly is the light distributed. With this in mind, it will be seen that the ratio of minimum to maximum on the line of the standards across the boardwalk for the old system is 0.32 and for the new system is 0.66. Thus the new system is much closer to unity in this respect than is the former installation. On a line midway between standards across the boardwalk, the ratios are 0.73 for the old and 0.96 for the new.

Lighting of the Beach

While the lighting of the beach was not a paramount consideration in the design of the new system, the intensity on the beach has nevertheless been increased. Of course, it is not to be expected that the increase will be of the same magnitude as that on the boardwalk, due to the action of the lower reflector in the unit.

It should be noted that at the location of the new system the beach is approximately 12 ft. below the boardwalk, whereas at the place the tests were made on the old system the beach is only 5 ft. below the boardwalk. If direct comparisons are made of readings immediately adjacent the boardwalk, it should therefore be remembered that the difference in reading level unduly favors the old system. If however comparisons are made at distances of some 50 ft. from the boardwalk, the effect of this difference in reading level will be greatly minimized. At such distances from the boardwalk, Figs. 9 and 10 show that the beach is much more evenly illuminated by the new system than by the old. At 50 ft., the ratio of readings midway between standards to readings on the line of standards has been raised from 0.75 to 1.07. It may be well to determine from observation over a period of time whether the new system is putting too much light on the beach. If it is desired to have just full moonlight intensity, the system could be easily designed to redirect more of the light toward the boardwalk and build up the intensity there even higher.

For their helpful co-operation throughout the determination of the service to be rendered by the new lighting installation, and for their assistance in the conduct of the tests, acknowledgments are due Mr. C. H. Howell, of the Atlantic City Electric Company, and Mr. Frank Shinnen, electrical engineer for the city.

Studies of Electric Discharges in Gases at Low Pressures

PART V

THE USE OF SPHERICAL COLLECTORS AND THE EFFECTS OF MAGNETIC FIELDS

By Dr. Irving Langmuir and Harold Mott-Smith, Jr.,
Research Laboratory, General Electric Company

This article of the series continues the earlier exposition of the use of spherical collectors to determine the characteristics of electric discharges in gases at low pressures, presents additional experimental data relative to this form of electrode, and then enters into a dissertation on the effects of magnetic fields upon the discharges. Starting from the equations of Townsend, for the mobility of ions in a magnetic field, a theory of these effects is developed, experimental results are recorded, and a comparison made. The installment concludes with an explanation of how the theory applies to the Goldstein experiments with magnetic fields.—Editor.

We have seen that the current that flows to small collecting wires in ionized gas enables us to determine the concentrations of electrons and ions, while cylindrical collectors of large diameter yield values of the electron and the positive ion random current densities I_e and I_p. But with cylindrical collectors of large diameter there may be very troublesome end corrections. The difficulty usually cannot be overcome by increasing the length of the collector, for the electron current taken by the collector becomes so great that the conditions in the discharge are seriously modified by the withdrawal of so many electrons. With plane collectors similar difficulties are met because of the edge corrections.[31] For these reasons it is sometimes desirable to use spherical collectors. Such collectors are easily supported from small insulated wires so that edge corrections are practically avoided. The current i collected by a sphere of surface A is given by

$$i = AIF \tag{74}$$

where I is the random current density of the electrons or ions in the ionized gas and F is a function given by[32] [33]

$$F = \frac{a^2}{r^2}(1-\epsilon^{-\phi}) + \epsilon^{-\phi} \tag{75}$$

where

$$\phi = \frac{r^2}{a^2 - r^2}\eta \tag{76}$$

and

$$\eta = \frac{Ve}{kT} = \frac{11{,}600V}{T} \tag{77}$$

When $\phi > 3$, the function F becomes almost exactly equal to a^2/r^2 so that the current collected is that which reaches the sheath. Thus under these conditions the current is calculated by the space charge equation for spheres, equation (16).

When the radius of the sheath is large compared to that of the collector, so that $a/r >> 1$, equation (75) reduces to

$$F = \eta + 1 - \frac{\eta^2 r^2}{2a^2} \tag{78}$$

or if a/r is sufficiently large

$$F = \eta + 1 \tag{79}$$

Thus the current to a very small spherical collector with accelerating field should be a linear function of the applied potential, and the intercept on the V-axis corresponds to $\eta_0 = -1$ or $V_0 = -T/11{,}600$ volts which is the same as in the analogous case for cylinders.

Typical Experimental Data with Spherical Collectors

In some experiments with spherical collectors molybdenum spheres 0.95 cm. in diameter mounted on molybdenum rods about 0.15 cm. in diameter were used. The rods were insulated from the ionized gas by closely fitting (although not touching) glass tubes which extended to within about 0.16 cm. of the surface of the sphere. The small current collected by the unprotected part of the rod was assumed to compensate for the shielding effect of the end of the glass tube where it was near the surface of the sphere.

The spherical collectors gave volt-ampere characteristics very much like those obtained with the plane collector.[31] With all reasonable current densities the sheath thickness is so small compared to the diameter of the collector that the currents are limited by space charge. It does not seem practicable to make spherical collectors of such small diameter that the equation for currents limited by orbital motion (equations 78 or 79) can apply. Thus with the collector either negative or positive, good ion- or electron-saturation currents were obtained. The electron currents in the intermediate region (retarding potentials) gave straight semi-logarithmic plots corresponding to a Maxwellian distribution as in the cases of plane and cylindrical collectors.

---

[31] Part II (Aug., 1924, p. 538).

[32] In referring to equations, it may be noted that equations (1) to (48) appeared in Part I (July, 1924, p. 449); equations (49) to (55) in Part II (Aug., 1924, p. 538); equations (56) to (71) in Part III (Sept., 1924, p. 616); and equations (72) and (73) in Part IV (Nov., 1924, p. 762).

[33] Equation (31), which was supposed to cover this case was in error owing to the omission of the last term. Equations (46), (47), and (48) which were based on equation (31) also involved the same error and should be disregarded. Equation (35) was also based upon (31) but is not in error for in this case the omitted term was properly neglected. The treatment of the spherical collector is repeated in these pages to correct these errors.

In many cases, particularly at low pressures of mercury vapor such as 1 bar, the dark positive-ion sheath was sufficiently distinct around a negatively charged collector to make possible cathetometer measurements of the sheath diameter. Of course since these sheaths must be viewed through a considerable thickness of luminous gas, the conditions for observation are not as favorable as with planes or cylinders. Table XVIII gives some measurements of the volt-ampere characteristics and the observed sheath diameter for a spherical collector in an arc of low current density (which thus gave thick sheaths).

Column 1 gives the potential of the collector with respect to the surrounding space. The current in milliamperes i is given in Column 2. Column 3 gives the ratio of the observed sheath radius to the collector radius (0.475 cm.). Column 4 gives the function α^2 calculated from V and from i by equation (16) which is the space-charge equation for spheres. The quantity ν which enters into equation (16) was found by equation (11) assuming a temperature $T_p = 10{,}000$ for the positive ions. Column 5 gives the value of a/r found from α^2 by means of a plot of this function.[34] Column 6 gives the positive ion random current density I_p calculated by dividing i (in Column 2) by the surface area of the collector (2.84 cm.^{2}) and then dividing by the square of (a/r) cal. given in Column 5. This is in accord with equation (74) since $F = a^2/r^2$, the current being limited by space charge, as we may see from the fact that ϕ lies between 70 and 180 whereas orbital motions are only important when ϕ is less than 3.

TABLE XVIII

TYPICAL DATA WITH A SPHERICAL COLLECTOR

Collector Diameter 0.95 cm.; Tube diameter 3.2 cm.; Arc current 0.2 amp.; Arc current density 0.025 amp. per cm.^{2}; Vapor pressure of mercury 1.0 bar (15 deg. C.)

1	2	3	4	5	6
V Volts	i m.a.	$\left(\frac{a}{r}\right)$ obs.	α^2	$\left(\frac{a}{r}\right)$ cal.	I_p ma. cm.$^{-2}$
−251	0.67	1.67	0.333	1.638	0.088
− 88	0.44	1.32	0.115	1.360	0.084
− 60	0.36	1.20	0.0825	1.303	0.075
− 20	0.30	1.11	0.0225	1.155	0.079

The agreement between the calculated and observed values of a/r and the practical constancy of I_p confirm the theory of spherical collectors with currents limited by space charge. The increase in current i with the negative voltage is thus explained by the increase in sheath area which may be determined either by direct observation or by calculation from the space-charge equation.

Table XIX gives some data obtained in another tube having an internal diameter of 5.1 cm. with very much higher arc current density. Data are given for accelerating fields with the collector both positive and negative. In the intermediate region where electron currents were flowing against a retarding field, the electron currents gave an excellent straight-line plot on semi-logarithmic paper whose slope indicated an electron temperature $T_e = 18{,}100$ deg.

With high-current densities where the sheath becomes thin compared to the radius of the collector, the collector may be assumed to have a plane surface and the space-charge equation for planes may be applied with very little error. This is illustrated in Table XIX. Column 3 gives the value of ν by equation (11), taking $T_p = 10{,}000$ when the collector is negative and $T_e = 18{,}000$ when it is positive. The values of x in Column 4 are the sheath thicknesses calculated from i and ν

TABLE XIX

POSITIVE ION AND ELECTRON DATA WITH SPHERICAL COLLECTORS

Collector diameter 0.95 cm.; Tube diameter 5.1 cm.; Arc current 10.0 amp.; Arc current density 0.500 amp. per cm.^{2}; Mercury vapor pressure 8.0 bars (40 deg. C.). Electron Temperature $T_e =$ 18,100 deg.

1	2	3	4	5	6
V Volts	i m.a.	ν	x cm.	$\left(\frac{a}{r}\right)$ cal.	I_p ma. cm.$^{-2}$
−75	12.5	840	0.0270	1.06	3.92
−65	12.4	675	0.0244	1.05	3.94
−35	12.1	290	0.0162	1.035	3.96
−15	11.8	95	0.0094	1.020	3.98
					I_e
+1.0	2260	4.3	0.0033	1.006	890
2.0	3250	8.6	0.0042	1.008	1120
3.5	3630	17.5	0.0057	1.012	1240
5.0	3720	26.5	0.0069	1.015	1270
10.0	3950	63	0.0103	1.021	1320
15.0	4100	106	0.0131	1.027	1360

---

[34] See Part I (July, 1924, p. 449) equation (17) and footnote 4.

by the space-charge equation (10) taking $\sqrt{m/m_e}$ equal to unity when the collector is positive and 605 when it is negative. Column 5 gives the ratio of the sheath radius to the collector radius (0.475 cm.) calculated from the values of x. Finally, in Column 6 are the values of I_p and I_e in milliamperes per cm.^{2} calculated from i and a/r in the same way as in Table XVIII.

The constancy of I_p indicates that the variation of i with voltage is fully accounted for by the change in sheath diameter. It should be noted that this variation with voltage is much less than for the data of Table XVIII, but this results from the thinner sheaths corresponding to the higher current densities. The electron currents i show a very definite approach to saturation as the positive potential is increased but, as may be seen from the gradual increase in I_p, the increase in i cannot be wholly accounted for by the change in the sheath diameter. The two factors discussed[35] in connection with plane collectors, viz., electron reflection as low potentials and increased ionization at higher potentials, are probably responsible for the variations in I_p.

Potential Gradients in Ionized Gases

The observations of sheath thickness which were possible at the lower current densities nearly always showed a sheath of uniform thickness around the whole sphere. In view of the fact that positive ions must lose energy on collision with atoms, it would seem that the positive ions should move principally in a direction towards the cathode so that the part of the surface of a spherical collector which faces the anode should receive more positive ions than the opposite side. The observed uniformity of the sheath thickness, however, seems to show that the positive ions move as much in random directions as the electrons do. This effect, however, may perhaps be brought about by the presence of the collector itself.

For example, imagine a case in which we have a volume of uniformly ionized gas in which the electrons move in random directions while the positive ions all move in a definite direction C. Let us now consider the effect of introducing a spherical collector. *If no potential gradients were set up in the gas*, except within the sheath surrounding the sphere, then there would be a positive ion shadow or region in the space extending from the sphere towards C which would be devoid of positive ions, but would contain the normal concentration of electrons. The resulting space charge would, however, exert an enormously great field which would extend even outside of the shadow and which would deflect position ions into it.

Thus we see that if the concentration of the electrons is to be the same on both sides of the sphere, potential gradients must be set up sufficient to bring the positive ions in nearly equal numbers to both surfaces. The potentials needed to do this will be comparable to the average energies of the positive ions (about 1 volt). Thus the space towards the cathode side of a large collector will in general be at a potential of a volt or so negative with respect to the space on the anode side.

Similar potential gradients must exist between the space near the axis and near the walls of a tube. Since the positive ions are generated in the tube and disappear on the walls, the positive ion concentrations n_p at the axis must be higher than near the walls at a point near the edge of the sheath. To prevent large space charge effects, the concentrations of negative and positive particles per unit volume must be equal, at least to a first order. Therefore the concentration n_e of electrons near the axis must also be greater than near the sheath on the walls. These electron concentrations, however, can only be brought about by potential gradients in accordance with the Boltzmann equation (equation 2). Thus the potential of the gas near the axis of an arc must be positive with respect to that nearer the walls and we may estimate this potential gradient by the Boltzmann equation. If the concentration of positive ions at the axis of a tube is twice that nearer the walls, the potential difference between these points must be

$$\frac{T_e}{11{,}600} \times \log_e 2 \text{ volts}$$

With $T_e = 30{,}000$ this gives 1.8 volts. With such radial potential gradients the positive ions are accelerated outwards and are thrown against the walls. It is probable that such factors as these determine the velocities of the positive ions.[36]

EFFECTS OF MAGNETIC FIELDS

A magnetic field of strength H exerts a force equal to eHv on a moving electron of charge e. Here v is the component of the electron's velocity which is perpendicular to the magnetic field. The force is exerted on the electron in a direction perpendicular to the direction of motion and also perpendicular to the magnetic field. Thus any motion of the electron in the direction of the magnetic field remains unaltered by this field, and may for the present be disregarded.

---

[35] Part II (Aug., 1924, p. 538).

[36] The use of the Boltzmann equation to calculate radial potential gradients and other potential distributions was discussed in a short paper by I. Langmuir and H. A. Jones (*Science*, 59, 380 [1924]) and also in more detail in a paper by Langmuir, Found, and Dittmer (*Science*, 60, 392 [1924]). Schottky has apparently arrived independently at similar views and is developing a "diffusion theory" of potential distributions in gaseous discharges along somewhat similar lines. See W. Schottky, *Physikalische Zeitsch.*, 25, 342 (1924) and a paper by him which is to appear in the *Zeit. fuer Physik.*

Consider a magnetic field parallel to the Z-axis acting on an electron moving with velocity v in the X-Y plane. The force due to the field causes the electron to describe a circular path of radius r given by

$$r=\frac{mv}{eH}=5.65\times 10^{-8}\frac{v}{H}\ cm. \qquad (80)$$

where r, v, and H are in electromagnetic units. The direction of motion is clockwise as seen in the direction of the magnetic lines of force.

Let us now consider the effect of an electric field. Any component of electric field parallel to the magnetic field produces its effect on the motion of the electron independently of the magnetic field and therefore may be disregarded for the present. Let the electric field component perpendicular to the magnetic field lie in the direction of the X-axis. Then a mathematical analysis[37] shows that the effect of an electric field of strength X is to superpose upon the circular motion due to the magnetic field a uniform motion of velocity X/H in a direction *perpendicular to that of the electric field* and also perpendicular to the magnetic field. Thus the electron describes a trochoidal path in the X-Y plane.

With a transverse magnetic field sufficiently strong to make the radius of curvature r small compared to the diameter of a discharge tube, the electrons *in free space* in a perfect vacuum could not move in the direction of the applied electric field so that no current should flow. Such conditions are in fact realized in the magnetron where there are crossed electric and magnetic fields. With tubes such as those that we have been studying there are, however, two factors which make it possible for current to flow in spite of strong transverse magnetic fields: (1) the effect of collisions of the electrons with gas molecules; and (2) the effect of the walls of the tube.

Effects of Collisions

Townsend has developed the theory of the motion of electrons in gases under the combined action of electric and magnetic fields.[38] After each collision the electron starts to move along its new path in a direction which is random. Thus each collision affords an opportunity for the electron to progress a step (less than $2r$) in the direction of the electric field. The average direction of motion therefore makes an angle θ with the direction of the electric field where θ is given by

$$\tan\theta=\frac{He\lambda}{mv} \qquad (81)$$

where λ is the mean free path of the electrons among the gas molecules. Since λ is inversely proportional to the pressure, we see that θ approaches zero deg. at very high pressures or at vanishing magnetic fields and tends to become 90 deg. at low pressures or with very strong fields. In this theory v has been assumed constant. Without serious error we may put v equal to the root-mean-square velocity of the electrons perpendicular to the magnetic field. We thus find

$$v=6.23\times 10^{5}\sqrt{T_e}\ \text{cm. sec}^{-1} \qquad (82)$$

Substituting this in equation (81) gives

$$\tan\theta=28.4\frac{H\lambda}{\sqrt{T_e}} \qquad (83)$$

Townsend finds that the diffusion coefficient D_H of electrons in a transverse magnetic field is given by

$$D_H=\frac{D}{1+\tan^2\theta} \qquad (84)$$

where D is the diffusion coefficient in the absence of a magnetic field (or in the direction of the magnetic field.) With mercury at 20 deg. C., the pressure is 1.5 bars and the free path λ of electrons is about 30 cm. Taking $T_e=30{,}000$ deg. this gives

$$D_H=\frac{D}{1+24H^2} \qquad (85)$$

We see that with these low pressures of mercury, the mobility of electrons, which is proportional to D_H, should be decreased to one twenty-fifth by a field of only one gauss.

Effects Due to the Walls

Because of the magnetic field the electrons are caused to move towards one side of the tube and are thus made to collide with the walls of the tube, or rather are brought to the edge of the positive ion sheath on the glass from which they are specularly reflected, being repelled by the negative charge on the glass. The electrons which are thus reflected progress in a series of approximately semicircular paths along the surface of the tube wall in a direction towards the anode, so that in the immediate neighborhood of the wall the mobility is not much decreased by the transverse magnetic field, although the mobility along the axis of the tube may be negligible.

---

[37] See for example "Conduction of Electricity Through Gases," J. J. Thomson, 2nd Edition (1906) page 111.

[38] J. S. Townsend, *Proc. Roy. Soc.*, 86, 197 and 571 (1912).

Another effect comes into play which increases the mobility near the tube wall on the side towards which the electrons are deflected. From equations (80) and (81) we see that to deflect positive mercury ions a given amount will take a magnetic field 605 times stronger than to give a similar deflection to electrons having the same kinetic energy. Thus moderate fields sufficient to control the motions of electrons will have a negligible effect upon positive ions.

If by a magnetic field the electrons have been forced close to one side of the tube so that n_e is larger near one wall than at the axis of the tube, there must be a similar difference in the positive ion concentrations n_p, for otherwise enormous potential differences would be set up as a result of the space charge that would develop. Since the positive ions cannot be concentrated near the walls by the magnetic field, the required concentration must be brought about by transverse potential gradients Y sufficient for the purpose. Thus the region of high electron concentration near the wall must be at a negative potential with respect to the region near the axis where the lower concentration prevails.

This transverse potential gradient Y is in such a direction as to cause the electrons to drift towards the *anode* with a velocity Y/H. This effect tends to increase the mobility near the walls.

Townsend gives the following differential equations for the motions and the partial pressure of electrons in gases in presence of magnetic and electric fields.

$$\frac{p}{D_H}\frac{dx}{dt} = -\frac{dp}{dx} + ne\left(X - \frac{YHe\lambda}{mv}\right)$$

$$\frac{p}{D_H}\frac{dy}{dt} = -\frac{dp}{dy} + ne\left(Y + \frac{XHe\lambda}{mv}\right)$$

$$\frac{p}{D}\frac{dz}{dt} = -\frac{dp}{dz} + ne\,Z$$

The magnetic field is taken parallel to the Z-axis with the lines of force in the direction of the +Z-axis. The electric field strengths X, Y, and Z are defined by

$$X = \frac{dV}{dx},\ Y = \frac{dV}{dy},\ \text{etc.}$$

The velocity components dx/dt, dy/dt, etc. are the average drift velocities of the electrons under the combined magnetic and electric field while v is the actual velocity of thermal agitation (parallel to the X-Y plane) along the path of the electron (assumed constant in this derivation). The partial pressure of the electrons p is related to the concentration n by the relation

$$p = n\,k\,T_e$$

so that we may eliminate p and obtain

$$\frac{1}{D_H}\frac{dx}{dt} = -\frac{d\log n}{dx} + \frac{e}{kT_e}\left[X - Y\tan\theta\right] \qquad (86)$$

$$\frac{1}{D_H}\frac{dy}{dt} = -\frac{d\log n}{dy} + \frac{e}{kT_e}\left[Y + X\tan\theta\right] \qquad (87)$$

$$\frac{1}{D}\frac{dz}{dt} = -\frac{d\log n}{dz} + \frac{eZ}{kT_e} \qquad (88)$$

Let us consider a portion of a discharge close to the wall of a tube. Let the wall be represented by a plane which includes the X- and Z-axes and let the anode lie along the +X-axis, the distance y being measured from the wall. By taking the magnetic field negative, the motion of the electrons in the X-Y plane will be clockwise and the electrons will be forced towards the walls of the tube.

Since the number of electrons that strike the walls must be equal to the number of positive ions, all but about one in 400 of the electrons which move towards the walls will be specularly reflected from the sheath. Thus, neglecting the small fraction that reach the wall, we may say that the *average* velocity component $\frac{dy}{dt}$ of the electrons normal to the walls must be zero. Thus equation (87) reduces to

$$\frac{d\log n}{dy} = \frac{e}{kT_e}\left[Y + X\tan\theta\right] \qquad (89)$$

When the magnetic field is zero this equation after integration reduces to the Boltzmann equation

$$n = n_0\,\epsilon^{\frac{eY}{kT_e}} \qquad (90)$$

Since H is negative we see that the effect of the field is to concentrate the electrons near the wall.

The potential gradient Y is determined by the ease with which the positive ions can be held within the region of high electron concentration. Assuming that the positive ions acquire by collision a random velocity of agitation corresponding to T_p we may apply the Boltzmann equation to calculate the potential gradient Y from the concentration gradient of the positive ions. But, outside of the positive ion sheath, the concentrations n_p and n_e (neglecting the possible presence of negative ions) must be very nearly equal so that we obtain by differentiation of equation (90) (or by direct use of equation (89) placing $m=\infty$)

$$\frac{d \log n}{dy}=-\frac{eY}{kT_p} \tag{91}$$

the negative sign being due to the fact that the charge of the ions is opposite to that of the electrons. Combining equations (89) and (91) we get

$$-\frac{X}{Y} \tan \theta=1+\frac{T_e}{T_p} \tag{92}$$

This equation enables us to calculate the transverse potential gradient Y in terms of the longitudinal gradient and other quantities which can be measured. It is interesting to note that Y is not a function of y, the distance from the wall. Of course this equation by its method of derivation does not apply within the positive ion sheath on the wall.

We may obtain another useful relation by means of equation (86). If we are dealing with a discharge which is longitudinally uniform, the first term in the second number of equation (86) vanishes and we get

$$\frac{dx}{dt}=\frac{D_H e}{kT_e}[X-Y \tan \theta] \tag{93}$$

By combining this with equation (92) we may eliminate Y and thus obtain after insertion of the value of D_H from equation (85) and simplification,

$$\frac{dx}{dt}=\frac{DeX}{kT_e}\,\frac{T_p+\dfrac{T_e}{1+\tan^2\theta}}{T_p+T_e} \tag{94}$$

With weak fields where $\tan \theta$ by equation (81) is small compared to unity, this equation reduces to

$$\frac{dx}{dt}=\frac{DeX}{kT_e} \tag{95}$$

while for strong fields where $\tan \theta$ is large compared to unity, it reduces to

$$\frac{dx}{dt}=\frac{DeX}{kT_e}\,\frac{1}{1+\dfrac{T_e}{T_p}} \tag{96}$$

In both cases the mobility of the electrons towards the anode, which is measured by dx/dt, is independent of the magnetic field strength and of the distance from the wall.

From equation (96) we see that the effect of even a strong field in cutting down the flow of current towards the anode is relatively small. For example, if T_p is $\frac{1}{3}$ of T_e the mobility is only decreased to one-quarter by a very strong field.

The reflection of electrons from the sheath on the glass wall causes the electrons which reach the sheath to drift towards the anode with a mobility nearly equal to that which they would have in the absence of the magnetic field. Since this action of the negatively charged walls could occur in absence of gas, it does not depend on the velocities of the positive ions as does the action in the body of the gas such as is described by equation (94). The longitudinal drift of the electrons which are reflected from the sheath is due of course to the transverse electric field which acts on them while they are within the sheath, but since in this region the concentration of electrons and ions are not equal, equations (92), (93), and (94) will not apply.

The assumption that the positive ions have a Maxwellian velocity distribution and that the Boltzmann equation (90) may be applied to them is probably only approximately true and any observed disagreement between experiment and equation (94) will be most likely due to a different velocity distribution from that assumed. As the positive ions lose on the average about one-quarter of their energy on each collision with a gas molecule, there seems to be no mechanism by which ions can acquire the high velocities which a few of them should possess according to Maxwell's distribution law. Thus we should expect that the transverse potential gradient Y, instead of being constant across the tube as indicated by equation 92, should at first remain constant but then further from the wall, as the concentration of ions and electrons decreases, Y should also decrease because of the deficiency of the ions of unusually high velocity.

It is felt, however, that these equations should give a general representation of the phenomena to be expected with transverse magnetic fields. A more complete mathematical analysis will probably be made in connection with experiments now in progress. It is planned to develop the theory also for the case of low pressures where the normal free path is large compared to the diameter of the tube, although the equations already presented are probably more or less applicable to this case in spite of the tacit assumption in their derivation that the pressures are high enough to make the free path small.

Experimental Study of the Effect of Magnetic Fields on the Positive Column of Mercury Arcs

A series of experiments were made with longitudinal and transverse magnetic fields with the tube shown in Fig. 3. All these experiments were made long before the foregoing theory had been worked out. Longitudinal fields up to 100 gauss had surprisingly little effect on the arc. The values of I_e, I_p, T_e, and dV/dx were all practically unaffected by the field except in some cases when the field caused a non-uniform distribution of current across the tube. There was a marked tendency for the electrons of the arc to follow the lines of magnetic force. Thus if the field was not quite parallel to the axis of the tube, the arc by following the direction of the field would be deflected to one side of the tube.

In the literature there are numerous statements that a longitudinal field causes a gaseous discharge to concentrate near the axis of the tube. Our observations have convinced us that a *longitudinal* field does not have this effect, and that a concentration near the axis is due only to the radial field at the cathode end of the longitudinal portion of the field, which occurs for example at the end of a solenoid used to produce the field.

If an electrode or other body is placed near the axis of the tube carrying an arc in a longitudinal field with mercury vapor at low pressure, a very definite shadow extends from the object towards the anode showing that the electrons which are responsible for the luminosity travel along the lines of force (in helical paths). At higher pressures these shadow effects were less distinct and require stronger fields to produce them.

Effect of Transverse Fields

A ring-shaped coil 30 cm. in diameter was mounted in a vertical plane close to the tube, of Fig. 3, so as to produce a uniform transverse field in the neighborhood of the collectors D and E of such polarity that the arc was deflected to the right, i.e., against the smooth wall of the vertical tube which faces the anode B. With a mercury vapor pressure of 8.0 bars (40 deg. C.), the following phenomena were observed as the field intensity was increased.

The arc, which without the field gave a nearly uniform luminosity across the tube, was thrown by the field against the wall so that the light appeared to come only from a segment of the circular cross-section. Thus with an arc current of 4 amp. and a field of 15 gauss, the luminosity was confined to a region about 7 mm. thick (measured along a radius perpendicular to the magnetic field). This luminous band was divided longitudinally by faint striations about 4 cm. apart, which seemed to depend on the presence of the side arm containing the anode B. The striations become closer together and less distinct as the field is increased, and they are most distinct with lower arc currents.

Each striation is sharp on the cathode side but indefinite on the anode side. The sharp surface is concave upward and from the point where it meets the glass (on the right) it curved downward and then radially inward toward the axis of the tube. If, as seems probable, the surfaces of these striations are approximately equipotential surfaces, we have here a direct indication that the region of high arc density near the wall is negative with respect to the region near the axis where the arc density is less. The curvature of the surface thus indicates that the transverse field Y decreases as we go from the wall out to the region of lower arc density.

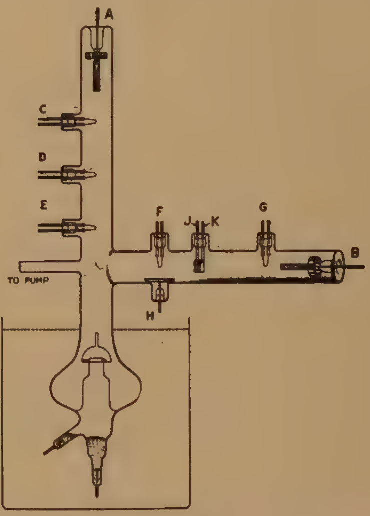

Fig. 3. Mercury Vapor Tube with Various Types of Collectors. *(Repeated from Part II)*

As the field is increased, the band of light as seen along a radius perpendicular to the field contracts in width but its edges are diffuse. At a certain critical field strength which depends on the arc current (and the mercury-vapor pressure) a narrow sharply defined and brilliantly luminous strip appears running down the middle of the original diffuse band. This phenomenon is more distinct at larger arc currents (2 amp. or more). The width of this brilliant strip was about 12 mm. and remained practically independent of the arc current and the field strength. With an arc current of 2 amp. the critical field was 27 gauss, while with 3.6 amp. it was 64 gauss.

With a mercury-vapor pressure of 33 bars (60 deg. C.) much stronger magnetic fields are required to produce these effects. When moderate fields (up to 45 gauss) are applied, there is only a relatively small change in the distribution of the light and this does not increase rapidly as the field increases. At the critical field strength, however, there appears quite sharply an exceedingly intense narrow strip of light (10 mm. wide) along the side of the tube. Faint striations, about 18 mm. long, could be seen in the bright strip although at the lower pressure (8 bars) the striations disappeared above the critical field strength. With an arc current of 0.5 amp. the critical field was 45 gauss, while with an arc of 4 amp. it was 60 gauss.

Some experiments were undertaken to determine the transverse concentration gradients resulting from a transverse magnetic field. A ring-shaped coil was mounted so as to deflect the electrons against the collector H (Fig. 3) or by reversing the polarity away from this collector. With an arc current of 2 amp. and mercury vapor at 1.0 bar (15 deg. C.), the data of Table XX were taken.

TABLE XX

Effect of Transverse Magnetic Field on Random Currents Measured by Collector H

1	2	3	4
H	I_e	I_p	T_e
+40	....	4.4	23000
0	170	0.4	22000
−40	25	0.1	.....

The positive sign for H refers to a field which forces the arc against the collector. The random current densities I_e and I_p are expressed in ma. per cm.² With the field $H = +40$ gauss, it was impossible to measure I_e as the collector drew the whole arc current before the current became saturated. With the field $H = -40$, the semi-logarithmic plot of the electron currents was far from straight, being concave downwards. The lower part of the curve gave a slope ranging from $T_e =$ 19,000 to 23,000 deg. With the field $H = +40$, the arc was in a narrow band not over one-half the width of the collector. The actual current density I_p was thus probably at least twice the uncorrected value 4.4 given in the table.

The positive-ion currents I_p were also measured at a series of different field strengths. A field of +5 gauss approximately doubled this current, while a field of −5 decreased it to about one-half. With negative fields from 20 to 50 gauss, I_p remained constant at about 0.1 and then increased at $H = -60$ to about 0.2 and remained again constant up to $H = -90$. With positive fields, I_p increased approximately linearly from 0.4 at $H = 0$ to 8.0 at $H = +90$.

A study of the longitudinal potential gradients with transverse fields was made with a transverse field in the neighborhood of collectors D and E (Fig. 3) and the results are summarized in Table XXI. The direction and polarity of the field was such as to force the arc (to the right) towards the smooth wall of the tube. Since the distance between the collectors was small (7.6 cm.) the data for the potential gradient (in Column 7) are probably not accurate to within less than ±0.15. Column 4 gives E_A, the voltage drop between the anode A and the mercury cathode. The current densities I_e and I_p are the averages of those obtained by the two collectors D and E. The electron temperatures were 30,000, 18,400, and 12,200 deg. at the three temperatures 15, 40, and 60 deg.[39]

TABLE XXI

EFFECT OF TRANSVERSE MAGNETIC FIELDS

Tube of Fig. 3. Collectors D and E. Runs 76 to 83

1	2	3	4	5	6	7
Bulb Temp., Deg C.	Hg Pressure bars	Field H gauss	E_A volts	I_e ma.cm.$^{-2}$	I_p ma. cm.$^{-2}$	$\frac{dV}{dx}$ volt cm.$^{-1}$
15	1.0	0	36.0	474	1.74	0.2
		9	43.4	210	0.50	0.3
		18	47.0	260	0.65	0.4
		37	60.6	250	0.63	1.1
		60	72.0	250	0.82	2.3
						0.3
40	8.0	0	37.0	490	1.67	
		9	42.5	220	0.66	0.4
		18	45.5	100	0.24	0.5
		37	54.2	110	0.19	0.7
		70	71.1	115	0.31	1.0
60	33.0	0	35.6	1530	5.0	0.5
		55	56.1	90	0.19	1.1
		92	64.2	45	0.08	1.5

---

[39] Runs 76, 79, and 83 of Table XIV are the same as those without field in Table XXI.

Comparison of Experimental Data and the Theory

It is seen that the phenomena observed agree qualitatively with the theory as outlined. The arc is deflected by a relatively weak transverse magnetic field but the concentration of electrons and ions on the side of the tube, where the concentration is lowest, does not continue to decrease as the field is increased but approaches a constant value independent of the field in general accord with the teachings of equations (89) and (92). Such behavior is undoubtedly due to transverse electric fields.

When, however, we use the ordinary values of the free paths of electrons in mercury vapor as calculated from the kinetic theory (for example 30 cm. at one bar), and thus calculate $\tan\theta$ by equation (83), and use this value to calculate by equation (92) the transverse potential gradient, and the mobility by equation (93), we find that the actually observed effects of the magnetic field are much less than those calculated. If we assume that the error lies in the value for the free path, we may proceed as follows to determine this free path from the data.

Let us assume that the transverse concentration gradient represented by $d \log n/dy$ is known from the experiments. By combining equations (89) and (91) we can eliminate Y obtaining

$$\tan\theta = \frac{\alpha k (T_e + T_p)}{e X} \tag{97}$$

where α is a measure of the transverse concentration gradient and is defined by

$$\alpha = \frac{d \log n}{dy} \tag{98}$$

Let us assume as a reasonable approximation that the total number of electrons involved in the carrying of current remains the same when the field is increased. Thus to carry a given arc current, dx/dt must remain constant. From equation (94) we then obtain

$$\frac{T_p}{T_e} = \frac{X_0 - \dfrac{X}{1+\tan^2\theta}}{X - X_0} \tag{99}$$

where X_0 is the longitudinal potential gradient in the absence of the magnetic field.

By eliminating T_p from equations (97) and (99) we find

$$\tan^2\theta + \beta \tan\theta + 1 = 0 \tag{100}$$

where β is defined by

$$\beta = -\frac{\alpha k T_e}{e(X - X_0)} \tag{101}$$

Solving equation (100) for $\tan\theta$ gives

$$\tan\theta = -\tfrac{1}{2}\left(\beta \pm \sqrt{\beta^2 - 4}\right) \tag{102}$$

Let us apply these equations to the data obtained with arcs in mercury vapor at 33 bars pressure. With a field of 92 gauss the current density I_e at the collecting electrodes D and E was 3 per cent of that observed in the absence of the field. According to equation (91) the concentration at any distance from the wall may be represented by

$$n = n_0\, \epsilon^{\alpha y} \tag{103}$$

α being defined by equation (101).

The average concentration n_a across the tube (considered as of square cross-section) from $y=0$ up to a point y_1, where the concentration is n_1, is then

$$n_a = \frac{n_1 - n_0}{\alpha Y_1} \tag{104}$$

If we let $y_1 = 2$ cm. corresponding to the position of the collectors D and E and consider that the diameter of the tube is about 3 cm., then if the total ionization is to remain constant we must put $n_a = 3/2$ of the average ionization observed in the absence of the field. Thus from the experimental data we know

$$\frac{n_1}{n_a} = 0.02$$

Placing $y=2$ and solving equations (103) and (104) for α we find

$$\alpha = -2.82$$

$$n_0 = 5.66 n_a$$

and $$n_0 = 280 n_1$$

For the mercury arc with 33 bars pressure we have $T_e = 12{,}000$, $\alpha = -2.82$, and from Table XXI $X_0 = 0.5$ and $X = 1.5$ volts per cm. Placing these together with the value $e/k = 11{,}600$ deg. per volt in equation (101) we obtain

$$\beta = 2.92$$

and from equation (102) we get

$$\tan\theta = -2.52 \text{ or } -0.30$$

The first of these values substituted in equation (99) gives

$$T_p = 2950 \text{ deg.}$$

whereas the second value corresponds to negative values of T_p and must be rejected.

From equation (91) we find

$$Y = 0.72 \text{ volts per cm.}$$

Similarly from equation (83) placing $H=-92$ we find

$$\lambda = 0.106 \text{ cm.}$$

This value of the free path of the electrons although of the right order of magnitude is about 8 to 10 times smaller than that calculated by the kinetic theory from the viscosity. Direct experimental determinations of the free paths in this laboratory have given values of about 30 cm. at 20 deg. C. and one bar, which would correspond to at least 1 cm. under the conditions of the experiment we are considering.

The other data in Table XXI, although the conditions are less in accord with those assumed in the derivation of the equations, agree in general with values of the free path, roughly about one-tenth of those usually found.

A similar discrepancy in the free path of about the same amount is also found when we attempt to calculate the longitudinal potential gradient in a mercury arc in the absence of a magnetic field from n_e, T_e, λ, and I_x (the drift current density) according to the Langevin (or other) equation for the mobility of electrons. The cause of this discrepancy is now being investigated experimentally and theoretically in this laboratory.

Goldstein's Experiments with Magnetic Fields

Many of the effects of magnetic fields which we may predict from the theory that we have developed are illustrated by some experiments made by Goldstein.[40]

Cylindrical discharge tubes of rather large diameter were used containing hydrogen at very low pressure. A cold cathode was used, the discharge being of the type of that in a Crookes' tube. The anode placed near one end of the tube was a piece of sheet metal (usually rectangular) in a plane which passed through the axis of the tube. A glass rod was usually mounted opposite the center of the anode and perpendicular to the plane of the anode, so that its nearer end was perhaps a centimeter from the anode. With a strong magnetic field parallel to the plane of the anode and perpendicular to the axis of the discharge tube (and the rod) some very remarkable effects were observed. A brilliant luminous skin formed on one side of the glass rod and passed along it to the point which was nearest the anode. Then instead of jumping across to the anode it passed through the space as a fine brilliant line in a direction nearly parallel to the surface of the anode and in a direction opposite to that side of the rod which was covered by the luminous skin. This brilliant line followed a nearly elliptical path around the anode until it intercepted the glass stem upon which the anode was mounted (even if it had to pass three-quarters of the way or more around the anode to do so). It then followed the surface of the glass stem as a luminous skin until it reached the anode. In many cases a beaded rod was used opposite the anode. A brilliant line, following an elliptical path, then started from each of the spaces between the beads forming a beautiful family of concentric ellipses.

Examination of Goldstein's paper shows that practically all the phenomena, which he illustrates in much detail, are completely explainable in terms of the theory we have given.

In the free space the "brilliant lines" follow paths which are *perpendicular to the direction of the electric field* and thus form approximately elliptical paths around the rectangular anode. The reason for Goldstein's emphasis on the necessity for very low pressure becomes apparent, since to have $\theta = 90$ deg., λ by equation (83) must be large. The luminous skins on the glass conductors are due to the reflection of electrons from the positive ion sheaths on the glass (and from the transverse fields near the glass resulting from concentration gradients).

Goldstein points out that these effects disappear if the anode is mounted on a metal rod instead of a glass stem. The "brilliant lines" in the glass are observed only when both ends can terminate on insulators. Goldstein calls them for this reason "insulator discharges."

The reason is that only by the presence of insulators can electrons pass to the anode and still move in a direction perpendicular to the field while in free space. A metallic support for the anode would be *positively* charged and therefore would produce a field which would cause the discharge to pass *parallel* to the surface of the support. Under these conditions the electrons of course do ultimately get to the anode but only by building up space charges which distort the field and destroy the simplicity of the phenomena.

---

[40] E. Goldstein, *Verh. deut. physik. Gesell.* 21, 559 (1919). Very striking photographs of the discharges in tubes of various shapes are given in this article.

The insulator discharges of Goldstein thus result from the fact that, by the presence of the negative charges on these insulators and the positive ion sheaths surrounding them, the electrons are able to reach the anode by a relatively direct path although they move perpendicularly to the electric and the magnetic fields. Of course a metallic electrode would have the same effect as a glass surface if it were maintained at a sufficient *negative potential* with respect to the surrounding space.

(*To be continued*)

The Steinmetz Memorial Scholarships

By C. M. Ripley

Publicity Department, General Electric Company

Steinmetz admired the useful things of life and did not believe in pomp or display; therefore no ordinary monument of stone or bronze would be suitable to commemorate his name.

Knowing this, the Directors of the General Electric Company had set about to establish a *living* memorial to their Chief Consulting Engineer who died last year; but it was no easy task to decide on something appropriate to a man who was so many-sided, yet withal a man of such plain and simple tastes. The recent announcement of their choice to endow in his name four scholarships at Union College will be gratifying to all who knew this genius of Schenectady or who knew of him only by reputation.

It is fitting that this remembrance should be an educational memorial because of the great passion which Dr. Steinmetz had for education. He was a tireless student himself, gave lectures on many subjects from soap bubbles to automatic electric plants, pointed out the defects in engineering education, and wrote a score or more of books covering a wide range of topics from international economics to the performance of alternating current and artificial lightning.

His title of Doctor of Philosophy, a degree conferred on him appropriately by Union College, and that of Master of Arts, given him by Harvard University, are in themselves evidence of his breadth of education. Besides, he was a mathematician, astronomer, naturalist, author, lecturer, teacher, sociologist, and a high municipal authority, being president of the Schenectady Board of Education for several years, as well as president of the Common Council.

Dr. Steinmetz believed that adequate education was an indispensable asset. "Any young man," he once said, "can do as well as I have done if he is given the right opportunity." And by right opportunity he meant a broad education, adequate training, and an opening in the line of work in which the young man is most deeply interested.

No young man ever approached Dr. Steinmetz for advice and encouragement without receiving both in large measure; and always he urged more study, broader reading, wider acquaintanceship. His early career with its hardships and bitter sacrifices, and the lack of appreciation which he suffered until he joined the General Electric Company over 30 years ago, gave him a keen sympathy for those less fortunate in life. He was always ready to lend a helping hand to young men compelled to struggle for education and to overcome the obstacles of life.

It is therefore most appropriate that his memorial shall be in the form of scholarships to aid boys who could not otherwise acquire a college education. These means are to be extended to:

Sons of employees of the General Electric Company.

Young men now employed by the Company.

Sons of residents of Schenectady if there should be no applicant from any of the Works of the Company.

The location of this Memorial is also appropriate because Dr. Steinmetz organized and for ten years personally conducted the course in Electrical Engineering at Union College, where he was beloved by the students and professors alike. So in this atmosphere, filled with the tradition of "The Great Torchbearer" the Memorial scholarship students will pursue their education.

The City of Schenectady, too, will thus be indebted in another and useful way to the man who loved it and who spent the last

25 years of his life there. For its good, he lavished time in working with any group that wished to carry out civic betterments. He was consulted by hundreds who wished to promote public improvements of all kinds; parks, playgrounds, a civic center, new boulevards, and city plans.

It is proper that this Memorial should be endowed by the General Electric Company, for the electrical industry benefited by his services for 30 years. Working in its laboratories he formulated many of the fundamental principles of electricity and clarified thought in electrical terms.

In addition to his many inventions, he created electrical yard-sticks by which the whole engineering world can not only measure, but can even foretell the performance of electricity in complex transmission and distribution systems.

Previous to this work of Steinmetz, the designers of electrical apparatus had to rely largely on the "cut and try" method, but with the help of Steinmetz and his lucid exposition of fundamental laws and principles they were no longer compelled to work so in the dark. As the x-ray shows the way to physicians and surgeons, so has Steinmetz shown the way to engineers.

A living memorial has been established—not an inanimate bust of cold marble—and it is like the achievements of Steinmetz himself "more durable than brass—more lasting than the pyramids."

Dr. Steinmetz would heartily approve the method adopted to perpetuate his name and his ideals, because this Memorial concerns itself with human beings. To thousands he was a good friend, and was always at home to callers day or night—no matter who they were. Hardly an evening passed that he was not consulted by teachers, municipal authorities, engineers, shopworkers, business men, or young folks—all in need of inspiration.

He was a lovable home-loving man with a warm heart and a kind word to all—engineer and watchman, chemist and elevator boy, trolley motorman or corporation official—everyone.

In his beautiful home and garden, amid well-kept grounds flanked by a brook, a glen, and a grove of trees, he was surrounded by those he loved. The noisy play of children at his very elbow would not disturb him while making abstruse mathematical calculations, or writing technical text books for senior students in engineering universities. In fact, he preferred to work amid animation and even the boisterous rioting of youth, either at home or at his camp on the bluff overlooking the Mohawk River.

In the conservatory adjoining his private museum and laboratory, he kept and tenderly cared for some of the wildest and most weird forms of animal and vegetable life. There were the cruel many-needled cactus plants from the desert, queer ferns, orchids from the jungles and swamps, and other exotic and little known plants from tropic lands. Alligators swam about in his fountains and a Gila monster which he pronounced "to lazy to eat" made its home within ten feet of the place where the great genius carried on his "home-work."

Who will replace him? Who *can* replace him? Who will be the Steinmetz of 1950 or the year 2000?

Since educational scholarships run on from generation to generation, it leaves one with the hope that perhaps one of the students to be educated at Union College through the Steinmetz Memorial Scholarships will be blazing the trail of the now undreamed electrical wonders 50 or 100 years from today inspired by the spirit of the great genius.

A moralist once referred to some great achievement and said: "Anyone can do the same thing if he is made of the right kind of stuff." To this Steinmetz objected: "The scientific fact is," he said, "that people *are* made out of the right kind of stuff but our problem is to find a way to *release* their creative energies."

Steinmetz found a way to release his own creative energies. He used a big electrical organization as the tool, as an instrument to make his ideas useful to the whole world. The corporation of which he was a part provided the organization, the laboratories, the assistance, the materials, the special machinery, and the money. Its big factories turned out tens of thousands of electrical devices. Salesmen marketed them throughout the Americas and the four corners of the world. Thus were Steinmetz's great creative engineering energies released to advance the human race on a truly international scale.

And now through these memorial scholarships his creative education will go on from generation to generation—not only released but multiplied, extended, and perpetuated.

Oil Circuit Breaker Investigations to Determine Interrupting Capacities

By J. D. Hilliard

Switchboard Department, General Electric Company

If oil circuit breakers were never called upon to interrupt more than the normal flow of power in a circuit, the problem of their construction would be comparatively simple. It is their emergency function of protecting apparatus and lines under short circuits and other abnormal conditions that gives rise to the real problems of their design, for consideration must then be given to their performance of interrupting amounts of current many times greater than their normal carrying capacity. In the case of the larger and higher voltage breakers, these volumes of power are truly huge and until recently have been far in excess of those consistently available to the designer for testing purposes. Now that there has been installed a power source of adequate capacity for research investigations in this field, our knowledge of circuit breaker performance is rapidly increasing. The following summary of some of the results already obtained is of great value and is here being reprinted from the Journal of the A.I.E.E., Sept., 1924, p. 818. A complete description of the testing equipment itself has already appeared in this magazine.[1]—Editor.

Although oil circuit breakers have been used for a number of years and many successful types produced, the work of the designer has been handicapped by the lack of definite design constants, based on experimental results. In some of the earlier designing, field tests were relied upon for the confirmation of the interrupting rating. Such tests were of great value, but, due to inherent erratic behavior of oil circuit breakers as a current interrupting device, the data obtained were not usually of a general or fundamental nature. To remedy this situation and to permit continuous and consistent research on the interrupting characteristics of alternating-current circuit-controlling devices, a special testing equipment was installed.

TESTING EQUIPMENT

The testing station[1] contains a three-phase specially built 26,700-kv-a. 25-cycle alternator of low reactance. The windings are arranged for connection to give 13,200, 7620, 6600 or 3810 volts. A three-phase 1500-horsepower direct-connected induction motor is used as the driving power. The generator and driving motor are shown in Fig. 1.

The current supplied on short circuit is controlled by means of reactors having ten taps and a maximum value of 6.1 ohms per phase.

In addition to the generator, high-voltage transformers of low reactance are provided. These transformers permit three-phase testing at any voltage up to 44 kv. and single-phase testing up to 132 kv.

The measuring equipment, in addition to the usual meters, consists of three oscillographs, pressure recorders, speed recorders, and such other apparatus necessary for the collection, analysis, and measurement of gas.

This equipment will produce short circuits approximating 300,000 kv-a., three-phase, at 13,000 volts. The equivalent three-phase kv-a. at 13,200 volts can be increased to approximately 600,000 kv-a. by single-phase test to ground at 7630 volts. Approximations of short circuits very much higher than 600,000 kv-a. can be obtained by testing one break on single-phase tests.

THE FACTORS INVESTIGATED

Break Distance

The satisfactory operation of any oil circuit breaker depends upon the break distance. This break distance must be ample to interrupt the arc under the severest condition of operation or there will be a permanent gas generation which will quickly result in the destruction of the breaker. The required break distance for any given voltage and interruption is determined by the circuit conditions, *i.e.*, grounded or ungrounded, power-factor, connected shunt load, amperes interrupted, pressure in the oil tank, tank cross-section, etc., and it is evident that to have an absolutely safe breaker the worst conditions must be assumed. This condition is fortunately a dead short circuit at the generator terminals on an ungrounded system without shunt load, and it is under these conditions that the rating tests are made. If the breaker is to be used on a line where less severe conditions exist, then the breaker may have a larger factor of safety than under its rated conditions. Cases have been observed where the break distance of breakers was inadequate for operation in generating stations but proved to be satisfactory in substations because, due to the arrangement and connections of the system, the arc length obtained for a given ampere interruption was less.

---

[1] For a complete description of this testing station, see "The High Capacity Current Interrupting Testing Station of the General Electric Company," by C. E. Merris, General Electric Review, June, 1923, p. 455.

Speed of Break

The interrupting capacity of a breaker depends upon the speed of the break, but one cannot say that the higher the speed the greater the interrupting capacity in every case. The interrupting capacity of a breaker depends not only upon the quantity of gas generated, but upon the speed of generation; and it may well be that a given breaker, if operated at higher speed, will have a lower interrupting capacity. The higher speed may well result in a longer arc, more gas, and more pressure than if operated at the lower speed, and this condition has been observed in test. Before the effect of a speed change can be determined, the many factors relating to that particular breaker must be known.

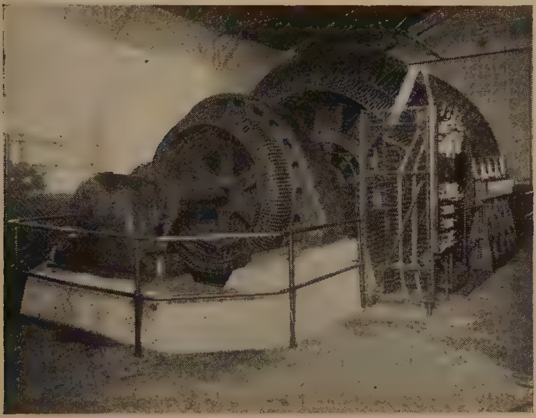

Fig. 1. Motor-generator Testing Set Used in Making the Oil Circuit Breaker Investigations

In what has been written about speed of break, it has been assumed that the moving contact was traveling at practically uniform speed. As a matter of fact, however, every breaker will have its own speed characteristic and this characteristic at no load may be decidedly different from the full interrupting capacity speed. In fact, at some load, the speed may not only slow down but actually stop and reverse in direction so as to reclose the breaker. There are several reasons for this behavior and none of the plain break breakers can be considered as entirely unaffected by it. Whether the defect is a serious one in any particular case can only be determined by actual test of the breaker under severe conditions.

In the case of fairly low voltage breakers, operating to interrupt large current, the actual speed of the moving contact may have little relationship to the interrupting capacity of the breaker, as such breakers interrupt the arc by the magnetic blowout effect instead of the physical separation of contacts. It may be found, however, that the heaviest stress is not produced by the largest current interrupted and that more gas and greater pressure are produced when interrupting a lesser current than that of the maximum rating. It is needless to say that the breaker must be safe when interrupting these smaller currents and that this fact must be considered in the rating of the breaker.

Oil Head

The head of oil over the contacts influences the interrupting capacity of the breaker, as it largely determines the pressure above and below the oil surface and therefore tank rupture. It also determines the arc stabilizing, shock to the entire breaker structure, oil throw, and gas ignition. Too much oil in the tank is as bad as too little. The correct quantity to use can be determined only by repeated tests at all loads up to the interrupting capacity rating of the breaker. In testing oil circuit breakers on skids, it is frequently noticed that the breaker jumps clear from the floor at the instant of interruption. This of course is due to the kinetic energy in the oil (as a result of being blown by the arc gas) which is expended when the oil mass strikes the top of the breaker. This shock may be so severe as to break the top casting of the breaker.

Air Space Above the Oil

The proper air space above the surface of the oil will vary with each individual breaker and the correct quantity has to be settled by the designer as a result of his observations of the action of various breakers under test. It should be noted that the tank pressure is not the only factor to be considered as affected by the air space, as there are also oil throw, arc stabilizing, secondary explosions, and gas ignition. Oil head and air space must be considered together.

Various Types of Venting

The venting of an oil circuit breaker is an important problem, as it affects the oil throw, tank pressure, and gas ignition. It has come to be recognized that the modern high class breaker must limit the ejection of oil or incandescent gases into the room at the breaker, and in order to accomplish this end a thorough investigation of the problem was made. As a result of these tests, the oil-throw problem is well in hand; but it should be realized that small and inexpensive breakers will not be free from oil throwing at extreme loads. The non-oil-throwing breaker is a comparatively modern product, and the vast majority of breakers now in use were designed with little regard to the question of oil throw. Hence their construction does not readily lend itself to their being rebuilt into a non-oil-throwing type.

Determination of Allowable Tank Pressure

In oil circuit breaker design, the maximum instantaneous pressure to which the structure may be safely subjected is of great importance, as it determines the safe interrupting capacity of the breaker. The foregoing statement refers particularly to those breakers having tanks of other than circular shape. Such information can be had only as a result of repeated tests when utilizing suitable recording instruments in connection with a source of power such as the large testing generator used in these investigations. Any calculations of static stresses which the structure will withstand are difficult to make and the results obtained, due to the lack of proper constants, are wide from the actual permissible pressures.

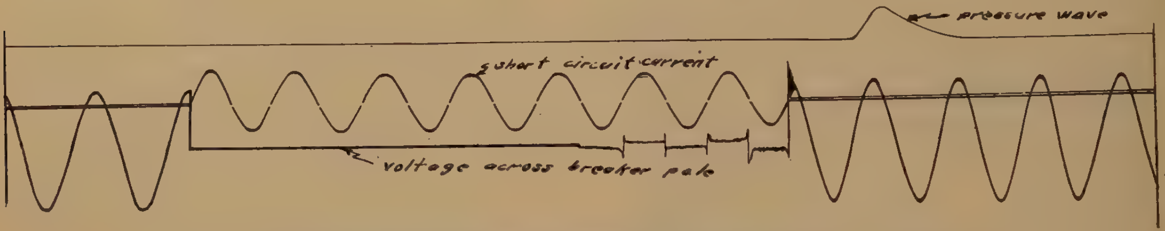

Fig. 2. Oscillogram Showing Secondary Explosion in an Oil Circuit Breaker, Explosion Occurring 0.014 Sec. After Current Was Interrupted

Method of Tank Construction and Best Material

Here also the use of the testing generator was invaluable as it settled questions which had been debated previously, but without any definite result, and the results of these tests are sure to show up in future records of performances.

Methods of Tank Support

Definite results have been obtained from the investigation of the method of supporting the tank and in all new breaker design advantage is taken of the findings from the tests.

Tank Lining Investigation

The question of what material should be used for the oil tank lining and, in fact, whether it should be lined at all, is one of great importance. The tests made with the large testing generator have definitely answered these questions. They have shown that linings are in most cases necessary, and that there is a decided difference in the efficiency of various linings. Just why one type is best in one case and another type better under other conditions has been determined.

Contact Investigation

One of the most important details in oil circuit breaker construction is that of the contacts, both main carrying contacts and arcing contacts; and more attention is given this one feature than any other entering into the breaker construction. The investigation of these contacts included not only their burning and carrying capacity, but also the heat generating and dissipating characteristics of the connected studs and busbars, the effect on the brush by the shock of closing the breaker, the degree of over-travel the brushes will stand, the permanency of the brush structure, the specification for the brush metal to give best results, the best contact pressure and area of contact, and the design of contacts so that they will not be affected by the magnetic stresses under short-circuit conditions.

The burning of the contact members of an oil circuit breaker is a very important factor in these investigations and probably receives more attention, while the breaker is undergoing tests, than any other single feature. Repeated tests are made at the standard number of duty cycles. This means that the breaker is tested in closing on a short circuit as well as opening the short circuit under duty conditions, which is the equivalent of the rated interrupting capacity of the breaker and the worst possible circuit conditions. Contacts are also tested to destruction in order that definite information may be obtained as to the maximum continuous duty the contacts will stand.

The brush heating is the chief feature of the circuit breaker which may be adversely affected by the action of the operating company. This may come from the improper adjustment of pressure at installation, by the use of insufficient busbar cross-section, by the heat insulation of that section, by the insulating tapings, by the running of cables carrying large currents causing eddy current losses, by installation of tanks close together, which decrease heat radiation, and by the installation in unventilated cells in locations where the ambient temperature is high.

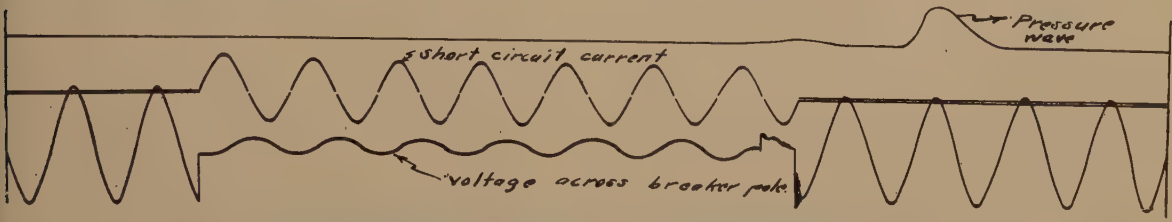

Fig. 3. Oscillogram Showing Secondary Explosion in an Oil Circuit Breaker, Explosion Occurring Approximately One Cycle After Current Was Interrupted

Ability of Breaker to Withstand the Shock of Oil Throw

Without a testing generator of large capacity, it would have been impossible to test for this condition which in the past has been responsible for serious breakages.

Reclosing Characteristics of the Breaker

The conditions under which the breaker contacts slow up or actually reclose have received special consideration and facts have been discovered which were not suspected at the time of starting the investigation.

Oil Throw and Gas and Oil Ignition

These features have been investigated in the case of the old style breakers; the newer breakers do not have these defects. It is, of course, impossible to stop the throw of oil and gas in the old type breakers without practically rebuilding them; however, the tests have shown how it would be possible to alter the breakers so as to prevent ignition.

Secondary Explosions

Attention was given to the cause and magnitude of secondary explosions. The tests were made with a bomb and also upon full-size oil circuit breakers. Oscillograms, Figs. 2 and 3, show such a secondary explosion. They indicate that the breaker interrupted the circuit with ease; that in 0.014 sec. after interruption, pressure developed in the air space (Fig. 2); that the maximum pressure was reached in 0.004 sec.; that the pressure below the oil, due to the necessary acceleration of the oil mass, was delayed 0.007 sec. behind the air space pressure. The breaker was not injured. These secondary explosions are nearly always caused by a static spark igniting the explosive gas mixture and may come while the breaker is open or closed. Their cause is well understood, and if the station operator exercises proper care there should be no such explosion in the newer breakers.

Acceleration and Retardation of the Moving Contact Member

The acceleration of the moving contact member under short-circuit conditions is extremely important and equally important is the retardation, especially in the case of the explosion chamber breakers. With these latter breakers any desired speed of opening may be readily obtained. The breakers are specially designed to give the desired opening speed and means have been developed to decelerate moving parts satisfactorily.

Investigation of Magnetic Stresses Produced in the Breaker

Magnetic stresses may cause the lifting of the brush or the throwing back of some types of arcing contacts at "Make." Such stresses may also cause movement of bushings and studs. The current limits of various designs have been determined and designs for higher duty developed.

Arc Stabilizing Tests

If the contact blocks under oil are not separated a sufficient distance or there is insufficient distance between these blocks and the metal part of the operating rod or cover or tank, an arc is liable to be stabilized across these insufficient distances and cause the destruction of the breaker. The safe distances depend upon the voltage, circuit conditions, and amount of current interrupted; and each type of breaker is tested many times under the most severe condition of operation in order to prove that the distances to prevent stabilizing are ample.

OIL VISCOSITY AND OTHER OIL CHARACTERISTICS

The characteristics of the oil used in oil circuit breakers is an important factor in the satisfactory operation of the breaker, and the oil supplied with the General Electric oil circuit breakers is rigidly held to specification. Miniature tests are not only made in the research laboratories, but tests are also carried out with the large testing generator. That oil is best which produces the least quantity of fixed gas for a given interruption, which has the least carbon production, the most suitable oil viscosity for the particular breaker in which it is to be used, the highest dielectric strength for the given interruptions, the smallest quantity of oil vaporized, the greatest percentage carbon precipitation, the least absorption of moisture, and the highest flash point. The oil affects the circuit breaker operation in ways little realized by those not intimately connected with breaker investigation.

Other arc-extinguishing liquids are also under constant observation by means of the full-size tests. Miniature tests show interesting results, but definite conclusions can be obtained only by comparing such tests with tests made on full-sized apparatus.

DUTY CYCLE TESTS

All breakers are tested at the new proposed duty cycle, *i.e.*, two open-close-open at the rated interrupting capacity, or if that cannot be obtained, at capacities which may be used to interpolate and thus obtain the full duty.

Tests have also been made at duty cycles other than standard, in order to determine the relative severity of these supplementary cycles.

Gas Production and the Resulting Stresses Upon the Breaker

An extended investigation into the gas generated by the arc has been carried on with the large testing generator and will be continued. In these tests, the gas volume generated, the speed of generation, the pressures above and below the oil level, and the current and voltage at the break, are all recorded on the oscillograph. The effect on the breaker structure is also recorded. These data are used in obtaining an empirical formula with which to calculate the interrupting capacity of any existing breaker and the design information for any new breaker of any proposed interrupting capacity. In this connection it can be stated that, theoretically, the quantity of gas generated depends upon a large number of variables. For instance, the r.m.s. current and voltage varies throughout the arcing period, the current decreasing and the voltage at the arc increasing with time. The resistance of the gas stream and the dielectric strength of the gas vary with the pressure and temperature of the gas, and since the gas generation is a heat phenomenon, this pressure affects the I^2R losses and the dielectric strength affects the duration of arcing. Then there is the effect of the magnetic blow-out which affects the arc duration. The power-factor and shunt load both affect the recovery voltage, which in turn affects the re-establishment of the arc at each zero value of the current wave, the available stored energy—electromagnetic and electrostatic—in the circuit, which may be discharged through the arc at the zero current value and aid re-establishment of the arc, and other causes—all of which combine to make the gas production extremely fluctuating. The extent of this fluctuation is shown in Fig. 4, on which has been plotted the volume of gas generated and current in the arc at definite voltage and circuit conditions. It is evident that

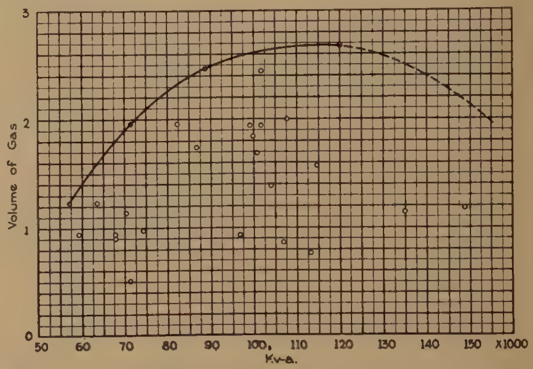

Fig. 4. Plot Showing Fluctuation in Volume of Gas Generated in Oil Circuit Breaker at Various Interrupted Currents at Constant Potential. Curve drawn through highest test values obtained

the empirical formula for interrupting capacity determination must be based upon the curve of the extreme points, as plotted from the tests, and that such a curve can be obtained only by means of a large number of tests made with a generator able to produce the conditions at the desired rating.

Investigation into the Action of the Oil Circuit Breaker Under Various Conditions

That the action of the oil circuit breaker is very erratic is soon realized when one attempts a systematic investigation of its action. Individual short circuits vary widely in effect, even when all conditions of the short circuit are made as nearly identical as possible. That is, given a generator, running at a definite speed, and excited to the same voltage, with the same impedance in circuit, and short circuited by the same breaker, under the same conditions of grounding, the gas generated may vary several hundred per cent. The gas generated is the final measure of the efficiency of a given breaker, but the speed of generation must, of course, be taken into consideration. If fluctuations to the foregoing extent are observed under constant and controlled conditions, what must be the variation during the ordinary short circuit on commercial systems where the field excitation, power-factor, shunt load, conditions of grounding, and other factors vary widely?

In general, on commercial systems the factors mentioned are usually combined so that the interrupting conditions are less severe than they are under the controlled conditions of test. Therefore, it is safe to assume that breakers which will pass tests with the testing generator equipment will give satisfactory service under normal operating conditions. By normal operating conditions is meant conditions limited by the normal generator and circuit characteristics and would not, for instance, include a heavy lightning stroke or cross with a higher voltage line.

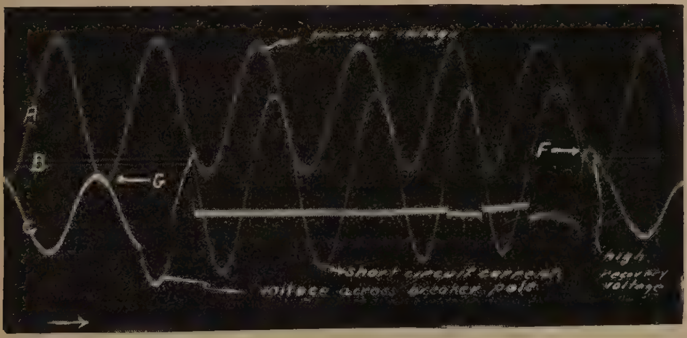

Fig. 5. Oscillogram Showing Recovery Voltage When Interrupting an Ungrounded Circuit

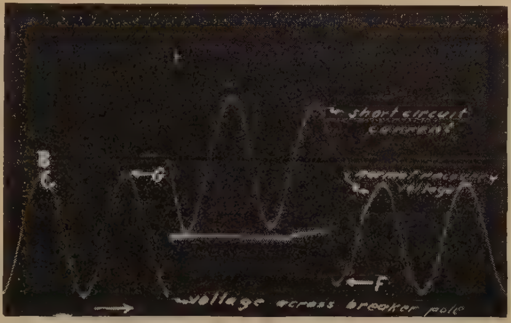

Fig. 6. Oscillogram Showing Recovery Voltage When Interrupting a Circuit Grounded at the Generator Neutral and at the Point of Short Circuit

The service condition where an oil circuit breaker in a generating station controls a single feeder is in general equivalent to the condition obtained with the testing generator and should produce equivalent results.

There is, however, considerable difference in the operation of breakers on ungrounded systems, as compared with operation on systems with the neutral grounded and a short circuit to ground.

Oscillogram Fig. 5 shows a short circuit upon an ungrounded system and oscillogram Fig. 6 shows a short circuit with the same apparatus upon the same system with the neutral grounded and a ground at the breaker. The feature to be noticed is the recovery voltage, which is characteristic of the two conditions and is considerably greater in the case of the ungrounded system. The greater recovery voltage means a longer arc and more gas generated in the breaker before final interruption of the circuit. By recovery voltage is meant the instantaneous voltage rise at the instant of circuit interruption, that is, it is the voltage which tends to re-establish the arc at the zero value of the current wave. In this connection, it might be said that while we state broadly that the interruption of the circuit always takes place at the zero value of current, this statement should not be taken too literally. It takes a certain voltage to maintain an arc; the longer the arc, the higher the required voltage, so that a time must come at every operation when the circuit tends towards interruption and before the absolute zero value is reached. This fact will largely account for the "kick" which will be made manifest by the use of spark gaps, but is not shown by the oscillograph, it being a steep wave-front phenomenon. The action of this phenomenon, however, is to aid in re-establishing the arc.

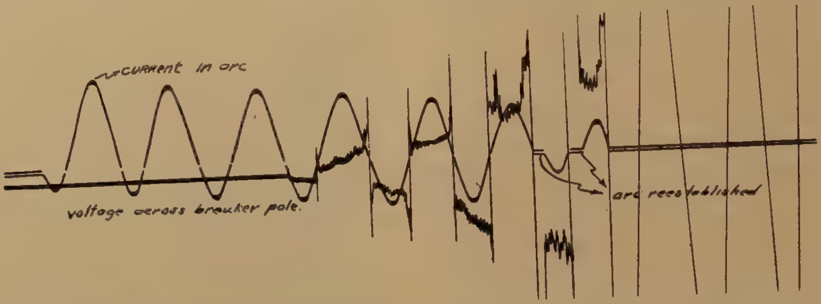

Fig. 7. Oscillogram Showing Re-establishment of Current in the Arc Drawn by an Oil Circuit Breaker, the Re-establishment Occurring a Considerable Time After the Zero Current Value

That the circuit may be re-established, some considerable time after the zero current value, is shown in oscillogram Fig. 7 in which case about 60 electrical degrees have elapsed before re-establishment. This case is not unusual, on the contrary it is quite frequently noticed. The arc is of course an energy phenomenon and the current and voltage in the arc are substantially in phase, but at the instant of final circuit interruption there is a change in the relationship of the two and the lag of current is then determined by the circuit as a whole. This is important, because it in a way explains why the lower power-factor circuits are the harder to interrupt. At zero current value and 90 deg. lag, the maximum voltage is available to re-establish the arc, while at unity power-factor there is zero voltage at zero current. This difference caused by power-factor variation is really one of time only, because if we assume a case of unity power-factor and a 25-cycle circuit, the same voltage is applied at the expiration of 0.01 second as would have been applied instantaneously at zero power-factor. During this 0.01 second, the gas has had a chance to cool, thereby increasing its dielectric strength, and the gap has been increased (assuming an opening speed of 5 ft. per second) by 0.6 in. Both of these factors act to increase the interrupting capacity of the breaker in the case of unity power-factor.

Investigation of the Magnitude of Current Interrupted upon Circuit Breaker Action

In the case of fairly low voltage, the magnetic blow-out effect has to be considered in connection with the interrupting capacity of the breaker. The curve in Fig. 8 shows such a study. This indicates that the maximum arc length corresponds to a fairly definite current value and that any increase in current above this value acts to decrease the arc duration.

The logical deduction is that at some current value, less than the maximum interrupting rating, the breaker may fail. This deduction is correct and many breakers are undoubtedly stressed more at partial rating than at their maximum rating.

Comparison of the Plain and Explosion Chamber Breakers

The oscillogram in Fig. 9 shows a plain break interruption, and the curve in Fig. 8 shows the plot of arc lengths and currents on such a breaker. The erratic behavior of the plain break breaker is striking but is characteristic of its class. The oscillogram in Fig. 10 shows an explosion chamber interruption in the same tank at substantially the same current and with the same mechanism,

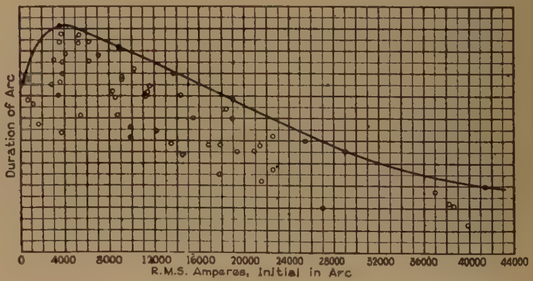

Fig. 8. Arc Duration as a Function of Current Interrupted by a Plain Break Oil Circuit Breaker

while the oscillogram in Fig. 11 shows the same explosion chamber breaker interrupting substantially double the current at 1.73 times the voltage of the plain break breaker in Fig. 9.

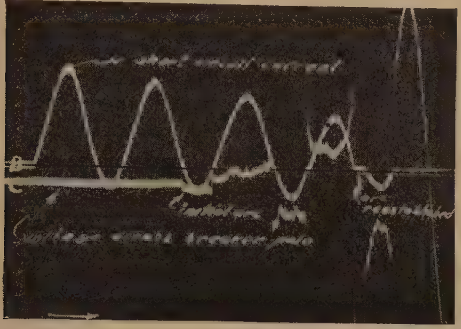

Fig. 9. Oscillogram Showing Arc Interruption by a Plain Break Oil Circuit Breaker

The curve in Fig. 12 shows the plot from tests of half cycles and currents of an explosion chamber breaker.

The foregoing oscillograms and plots are characteristic of the two types of breakers and comments are not needed as to the story they tell in reference to breaker efficiency, an efficiency which increases with the voltage increase in the case of the explosion chamber breaker.

Testing of Breakers to Operate Under Special Conditions

For this class of work the testing generator equipment is invaluable, as it obtains results and definitely settles questions that would be impossible without such an equipment. Miniature tests are of little value unless they can be compared directly with tests made on regular apparatus under operating conditions.

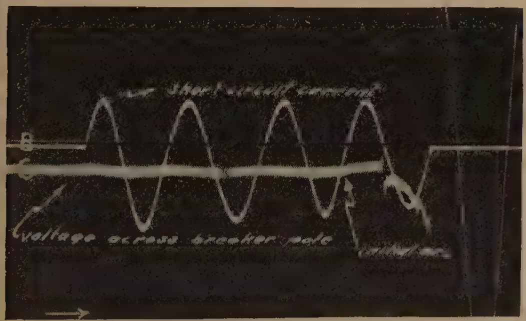

Fig. 10. Oscillogram Showing Arc Interruption by an Explosion Chamber Oil Circuit Breaker

In order to be proved safe, every breaker must be tested under full maximum operating conditions or must be compared with a similar breaker which has operated under these conditions.

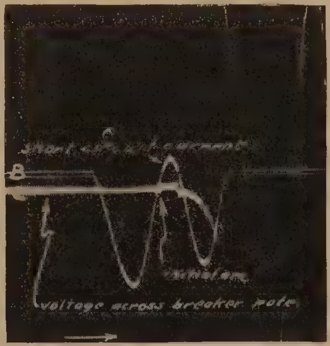

Fig. 11. Oscillogram Showing Behavior of Same Breaker as in Fig. 10 at Higher Current

CONCLUSIONS

What has preceded shows the large number of variables which enter into the determination of the oil circuit breaker interrupting capacity. It shows that each variable depends upon the others and that the breaker as a whole must be judged from results obtained when actually performing under loads which vary from the smallest up to its maximum rating and under repeated operations at each value. A single shot at any particular load is far from conclusive and the only safe rating is that obtained from plotting many tests made at all capacities.

For this work, the large testing generator has proved indispensable. It has made clear phenomena previously not understood. It has brought out facts not dreamed of until they were shown up by the tests. It has pointed the way as to what features to avoid and what improvements to make, and its influence is showing in the design and performance of breakers and will continue to show its value in the research which is already planned for years ahead.

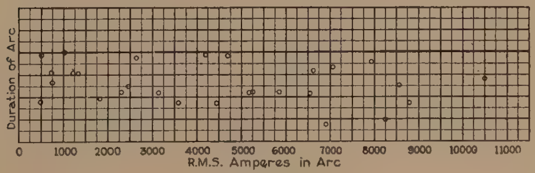

Fig. 12. Relation of Arc Duration to Current Interrupted by an Explosion Chamber Oil Circuit Breaker

Studies in the Projection of Light

PART XV

DESIGN AND OPTICS OF SECOND-SURFACE MIRRORS

By Frank Benford

Physicist, Illuminating Engineering Laboratory, General Electric Company

Familiarity is said to breed contempt, and we are inclined to accept the plane second-surface mirrors that we look into many times daily as being exceedingly plain in nature. But, as the author points out, the plane mirror is rather complicated in its optical action and there results what may be a serious deviation from really plane reflection when used in connection with precision work. The rules governing the construction of an optically plane mirror lead to a curved surface with a fixed focal point. The development of this surface is important because it establishes mathematically the validity of the rules that are known to be practically correct for the paraboloid, the hyperboloid, and the ellipsoid. The two latter surfaces are taking their places alongside the paraboloidal mirror as more or less common articles of commerce, and as the art advances there is every reason to believe that the optically correct forms here presented will supplant the more or less haphazard forms now seen. A point of minor importance that is discussed is the surface of virtual reflection, which is used by the author to demonstrate that there is no short cut to the design of a second-surface mirror.—Editor.

In solving for an expression for the co-paraboloid the extremely simple relation

$$T=\frac{T_o}{\cos c}$$

was found to describe the surface accurately, and as the parabola is one of a number of related curves—the conic family—it might reasonably be expected that the same relation will hold for the others. Several mirrors—ellipsoids, paraboloids, and hyperboloids—have been designed with the aid of the foregoing equation and care has been taken to check up points by means of the longer and more accurate path-length method. The nature of the agreement, or lack of it, will be given in some detail later, using data that are from computation on mirrors designed for special purposes that required more than the usual accuracy of projection.

In developing the co-paraboloid, the fundamental condition was that the independent first-surface beam and the beam reflected from the second surface should coincide in position of the image. The same conditions will be imposed on the several mirrors discussed later. When the light is converged to a focal point both surfaces must concentrate the light at the same point, and when the reflected light diverges from a virtual image the several components of the beam must again agree on a common point of divergence.

In every case, the source of light is a point source at a focal point of the first surface, and the highly important features of image size and beam formation from a finite source are not touched upon. This part of the work has previously been considered in detail in the case of the paraboloid, and much of the graphical exploration is directly applicable to the other conic mirrors. It will be realized, of course, that once the two surfaces of a mirror are brought into optical co-operation we may treat both surfaces as a unit, and the mirror becomes, for our purpose at least, a simple first-surface mirror.

By taking a slight liberty in the matter of definitions, the plane mirror may be included among the conics. The plane mirror has many interesting and important properties, chief among which is the fact that a physically plane mirror is not optically plane, and also the demonstration of the triangle solution for thickness can be carried out readily for any angle, thus giving a general demonstration of this relationship between the thickness of glass at various parts of the mirror and the angle of refraction.

There are several features of the plane mirror in addition to its thickness that are of importance, and these features will be taken up as a preliminary to the discussion of the thickness of glass.

SECOND-SURFACE MIRROR WITH TWO PLANE FACES

A second-surface mirror with two plane parallel faces is not optically a plane reflector. The first surface reflects its portion of light as a plane, that is, the virtual image is as far back of the surface as the object is in front of it and the object and image are on a common perpendicular to the surface. This condition holds for any angle from which the image is viewed and for any position of the source. But when the second-surface image is investigated, it is found that this simple and universal rule does not hold. Not only is the image variable in position depending upon the angle of reflection but, as will soon be shown, the image is distorted into two line images (of a point source) similar to the images from meridian and sagittal lines in the parabolic mirror.*

It is occasionally necessary to use a second-surface mirror either for experimental work or as part of an instrument, and the precise mechanism of the reflecting action is therefore a matter of some importance, particularly if the glass is thick, as is usually the case for the best quality of large mirrors.

Images for Meridian and Sagittal Sections

In Fig. 157, a point source is shown located at M and at a distance F from the first surface of a second-surface mirror. A ray from the source to point P_1 on the first surface makes an angle a with the normal, and an angle c with the normal after refraction. The second surface being parallel to the first, the internal angle c and the external angle a at the point of exit P_3 will be the same as at P_1, that is, the path of the ray will be symmetrical about a normal at P_2.

A second ray given off at a slightly increased angle $a+da$ pursues a path that diverges from the first path; up to the point P_1 the divergence is da, but within the glass the divergence is dc, and upon emerging the original divergence da is resumed. These two rays, if extended behind the mirror to their point of virtual intersection will meet at some point F_m, which it is now proposed to locate.

In Fig. 157 the length of the meridian element between the points of incidence of the two rays at P_1 is

$$ds_1=\frac{da}{\cos^2 a} \tag{225}$$

and from P_1 to P_2 a further separation by the angle dc takes place, so that

$$ds_2=ds_1+T\frac{dc}{\cos^2 c} \tag{226}$$

This separation is doubled in passing to P_3, so that

$$ds_3=ds_1+2T\frac{dc}{\cos^2 c}$$

$$=\frac{da}{\cos^2 a}+2T\frac{dc}{\cos^2 c} \tag{227}$$

It was previously shown that from Snell's equation

$$\sin a=n \sin c \tag{228}$$

the relation

$$dc=\frac{\cos a}{n \cos c}\,da \tag{229}$$

is obtained by differentiation.

Substituting in equation (227), we get

$$ds_3=\frac{da}{\cos^2 a}+\frac{2T}{n}\frac{\cos a}{\cos^3 c}\,da \tag{230}$$

The length of ds_3 may also be expressed in terms of the divergence da of the rays refracted at P_3 and the distance F_m from P_3 to the point of intersection.

$$ds_3=\frac{F_m}{\cos a}\,da \tag{231}$$

Equating (230) and (231)

$$\frac{F_m}{\cos a}\,da=\frac{da}{\cos^2 a}+\frac{2T}{n}\frac{\cos a}{\cos^3 c}\,da$$

$$F_m=\frac{1}{\cos a}+\frac{2T}{n}\frac{\cos^2 a}{\cos^3 c}$$

$$=\frac{1}{\cos a}\left[1+\frac{2T}{n}\frac{\cos^3 a}{\cos^3 c}\right] \tag{232}$$

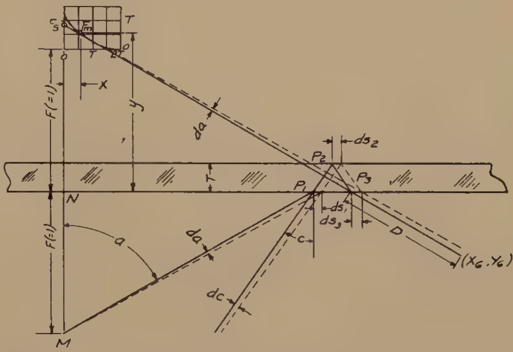

Fig. 157. In this diagram two adjacent rays in the plane of the paper are traced through the glass and their point of virtual origin is found to fall on the small curve in the upper left-hand corner of the illustration and two rays in adjacent vertical planes through MN Meet at F_s; the image can therefore be considered as being divided into two sections, one at F_m and one at F_s

To locate the point F_m in space we may take the perpendicular through M as the Y-axis and the first surface as the X-axis. The origin is at the intersection of the perpendicular with the first surface.

$$x_1=\tan a+2T \tan c-F_m \sin a$$

$$=\tan a+2T \tan c-\tan a-\frac{2T}{n}\frac{\cos^2 a}{\cos^2 c}\tan c$$

$$x_1=2T \tan c\left[1-\frac{\cos^2 a}{\cos^2 c}\right] \tag{233}$$

and

$$y_1=F_m \cos a$$

$$=1+\frac{2T}{n}\frac{\cos^3 a}{\cos^3 c} \tag{234}$$

In Fig. 157 the small curve shown in the region of the image of M illustrates the path taken by the focal point F_m for different angles of the reflected ray. The image formed by a meridian section of the complete mirror is therefore variable in position and is not on the perpendicular through the source except at normal incidence.

---

*Part I of this series, February, 1923, pp. 77-78.

A sagittal section of the mirror, which in this case is a segment of a circle concentric about the foot of the perpendicular through M, forms an image that falls on this perpendicular. This is obvious from the fact that a ray in a given vertical plane through M remains in that plane after reflection. Thus two rays in adjacent vertical planes will meet at a point of virtual intersection at the intersecting lines of the planes. This line is of course the perpendicular through M and it remains only to find the point of intersection on this line.

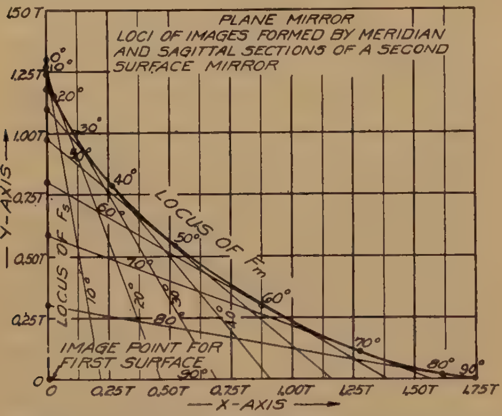

Fig. 158. The loci of images formed by meridian and sagittal sections of a plane mirror are here illustrated. This division of the image into "Sturm's conoid" makes the plane mirror an optical device of some complexity

From the similar triangles $M\ P_1\ N$ and $F_s\ P_3\ N$ of Fig. 157, we have the relation

$$\frac{NF_s}{NM}=\frac{NP_3}{NP_1}$$

$$NF_s=NM\frac{NP_3}{NP_1} \qquad (235)$$

But NM is taken as unity, and

$$NF_s=\frac{\tan a+2T\tan c}{\tan a}$$

$$NF_s=1+2T\frac{\tan c}{\tan a} \qquad (236)$$

The focal length, F_s, from the axis to P_3, Fig. 157, is

$$F_s=(NF_s)\frac{1}{\cos a}$$

$$=\frac{1}{\cos a}\left[1+2T\frac{\sin c\cos a}{\cos c\sin a}\right] \qquad (237)$$

and using equation (228) this may be put into the form

$$F_s=\frac{1}{\cos a}\left[1+\frac{2T}{n}\frac{\cos a}{\cos c}\right] \qquad (238)$$

The co-ordinates of the point F_s are

$$x_2=0 \qquad (239)$$

$$y_2=1+\frac{2T}{n}\frac{\cos a}{\cos c} \qquad (240)$$

In Fig. 158 the curve gives the locus of F_m, and the rays drawn from the curve indicate by their intersection with the left-hand edge of the web (the perpendicular through M) the corresponding locus of F_s. The ordinates of this curve are in terms of the thickness of glass, so that if the glass is say 8 mm. thick these loci will be to actual scale when both the X- and Y-axis are marked 8 mm. at the points now marked 1.00. The photometric error made by assuming the image to be fixed can be determined by noting the distance between the assumed point of radiation and the points F_m and F_s. The curve in Fig. 158 makes this computation relatively simple in any given case, but better still, it points out the advisability of avoiding the use of a plane mirror under conditions where the shifting image may lead to error.

Equivalent Position of Single Image

The equivalent position of the image in a plane mirror may be found as follows:

The width of the beam from the virtual focal point F_m, Fig. 157, is da, where da is measured in the plane of the paper. The component of light from the sagittal element apparently originates at the virtual focal point F_s, and we may call its divergence dp. If the light source at M has an intensity of I candles, the quantity of light dF contained within the solid angle (da) (dp) is

$$dF=I\ (da)\ (dp) \qquad (241)$$

The area covered by the rectangular beam (da) (dp) at some distance D, Fig. 157, from the point of exit P_3 is

$$dA=(F_m+D)\ da\ (F_s+D)\ dp \qquad (242)$$

The illumination at the distance D is

$$E=\frac{dF}{dA}=\frac{I}{(F_m+D)\ (F_s+D)}\text{ ft-cd.} \qquad (243)$$

This equation is not in the most convenient form for use, principally on account of the difficulty of measuring the distance D, but if the coordinates (x_6, y_6) of the latter point, Fig. 157, are used, the illumination equation can be given the more usable form

$$E = \frac{I}{[(x_6 - x_4)^2 + (y_6 - y_4)^2]^{\frac{1}{2}} [x_6^2 + (y_6 - y_5)^2]^{\frac{1}{2}}} \qquad (244)$$

where

(x_4, y_4) are the co-ordinates of the F_m point
(x_5, y_5) are the co-ordinates of the F_s point $(x_5 = 0)$
(x_6, y_6) are the co-ordinates of the D point, using the same origin as for the F_m and F_s points (y_6 is negative)

The curve of Fig. 159 indicates the extent of the error caused by assuming the image to be stationary at a point. The data are for the particular case of an extremely thick mirror, $T = 0.18\ F$, and the points of photometric measurement are on a circle centered on the first surface image and having a radius 2 F. The determination was made graphically. From the form of equation (243) the error in reading is inversely proportional to the radius of the test circle and this leads to a working rule: "Photometric measurements made on the image of a small source seen in a plane mirror should be at least 250 times the thickness of the mirror removed from the first-surface image if the errors are not to exceed one per cent."

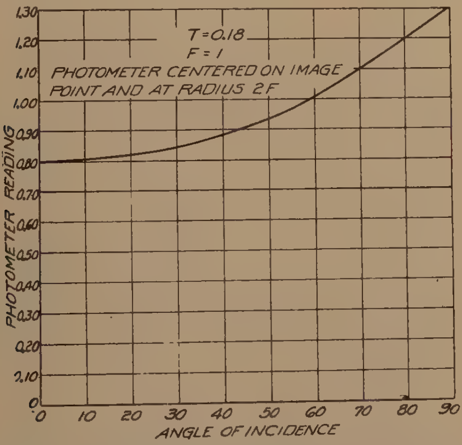

Fig. 159. The photometric readings made by a photometer swinging about the first-surface-image point at a radius of $2F$ will vary as shown by this curve. In this case $T = 0.25\ F$, but since the error varies as the thickness T, the curve may readily be reduced for more usual thicknesses of glass. This curve is imaginary beyond 60 deg. but that section of the curve may be used to compute values for any physically possible location of the photometer

There are two interesting facts brought out by Fig. 159. The negative error at normal incidence is equal numerically to the positive error at 90 degrees or grazing incidence. Also, and this is a useful fact, at 60-degree incidence the first- and second-surface images are at equal average distances from the point of measurement and the coefficient of the mirror can be measured at this angle without error. There still remains an error in the direction of the reflected light and a plane mirror can therefore not be used in any case where direction of reflection is important.

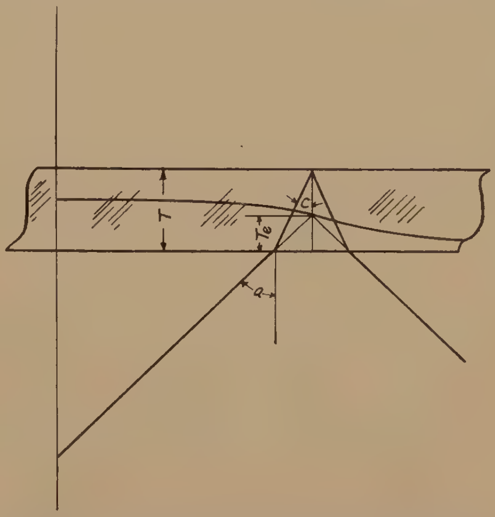

Fig. 160. The point of intersection of the incident and reflected rays, extended into the glass, gives a curved surface for the virtual point of reflection as here shown

Points of Virtual Reflection

The apparent point of reflection in a plane second-surface mirror is at a variable depth in the glass. In Fig. 160 the distance between the points of entrance and exit of a given ray may be used to locate the point of apparent reflection at a distance T_e from the first surface.

We have

$$2T \tan c = 2\ T_e \tan a$$

$$T_e = T \frac{\tan c}{\tan a}$$

$$= \frac{T \cos a}{\sqrt{n^2 - \sin^2 a}} \qquad (245)$$

At normal incidence the point of virtual reflection is at 0.66 the thickness of the glass, measured from the first surface. This depth of the virtual points decreases to zero at grazing incidence and for either plane or curved mirrors having high angles of incidence a correction should be made for the point of virtual reflection. Thus a 60-degree 36-in. parabolic mirror of 0.50-in. thickness and a focal length of 15 in. has an equivalent focal length of 15.33 in. and the virtual point of reflection at the edge of the mirror is 0.30 in. or more back of the first surface. In photometric tests for focal adjustment this small distance is a matter of some importance. In Fig. 161 the lower curve illustrates how the thickness to the point of virtual reflection varies with the angle of incidence.

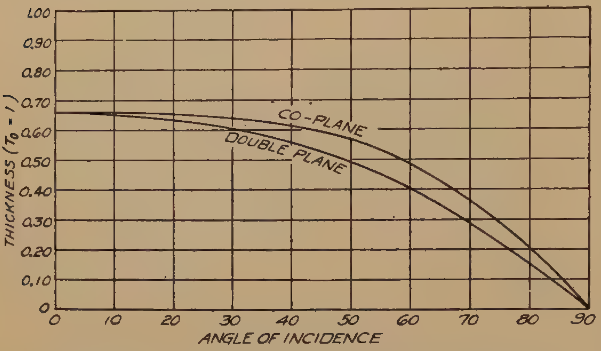

Fig. 161. The depth of the surface of virtual reflection is illustrated by these curves for both a geometrically plane mirror and a mirror that reflects as an optical plane. In both cases the virtual surface is curved

PLANE AND CO-PLANOID SECOND-SURFACE MIRROR

The derivation of the triangle solution for mirror thickness was in the case of the paraboloid based on the extreme edge of a mirror whose angular enclosure approached 180 degrees. The equation was found to reduce to a correct value for the thickness on the axis, and in the particular case of a certain mirror the errors were found to be alternately positive and negative, indicating that the triangle solution gave results correct at more than two angles. The plane mirror offers a complete solution for the triangle formula at any desired angle, which is preliminary to showing that the triangle solution is a universal rule that is not exact but is of a high degree of precision.

In Fig. 162, the source is at I_1, and the mirror is so constructed that the virtual source of light is at I_2 for both first and second surfaces. The wavefronts of both reflections are spherical and concentric about I_2 as a common center, but the light from the second surface will be retarded by a certain amount, which must obviously be a constant if the two wavefronts are concentric. Drawing a circle about I_2 at any radius $F+F+y$ as measured from the image point along the perpendicular to the mirror, we can write

$$2F+y=R_1+R_2 \qquad (246)$$

for the first-surface ray, and for a second-surface ray

$$2F+2n\ T_o+y=R_1+nL_1+nL_2+R_4 \qquad (247)$$

Subtracting equation (246) from (247)

$$2n\ T_o=n\ (L_1+L_2)+R_4-R_2 \qquad (248)$$

but

$$R_4-R_2=R_1-R_3 \qquad (249)$$

and

$$2n\ T_o=n\ (L_1+L_2)+R_1-R_3 \qquad (250)$$

which is another statement of the condition of concentricity of the two wavefronts.

In order to determine the relation of the second surface to the plane first surface when the foregoing condition is satisfied, we may proceed as follows:

Let a in Fig. 163 be a mid-angle between the ray to the point of entrance x_1, and the ray to the point of exit x_2. The former ray then has an angle $a-i$ and the latter $a+i$ when i is half the angle between the two rays.

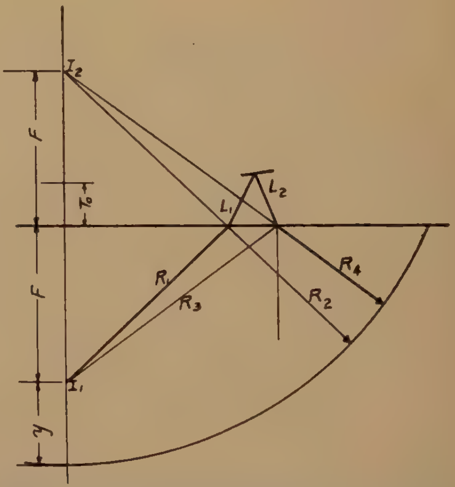

Fig. 162. In this diagram the reflected rays R_2 and R_4 ar directed so that the images formed by the first and second surfaces coincide at the point I_2

Let the second surface at x_3 be rotated through a small angle s; the normal will be rotated through the same angle s, and the reflected ray will be rotated through 2 s. The angle s being small, we may assume the normal to be common to both surfaces, that is triangles $x_1x_3x_4$ and $x_2x_3x_4$ are both assumed to have right angles at x_4. Equation (250) can now be written in terms of these new quantities.

$$2n_o\, T = n\left[\frac{T}{\cos\,(c+s)}+\frac{T}{\cos\,(c-s)}\right] + \frac{1}{\cos\,(a-i)}-\frac{1}{\cos\,(a+i)} \qquad (251)$$

which reduces to

$$2n\, T_o = nT\frac{2\cos c\,\cos s}{\cos^2 s-\sin^2 c}-\frac{2\sin a\,\sin i}{\cos^2 i-\sin^2 a} \qquad (252)$$

The angles i and s will in general be less than a quarter degree, and the square of their cosines will therefore be greater than 0.99992, so that we can without introducing any serious error write equation (252) in the simpler form

$$\begin{aligned} 2n\, T_o &= 2n\, T\frac{\cos c\,\cos s}{\cos^2 c}-\frac{2\sin a\,\sin i}{\cos^2 a} \\ &= 2\, nT\frac{\cos s}{\cos c}-\frac{2\sin a\,\sin i}{\cos^2 a} \qquad (253) \end{aligned}$$

The distance x_1x_2, Fig. 163, can be expressed in terms of a and i and also in terms of c and s.

$$\begin{aligned} &T\,[\tan\,(c-s)+\tan\,(c+s)] \\ &\quad=\tan\,(a+i)-\tan\,(a-i) \qquad (254) \end{aligned}$$

from which is derived

$$T=\frac{\cos i\,\sin i\,(\cos^2 s-\sin^2 c)}{\cos c\,\sin c\,(\cos^2 i-\sin^2 a)} \qquad (255)$$

Putting $\cos^2 s$ and $\cos^2 i$ equal to unity as before

$$T=\frac{\cos i\,\sin i\,\cos c}{\sin c\,\cos^2 a} \qquad (256)$$

from which is derived

$$\sin i = T\frac{\sin c\,\cos^2 a}{\cos i\,\cos c} \qquad (257)$$

Substituting this value of $\sin i$ in equation (253) we get

$$\begin{aligned} 2n\, T_o &= 2n\, T\frac{\cos s}{\cos c}-2T\frac{\sin c\,\sin a}{\cos c\,\cos i} \\ &= \frac{2n\, T}{\cos c}\left[\cos s-\frac{\sin c\,\sin a}{n\,\cos i}\right] \qquad (258) \end{aligned}$$

By Snell's Law

$$\frac{\sin\,(a-i)}{n}=\sin c \qquad (259)$$

but it has been found by trial that i reaches a maximum of about 0° 36′ when $a=30°$, and $T=0.04\, F$, and therefore we may write as an approximation

$$\frac{\sin a}{n}=\sin c \qquad (228)$$

Substituting in equation (258) we get

$$2n\, T_o=\frac{2n\, T}{\cos c}\left[\cos s-\frac{\sin^2 c}{\cos i}\right] \qquad (260)$$

Again placing

$$\cos s=\cos i=1 \qquad (261)$$

$$2n\, T_o=\frac{2n\, T}{\cos c}\,[1-\sin^2 c]$$

or, a further reduction

$$T=\frac{T_o}{\cos c} \qquad (150)$$

which is the identical expression obtained for the special case of the limits of the paraboloid.

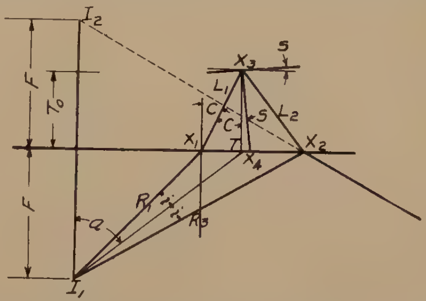

Fig. 163. This diagram shows the angle a taken as an average between the points of entrance and exit. The construction at the point x_3, where the surface is at an angle s with the front surface, leads to a figure of revolution for the second surface

The second surface is therefore not plane but is a surface of revolution that gives a gradually increasing thickness up to the limit

$$T=\frac{T_o}{\sqrt{1-\left(\frac{1}{n}\right)^2}} \qquad (152)$$

As a result of the several approximations made in simplifying, equation (150) is in maximum error at $a=30$ degrees by one part in 1000 for a mirror having a thickness of two per cent of the focal length. This error will increase in direct proportion to the thickness of glass. The focal point is fixed in this type of mirror so that no more freedom of movement is allowed than in any of the conic mirrors, and we may in fact consider the plane mirror as simply a limiting hyperboloid in which the eccentricity e is very large and the distance between the two branches of the curve is vanishingly small.

Points of Virtual Reflection

The determination of the points of virtual reflection is not so readily made in the case of a co-planoid second-surface mirror because the angles of refraction are not equal, but the points may be approximated as follows, reference being made to Fig. 161 and equation (245).

We have

$$T = \frac{T_o}{\cos c} \qquad (150)$$

and, substituting in equation (245)

$$T_e = \frac{T_o \cos a}{n - \frac{\sin^2 a}{n}} \qquad (262)$$

The important feature of this equation is that it shows the apparent points of reflection do not lie on a straight line and there is therefore no short-cut by this means to the determination of the back surface of the optically plane reflector. Also, by the form of the equation it is allowable to extend the same observation to curved mirrors, for the points of virtual reflection will in no case be a curve parallel to the front surface.

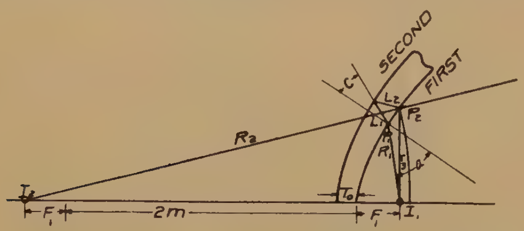

Fig. 164. This concave mirror is hyperbolic on the concave face and co-hyperbolic on the silvered or convex face

HYPERBOLOID AND CO-HYPERBOLOID

Light generated at one focus of a hyperboloid is reflected as if coming from the other focus. The two foci are interchangeable and the hyperbolic double-surface mirror may be either concave or convex. In either case the first surface is hyperbolic and the second surface is co-hyperbolic, as will be demonstrated.

In Fig. 164 a wavefront is shown concentric with the virtual source at I_2, and having a radius R_2. Equating the optical distances, measured from the source I_1, to this wavefront on the axis and at P_2, we get

$$F_1 + 2n T_o + R_2 - 2m - F_1 = R_1 + nL_1 + nL_2 \qquad (263)$$

which reduces to

$$2n\,T_o = n\,(L_1 + L_2) + R_1 - (R_2 - 2m) \qquad (264)$$

but

$$R_2 - 2m = R_3 \qquad (265)$$

and

$$2n\,T_o = n\,(L_1 + L_2) + R_1 - R_3 \qquad (266)$$

If now the points of refraction and reflection are carried out along the mirror until both the incident light and the reflected light are at grazing incidence, the triangle becomes isosceles, with the angle of incidence *a* equal to 90 degrees. Equation (264) can then be written

$$2n\,T_o = n\left(\frac{T}{\cos c} + \frac{T}{\cos c}\right) - 2T \tan c$$

$$T_o = \frac{T}{\cos c} - \frac{T}{n} \tan c$$

$$= \frac{T}{\cos c}\left[1 - \frac{\sin c}{n}\right] \qquad (267)$$

but

$$n = \frac{\sin a}{\sin c} \qquad (228)$$

therefore

$$T_o = \frac{T}{\cos c}\left[1 - \frac{\sin^2 c}{\sin a}\right] \qquad (268)$$

Putting

$$\sin a = 1 \qquad (269)$$

the final result is

$$T_o \doteq T \cos c$$

or

$$T = \frac{T_o}{\cos c} \qquad (150)$$

which is the same expression as derived for plane and parabolic mirrors.

The same demonstration can readily be made for a convex hyperboloid, using the notation of Fig. 165 which will give identical equations from equation (266) onward. In this case also the hyperboloid is next to the light source, that is, it is the first surface, and the co-hyperboloid is the convex or second surface. This order of surfaces is just the reverse of that for the concave hyperbolic mirror, and the two are therefore not interchangeable by simply transferring the silver backing from one face to the other.

ELLIPSOID AND CO-ELLIPSOID

The ellipsoid is the member of the conic family that is a closed curve and does not extend to infinity. The derivation of the triangle formula therefore is not possible in the ordinary way but it is possible to show that, as a practical design formula, the triangle solution may be used. Later, some design data will be given to illustrate the order of accuracy of the results. It might be remarked that when dealing with reflectors intended for illuminating purposes the required accuracy is greater in the paraboloid and less for the ellipsoid, which is used for short-range projectors; and it may also be less for the hyperboloid which is used when a certain amount of spread is desired.

In the field of motion-picture projection the ellipsoid is coming into use. The greatest collecting angle of a single condensing lens is about 60 degrees from the axis, and the light to the outer edge suffers considerable reduction due to reflection at the lens surface. There are other optical difficulties encountered and even if a train of two or three condensers is used, the outer angular limit remains about the same. The ellipsoid is not thus limited and its angle of collection may approach 180 degrees. The limits to the generating angle of the ellipsoid are set by other elements of the optical parts, such as the relative size of source and aperture, the focal length and diameter of the projecting lens, etc. These elements will not be discussed here, but they are mentioned to point out that ordinarily the ellipsoid is constructed with a greater depth, in proportion to diameter, than either the paraboloid or the hyperboloid, and while the curve cannot be extended to 180 degrees it does in practice come closer to that angle than either of the others.

In Fig. 166 the light source is at A_1, and the two rays shown, after reflection, are converged on the other focal point A_2. The axial ray to the left has an optical path length

$$P_1 = 2F_1 + 2n\,T_o + 2em \tag{270}$$

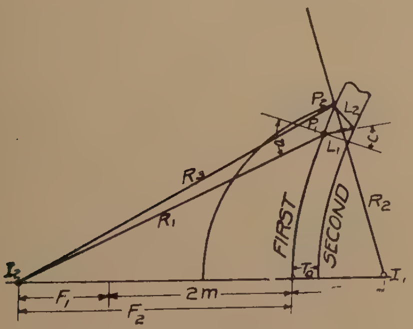

Fig. 165. This convex mirror is hyperbolic on the convex face and co-hyperbolic on the silvered or concave face

and the path starting with R_1 has the optical length

$$P_2 = R_1 + nL_1 + nL_2 + R_2 \tag{271}$$

Equating these two expressions

$$2F_1 + 2n\,T_o + 2em = R_1 + nL_1 + nL_2 + R_2$$

$$2n\,T_o = nL_1 + nL_2 + R_1 + R_2 - 2F_1 - 2em \tag{272}$$

But, from the definition of an ellipse,

$$R_2 + R_3 = 2F_1 + 2em$$

$$R_2 = 2F_1 + 2em - R_3 \tag{273}$$

and substituting in equation (272)

$$2n\,T_o = nL_1 + nL_2 + R_1 - R_3 \tag{274}$$

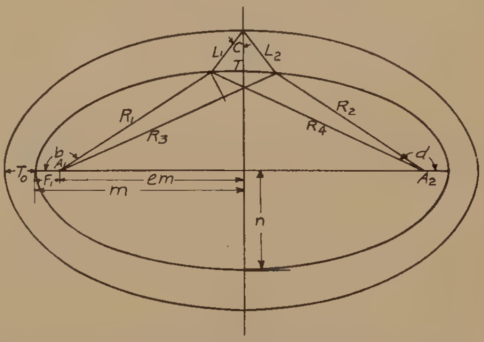

Fig. 166. This second surface ellipsoid is drawn to scale but to a greatly exaggerated thickness. The difference between the thickness on the major and minor axes is clearly visible

Calling the thickness of glass on the minor axis T, the optical path lengths over L_1 and L_2 are

$$nL_1 = nL_2 = \frac{T}{\cos c} \tag{275}$$

where there is an error involved in the assumption that the surface between the points of entrance and exit is straight instead of concave as in Fig. 166.

Also

$$R_3 - R_1 \simeq 2T \tan c \cos b, \text{ approximately.} \tag{276}$$

But the angle of incidence i at the end of the minor axis is

$$i = b - 90 \tag{277}$$

or

$$b = i + 90 \tag{278}$$

therefore

$$\cos b = -\sin i \tag{279}$$

and equation (274) may be written

$$2n\,T_o = \frac{2n\,T}{\cos c} - 2T \tan c \sin i \tag{280}$$

leading to

$$T_o = \frac{T}{\cos c}\left[1 - \frac{\sin c \sin i}{n}\right]$$

$$= \frac{T}{\cos c}[1 - \sin^2 c] \tag{281}$$

and finally

$$T = \frac{T_o}{\cos c} \tag{150}$$

which was to be demonstrated.

Instead of making a geometrical demonstration of the probable accuracy of equation (150) as applied to an ellipsoid, the following data are offered as the results of a complete set of computations made during the design of a mirror. The physical constants of the mirror were

$F_1 = 11$ in.
$em = 20$ in.
$T_o = 0.33645$ in.
$e = 0.64516$

and in Table XXI the computed data by the equal-path method and the triangle method are given in two columns.

TABLE XXI

THICKNESS OF GLASS IN AN ELLIPSOIDAL MIRROR

Angle Between R_1 and R_4	THICKNESS BY	
	Equal-path Method	Triangle Method
0°	1.000	1.000
23°	1.008	1.008
45°	1.033	1.032
64°	1.066	1.065
77° (max.)	1.096	1.095

These results seem to indicate a lower order of accuracy for the ellipsoid than has been encountered in any of the other conics. This view must be qualified by the observation that when the ellipticity is small and the ellipse becomes nearly circular the error reduces toward zero, which is attained when the ellipse reaches its limit, the circle. Also, when the ellipticity is approximately 1, that is, the curve is almost a parabola, the errors are again very small. Therefore, no generalization is here possible and the particular case given must stand alone as an example of the accuracy attained under a specific set of conditions.

This particular mirror was designed for use with a motion-picture projection machine, and the distance from the mirror to the working plane, the film, was only about 45 in. For this range, no high optical accuracy is needed and therefore the design data are far more accurate than needed for this mirror. In this type of projection we desire to avoid the streaked and uneven screen illumination that would result from a high accuracy of image formation, but the particular kind of optical error exhibited in Table XXI will not assist in this smoothing-out process.

Another application of the ellipsoidal reflector is found in a large lighting unit that has recently been designed for use on the boardwalk at Atlantic City.* The optical accuracy of this mirror need not be high because of the short distance (some 50 ft.) to the working plane, which in this case is the boardwalk. In both of these examples, the refinements of the design in Table XXI are not necessary, and certainly should not be insisted upon in the manufacturing specifications.

At the other extreme is the mirror which is claimed to have an ellipsoidal form with the conjugate focus at 2000 meters. The difference between a paraboloid and this ellipsoid is extremely minute, measured in terms of the best obtainable commercial mirror. While a projection accuracy of 1 minute of arc, which is the difference in projection direction from the paraboloid and ellipsoid to bring the edge rays to a focus at 2000 meters, is perhaps desirable, there is some doubt of its being at present attainable. The beam from the foregoing so-called ellipsoidal mirror, assuming correct curvature at all points, would differ from a parabolic beam only in a few minor details, and for practical projection purposes the difference is nil.

Between these two extremes there is a wide field of usefulness for an accurate ellipsoid and it should not be handicapped by the optical defects† that have operated to prevent the wider use of the glass paraboloid.

(To be continued)

---

*A cross-section of this lighting unit is given as Fig. 4 in the article by Mr. T. P. Brown, in this issue, page 803.

†Previously discussed in this series in Part XII, "Design of the Glass Paraboloidal Mirror" (Sept., 1924, p. 625), and Part XIII, "The Double Paraboloidal Mirror" (Oct., 1924, p. 698).

LIBRARY SECTION

Condensed references to some of the more important articles in the technical press, as selected by the G-E Main Library, will be listed in this section each month. New books of interest to the industry will also be listed. In special cases, where copy of an article is wanted which cannot be obtained through regular channels or local libraries, we will suggest other sources on application.

Alternators

Large Alternators, Field, A. B.
Engng., Oct. 17, 1924; v. 118, pp. 565-566.
(Abridgment of a paper presented at the World Power Conference.)

Alternators, High Frequency

Note on Polyphase High-Frequency Alternators. Chiba, Shigetaro.
I. E. E. Jour., Nov., 1924; v. 62, pp. 947-954.
(Mathematical paper.)

Ball Bearings

Ball Bearings for Motors. Huey, C.
Am. Soc. Nav. Engrs. Jour., Nov., 1924; v. 36, pp. 624-647.
(Advantages, disadvantages, limitations, and design data, as applying particularly to motors for the Navy Department.)

Capacitance

Measurement of Capacity by Analogy. Cramp, Wm.
Wld. Power, Nov., 1924; v. 2, pp. 267-273.

Circuit Breakers

Maintenance of Oil Circuit Breakers—Contacts and Oil. Biggin, H. L.
Power, Nov. 18, 1924; v. 60, pp. 797-800.

Coal, Pulverized

Pulverized-Coal Boiler Performance, Brunot Island Power Station. Heller, L. W.
Power, Oct. 14, 1924; v. 60, pp. 600-603.

Converters, Synchronous

Pressure Regulation of Rotary Converters by Means of Choke Coils. Thaning, O.
Brown Boveri Rev., Oct., 1924; v. 11, pp. 220-229.
(Mathematical article presenting data for use in design.)

Rectification of Polarity of Rotary Converters.
Bul. Oerlikon, Oct., 1924; pp. 170-171.

Electric Cables

Comparative Cable Wear with Different Types of Duct Endings. Rohrbach, F. L.
Elec. Wld., Oct. 18, 1924; v. 84, pp. 845-846.

High Tension Cables. Atkinson, Llewelyn B.
Wld. Power, Oct., 1924; v. 2, pp. 218-225.
(Abridgment of a paper presented at the First World Power Conference.)

Electric Distribution

Conducting a Distribution Survey—I. Nichols, E. G. and Eyre, J. R.
Elec. Wld., Oct. 11, 1924; v. 84, pp. 781-784.
(Method used by the Iowa Railway & Light Company, Cedar Rapids, Ia.)

Electric Distribution

Cost Data on a 6600-volt Rural Line. Robinson, J. C.
Elec. Wld., Oct. 4, 1924; v. 84, pp. 730-733.
(Gives cost data on a 12-mile line between Lincoln, Ill., and Atlanta, Ill.)

French Rural Electrification. Carney, H. Ambrose.
Elec'n., Nov. 21, 1924; v. 93, pp. 579-581.
(Gives some details of the transmission line and substation equipment used.)

Electric Drive—Mining

Cutting Down the Power Bill. Scott, L. Wilson.
Mod. Min., Oct., 1924; v. 1, pp. 72-75.
(On the economies that may be effected in the use of electric power at mines.)

Electric Drive—Pumps

Oerlikon Oil Circulating Pump, Built as Integral Part of Electric Motor.
Bul. Oerlikon, Oct., 1924; p. 172.
(Brief description of a small induction motor and pump unit for transformer oil circulation, and the like.)

Electric Drive—Steel Mills

Adjustable Speed Drives for Rolling Mills. Umansky, L. A.
Iron & St. Engr., Sept., 1924; v. 1, pp. 515-532.

Electrification of Tata Iron Works at Jamshedpur, India. Ghosh, S.
Iron & St. Engr., Oct., 1924; v. 1, pp. 545-552.

Experiences When Changing a Steel Mill Main Roll Motor Drive to Give Increased Capacity. McAuly, A. W.
Ind. Engr., Sept., 1924; v. 82, pp. 423-427, 457-458.
(Describes changes made by the Edgewater Steel Co.)

Problems of Steel Mill Operation. Whitcomb, Arthur J.
Ind. Engr., Sept., 1924; v. 82, pp. 408-416, 456-457.
(On electric drive. Includes table showing a list of electric drive main roll installations purchased during the past year.)

Electric Furnaces

Electric Melting Furnaces. Seede, J. A.
Iron & St. Engr., Sept., 1924; v. 1, pp. 490-494.
(Points out the more recent progress in design and use of melting furnaces.)

Medium and Low Temperature Applications. Hurme, E. A.
Iron & St. Engr., Sept., 1924; v. 1, pp. 503-513.
(Illustrated article showing possible applications of the electric furnace.)

Electric Furnaces

Medium Temperature Furnace Installations. Cone, C. F.
Iron & St. Engr., Sept., 1924; v. 1, pp. 494-503.
(Illustrated description of electric furnace installations in several different industrial plants.)

Electric Heating, Industrial

Costs of Electric Heating. Collins, E. F.
Elec. Wld., Oct. 25, 1924; v. 84, pp. 885-886, 887.
(Considers the factors which determine costs.)

Electric Heating with Special Reference to Central Stations. Sibley, E. D.
Iron & St. Engr., Sept., 1924; v. 1, pp. 513-515.

Electric Lighting

Year's Progress in Illumination 1923-1924.
Illum. Engng. Soc. Trans., Oct., 1924; v. 19, pp. 711-800.
(Report of the Illuminating Engineering Society Committee on Progress, 1924. Includes numerous footnote references to articles on the subject, and a list of the recent books.)

Electric Locomotives

Electric Locomotives for the Detroit & Ironton. Allison, Fred and others.
Rwy. Age, Oct. 18, 1924; v. 77, pp. 685-686.
(Describes locomotives designed to operate on a 22,000-volt, 25-cycle trolley supply. The electrical equipment is to be of Westinghouse manufacture. Also in *Electric Traction*, Oct., 1924, pp. 475-476.)

Electric Passenger Train Locomotive for the Railway Line Görlitz-Königsberg. Müller, Paul.
Engng. Prog., Sept., 1924; v. 5, pp. 173-174.
(Short description with illustrations, of a locomotive built by the Bergmann-Electricitäts-Werke for a German railway.)

Motor-generator Locomotives for the New Haven.
Rwy. Age, Oct. 18, 1924; v. 77, pp. 697-698.
(Short description of d-c. freight and switch locomotives with G-E electrical equipment. The 11,000-volt, 25-cycle, single-phase trolley current will be converted to d-c. on the locomotives.)

Electric Motors, D-C.

Economics of Power Consumption with Special Reference to Small D-C. Motors. Bolton, D. J.
I. E. E. Jour., Nov., 1924; v. 62, pp. 901-908.
(Viewpoints in the selection of motor sizes.)

Electric Ovens

How Electric Heat Has Been Put to Work in Low Temperature Enameling. Scott, Wirt B.
Auto. Ind., Nov. 20, 1924; v. 51, pp. 892-896.
(Author is Manager, Industrial Heating Section, Westinghouse Electric & Manufacturing Company.)

Electric Transformers

Special Applications of Standard Transformers. Gibbs, J. B.
Power, Nov. 25, 1924; v. 60, pp. 841-843.
("Factors to be considered when transformers are to be operated under other than rated conditions.")

Electrical Machinery—Temperature

Measuring Temperature in Electric Machinery. Stein, I. Melville.
Power Pl. Engng., Dec. 1, 1924; v. 28, pp. 1209-1211.

Ventilating Electrical Machinery.
Iron Tr., Nov. 27, 1924; v. 75, pp. 1443-1446.
(Applies especially to steel mill electrical machinery.)

Elevators, Electric

Operation of Electric Elevator Machines—Drum-type Equipment. Annett, F. A.
Power, Oct. 14, 1924; v. 60, pp. 609-612.

Excess Voltage

Excessive Voltage in Generators. Lyon, Waldo V.
Elec. Wld., Oct. 11, 1924; v. 84, pp. 784-785.

Excitation

Self-excitation of the Dynamo. Heather, H. J. S.
Wld. Power, Oct., 1924; v. 2, pp. 232-236.

Frequency Changers

Frequency Changers. Lubowsky, Kurt.
Elec'n, Oct. 10, 1924; v. 113, pp. 404-405.
(Explains the various systems employed, the control problems, load distribution, etc. Serial.)

High Voltage

High Voltage Phenomena. Faccioli.
Power Pl. Engng., Nov. 15, 1924; v. 28, pp. 1151-1155.
(An address before the American Institute of Electrical Engineers and the Western Society of Engineers, at Chicago.)

Hydroelectric Development

Building a Hydroelectric Plant on Saguenay River—I.
Engng. News-Rec., Oct. 16, 1924; v. 93, pp. 616-619.
(Describes the construction of the hydraulic features of a plant in Quebec, Canada. Serial.)

Power Developments at Stave Falls.
Elec. News, Oct. 15, 1924; v. 33, pp. 68-72.
(Illustrated account of a hydroelectric plant of the British Columbia Electric Railway Company.)

Inductive Interference

Inductive Interference with Communication Circuits. Russell, Alexander.
I. E. E. Jour., Nov., 1924; v. 62, pp. 941-946.

Insulating Oils—Testing

Testing Oil of High Voltage Transformers on the Premises. Orr, Frank.
Mod. Min., Oct., 1924; v. 1, pp. 76-77.

Insulators—Testing

High Voltage Insulators. Collins, A.
Elec'n, Oct. 17, 1924; v. 93, pp. 438-439.
("An accurate method of commercial testing.")

Locomotives, Mine

Efficiency of Electric Haulage in Mines. Harmon, C. A.
Mod. Min., Oct., 1924; v. 1, pp. 66-69.
(Discusses the economical installation and use of electric locomotive mine haulage systems.)

Locomotives, Mine

High-power Battery Locomotives for Shunting Purposes. Hiertzeler, M.
Brown Boveri Rev., Oct., 1924; v. 11, pp. 215-219.
(Illustrated account of various types manufactured by Brown, Boveri & Company.)

How to Proportion a Locomotive Storage Battery. Minnium, Byron B.
Mod. Min., Nov., 1924; v. 1, pp. 101-103.
(On the choice of battery capacity for mine locomotives.)

Unusual Electric Mine Locomotive. Bjornson, Edwin.
Engng. & Min. Jour.-Press. Oct. 25, 1924; v. 118, p. 674.
(Brief description of a Westinghouse locomotive built for the Alaska Juneau Gold Mining Company.)

Machinery—Erection

Erection of Overhead Crane Made Easy. Laing, William L.
Power, Nov. 25, 1924; v. 60, pp. 836-839.
(Presents practical methods.)

Installing an 1875-kv-a. Impulse Steam Turbine. Brown, Claude C.
Power, Oct. 21, 1924; v. 60, pp. 648-650.

Procedure for Alining Power Equipment.
Power Pl. Engng., Oct. 15, 1924; v. 28, pp. 1051-1054.

Machinery—Foundations

Foundations for Machinery Are Important.
Power Pl. Engng., Dec. 1, 1924; v. 28, pp. 1213-1214.

Machinery—Inspection

Transformer Inspection Practice.
Elec. Wld., Oct. 11, 1924; v. 84, pp. 794-795.
(Inspection procedure used by the Worcester Electric Light Company.)

Power Plants, Electric

Diesel Engines Eliminate Losses in Carthage Light Plant.
Power, Oct. 28, 1924; v. 60, pp. 684-686.
(Shows comparative costs of steam and Diesel power generation.)

New Plant at Fort Dodge Shows High Economy.
Power, Oct. 28, 1924; v. 60, pp. 676-681.
(Illustrated description of the Fort Dodge plant of the Northwestern Manufacturing Company.)

Steel Company Builds New Power Plant.
Power Pl. Engng., Oct. 15, 1924; v. 28, pp. 1034-1041.
(Illustrated account of equipment in the steam-driven power plant of the Columbia Steel Corporation, Provo, Utah.)

18,000-kw. Plant Serves Lumber Company.
Power, Oct. 21, 1924; v. 60, pp. 638-641.
(Short, illustrated description of the plant of the Long-Bell Lumber Company, Longview, Wash.)

Protective Apparatus

German System Re-adopts Petersen Coil.
Elec. Wld., Oct. 11, 1924; v. 84, pp. 786-787.
(Short article outlining a German concern's experiences with Petersen coils.)

Refrigeration

Development of Electrical Refrigeration for Ice-Cream Retailers.
Elec. Wld., Oct. 25, 1924; v. 84, pp. 890-892.

Regulators, Induction

Polyphase Induction Regulators. Carr, Laurence H. A.
Elec. Rev., Oct. 10, 1924; v. 95, pp. 528-530.
(Illustrated article on the principle of operation of such apparatus.)

Spot Welding

Spot Welding.
Am. Weld. Soc. Jour., Sept., 1924; v. 3, pp. 23-26.
(Report of the Resistance Welding Committee of the American Bureau of Welding.)

Standards

Test Code for Speed-Responsive Governors.
Mech. Engng., Nov., 1924; v. 46, pp. 713-716.
("Preliminary draft of a special supplementary code formulated by the American Society of Mechanical Engineers Committee on Power Test Codes.")

Steam

Experiments on the Generation of "Critical" Steam. Overwyn, Jacques F.
Power, Oct. 28, 1924; v. 60, pp. 693-694.
(Brief account of attempts to develop an extremely light-weight steam power plant for airplanes and the like.)

Steam Flow

Simplifying Steam-discharge Computations. Barclay, S. D.
Power, Oct. 14, 1924; v. 60, pp. 613-614.

Steam Turbines

Conditions Affecting Steam Turbine Economy. Dahlstrand, J. Y.
Power Pl. Engng., Oct. 15, 1924; v. 28, pp. 1041-1043.
("Outline of conditions which interfere with maintenance and high economy. Suggestions for obtaining best results.")

High Pressure Steam Turbines.
Bul. Oerlikon, Sept., 1924; pp. 165-168.
(Describes such turbines manufactured by the Oerlikon Company.)

Turbine Packing, Bleeding Arrangements and Other Features of Westport Station Addition.
Power, Oct. 14, 1924; v. 60, pp. 605-608.

Steam Turbines—Testing

Turbine Performance from Steam Quality Measurements. Johnson, N. L.
Power, Oct. 28, 1924; v. 60, pp. 691-692.

Steel—Electrometallurgy

Multiple System of Electric Melting. Hanff, E. A.
Iron Age, Oct. 16, 1924; v. 114, pp. 999-1003.
(The "twin furnace" plan as applied to a steel foundry.)

Street Lighting

Common Return for Street Lighting. Richter, H.
Elec. Wld., Oct. 18, 1924; v. 84, pp. 831-833.
(Advantages and disadvantages, testing, maintenance methods, etc.)

Substations

Features of 60,000-kv-a. Substation. Goodale, J. E.
Elec. Wld., Oct. 25, 1924; v. 84, pp. 881-884.
(Illustrated description of the Maspeth substation of the New York & Queens Electric Light and Power Company.)

Wattmeters—Testing

Testing Single-phase Induction Watthour Meters. Walsh, Willard F.
Power, Oct. 28, 1924; v. 60, pp. 687-689.

Wind Power

Wind Power for Farm Electric Plants. Pancratz, F. J.
Mech. Engng., Nov., 1924; v. 46, pp. 675-682.
(Presents the results of extensive tests.)

X-Rays

Using X-rays to Detect Hidden Dangers in Plant Equipment. Lester, H. H. and others.
Chem. & Met. Engng., Oct. 20, 1924; v. 31, pp. 619-622.

NEW BOOKS

Analytical Mechanics. Ed. 2, rev. and enl. Edwin H. Barton. 593 pp., 1924, N. Y., Longmans, Green & Co.

Charles Proteus Steinmetz; a Biography. John Winthrop Hammond. 489 pp., 1924, N. Y., Century Co.
(We now have an intimate story of the life of Steinmetz the world-builder and idealist—the story of one who was at once a celebrated engineer and a lovable personality. His biographer writes from the standpoint of one who knew both Dr. Steinmetz and many of his friends and fellow workers. The result has been that we have an accurate biography of a great man presented in a truly fascinating style. There is surely romance in this story of one who rose from a penniless immigrant to a position of acknowledged pre-eminence in the field of electrical engineering, and through it all the author has retained that atmosphere of the thoroughly likable personality for which Dr. Steinmetz was justly noted.)

Coal Carbonization. Horace C. Porter. 442 pp., 1924, N. Y., Chemical Catalog Co.

Electro-deposition of Metals. Ed. 9. George Langbein; trans. by William T. Brannt. 863 pp., 1924, N. Y., Henry Carey Baird & Co., Inc.

Elements of Electrical Engineering; a Textbook of Principles and Practice. Arthur L. Cook. 568 pp., 1924, N. Y., John Wiley & Sons, Inc.
(An elementary text intended for electrical and for non-electrical students in colleges. The use of formulas is reduced to a minimum, the student being encouraged to derive the result from fundamental laws. Practical problems are appended to each chapter, the solution of these being intended to provide a thorough grounding in the fundamentals brought out in that chapter. Special attention is given to the magnetic circuit and to alternating currents and alternating-current machinery.)

Engineering in American Industry. Conrad Newton Lauer. 94 pp., 1924, N. Y., McGraw-Hill Book Co., Inc.

Fuel Economy in Steam Plants. Arthur Grounds. 106 pp., 1924, N. Y., Isaac Pitman & Sons.

Fuel Oils and Their Applications. H. V. Mitchell. 171 pp., 1924, N. Y., Isaac Pitman & Sons.

Practical Radio; Including the Testing of Radio Receiving Sets. James A. Moyer and James F. Wostrel. 249 pp., 1924, N. Y., McGraw-Hill Book Co., Inc.
(Written with the object of presenting the fundamentals accurately and in a manner that can be understood by anyone of average training. Describes the various kinds of receiving sets, their construction, operation and testing. A chapter is devoted to detailed instructions for the building of several different sets, and another to the more common difficulties of reception, with their remedies. The volume concludes with an appendix which presents a chronology of the more important events in the development of radio engineering.)

Railway Rates and Cost of Service. Owen Ely. 148 pp., 1924, Boston, Houghton Mifflin Co.

Scales and Weighing; Their Industrial Applications. Herbert T. Wade. 473 pp., 1924, N. Y., Ronald Press Co.

Theorie der Schüttelschwingungen, und Untersuchung der Schüttelerscheinungen von Elektrischen Lokomotiven mit Parallelkurbelgetrieben. A. Wichert. 120 pp., 1924, Berlin, V. D. I.-Verlag.
(On the theory of chattering vibrations, especially with reference to chattering wheel-slip in electric locomotives having parallel rod drive. Discusses causes and remedies, and presents results of tests. A short bibliography is included.)

Theory and Practice of Public Utility Valuation. W. H. Maltbie. 201 pp., 1924, N. Y., McGraw-Hill Book Company, Inc.